

Department of Mechanical and Aerospace Engineering

**Design and Technical Assessment of Air Source Heat
Pump Systems for Domestic Heating Systems.
A Case Study in the Republic of Cyprus**

Author: Andreas Miltiadous

Supervisor: Dr. William Dempster

A thesis submitted in partial fulfilment for the requirement of degree in
Master of Science
Sustainable Engineering: Renewable Energy Systems and the Environment

2022

Copyright Declaration

This thesis is the result of the author's original research. It has been composed by the author and has not been previously submitted for examination which has led to the award of a degree.

The copyright of this thesis belongs to the author under the terms of the United Kingdom Copyright Acts as qualified by University of Strathclyde Regulation 3.50. Due acknowledgement must always be made of the use of any material contained in, or derived from, this thesis.

Signed: 

Date: 11/08/2022

Abstract

The mitigation of climate change and global warming is an important environmental aspect that needs to be tackled urgently. Air source heat pumps have the potential to contribute significantly, in reducing the greenhouse gas emissions associated with the domestic sector in space conditioning and direct hot water for use. Heat pumps in general is a technology which is rapidly growing and has a substantial prospective in improving the energy performance of heating and cooling systems due to their efficiencies which are relatively high. In this thesis a complete methodological design approach is proposed for the designing and optimization of a sustainable heating system using heat pumps. An economic analysis followed by an environmental assessment was also performed, to evaluate the performance of the proposed system in terms of initial investment cost and the potential CO₂ emission reductions.

The whole thesis was concentrated on a double story residential building in the republic of Cyprus with estimated yearly heating demand of 14.6 MWh deduced from an ESP-r model. An air to water heat pump system with a heating capacity of 16kW and a COP of 4.20, coupled with solar thermal collectors and thermal energy storage, was analysed to determine the suitability and reliability of such a system in fully meeting the overall heating demands. The modelling results has shown that the proposed design was reliable in meeting the demands by 100% with a final SPF of 6.15. The thermal energy storage with a total volume of 1500l has shown the effectiveness of such a technology in mitigating the time of peak loads. To assist the performance even further, an investigation for the integration of renewables was also performed to evaluate the feasibility of implementing PV arrays for the production of renewable power and solar thermal collectors for thermal energy production. The total PV array size consisted of 10 panels with an installed capacity of 4kW and an estimated yearly electrical power output of 8MWh covering 92% of the power consumption of the system. The solar loop system consisted of two flat plate collectors connected in series with a total surface area of 4m². An in-depth investigation on the effect of tilt angle both of the solar thermal collectors and the PV panels was performed to identify the optimum inclination of 31.5°. The total thermal energy production for the solar loop has shown that the entire hot water demand can be met. Finally, an economic analysis was performed to estimate the initial investment cost of such a sustainable system which was found to be £15 600 with a payback time of 8.4 years and a return on investment of 11.4%. From the environmental analysis, which was the most crucial aspect of this thesis, it was identified that a 60% reduction in the CO₂ emissions can be achieved.

Acknowledgements

Firstly, I would like to express my special thanks to my supervisor Dr. William Dempster for providing assistance and guidance throughout the whole duration of the project. His valuable help and support helped me to complete my thesis at high standards. Furthermore, I would like to thank the module leader of this course Dr. Paul Tuohy for his valuable advice from the beginning of my studies at the University of Strathclyde, and also all the staff in the Sustainable Engineering department.

Finally, I would like to thank my parents for constantly motivating me to reach my goals and for their financial support for my studies. I would also like to thank my cousin Michalis Michaelides who helped me with the data analysis and data processing in Excel and Matlab. Sincere thanks to my close friends and classmates who were always by my side whenever I needed them.

Table of Contents

1.0	Introduction	13
1.1	Background.....	13
1.2	Aim and Objectives	14
1.3	Thesis plan.....	15
2.0	Literature review	16
2.1	Heat pumps	16
2.1.1	Heat sources and heat pump classification.....	17
2.1.2	Refrigerants	17
2.1.3	Principle of operation- vapour compression cycle.....	19
2.1.4	Thermodynamics and ideal vapour-compression cycle	21
2.1.5	Effectiveness of the system performance.....	23
2.1.6	Seasonal performance factor	24
2.1.7	Energy Balance and System Efficiency	25
2.1.8	Heat exchangers in heat pumps.....	25
2.1.9	Heat pump systems vs conventional boilers	26
2.2	Thermal energy storage system	27
2.2.1	Heat capacity	28
2.2.2	Thermal stratification	29
2.2.3	Rate of heat loss	30
2.2.4	Importance of TES implementation with air source heat pumps.....	31
2.3	Integration of renewables	32
2.3.1	Renewable thermal energy production.....	32
2.3.1.1	SAHPS components	32
2.3.1.2	Solar thermal collectors.....	33
2.3.1.3	Thermal efficiency of solar thermal collectors	35
2.3.2	SAHP system configuration.....	36
2.3.2.1	Direct expansion.....	36
2.3.2.2	Indirect expansion	37
2.3.3	Renewable electrical power generation	38
2.3.3.1	Mode of operation of solar cells.....	39
2.3.3.2	Importance of semi-conducting materials	39

- 2.3.3.3 Solar PV cell types40
- 2.3.3.4 Solar PV system configurations41
- 3.0 System Design Methodology.....42**
- 3.1 Software Assessment and Selection43
- 4.0 Case Study Description: Cyprus.....45**
- 4.1 Climate.....45
 - 4.1.1 Temperature45
 - 4.1.2 Solar radiation46
- 4.2 Energy provider47
- 4.3 Housing Stock in Cyprus.....48
- 4.4 Current Heating Systems48
- 4.5 Site Selection50
- 5.0 Existing heating system.....50**
- 5.1 Heating Demands51
 - 5.1.1 Space Heating.....51
 - 5.1.2 Hot water demand54
 - 5.1.3 Overall estimate heating demands56
- 6.0 System Technology Design57**
- 6.1 System Capacity59
- 7.0 Results and Discussion60**
- 7.1 Performance Evaluation of ASHP.....60
- 7.2 Enhancing Performance.....63
 - 7.2.1 Introducing a TES63
 - 7.2.2 Solar Assisted Heat Pump Modelling65
- 7.3 PV Electricity Generation.....70
- 8.0 Financial Evaluation78**
- 8.1 Capex78
- 8.2 Total Savings79
- 8.3 Payback Period80
- 8.4 Return on Investment80
- 9.0 Environmental Analysis.....80**
- 9.1 CO₂ Savings81

10.0 Conclusion81
11.0 Future Work82
12.0 References83

List of Figures

Figure 1: Global share of residential sector in final energy use [3].	13
Figure 2: Simple energy flow diagram for refrigeration and heat pump [9]	16
Figure 3: Refrigerant selection graph based on temperature and pressure [17].	19
Figure 4: Vapor compression cycle of a heat pump [18].	20
Figure 5: Theoretical and actual vapour-compression cycle.	21
Figure 6: Thermodynamic processes in the ideal vapor compression cycle [19].	22
Figure 7: Evaporator and condenser temperature difference on COP[22].	24
Figure 8: Energy balance schematic on building.	25
Figure 9: Internal temperature variations while phase change is occurring [30].	28
Figure 10: Variation in the thermal stratification based on temperature difference [35].	30
Figure 11: Heat trap piping schematic [35].	31
Figure 12: Flat plate collector system schematic and component configuration [43].	33
Figure 13: Evacuated tube collector system schematic and components configuration [45].	34
Figure 14: Different system configurations of SAHP systems.	36
Figure 15: System configuration difference of ASHP and DX-SAHP[48].	37
Figure 16: (a)Serial;(b) Parallel; and (c)Complex configurations [53]	37
Figure 17: Photovoltaic effect on solar cell [58].	39
Figure 18: Solar PV cell types solar [61].	40
Figure 19:Classification of solar PV system types [64].	41
Figure 20: Example of supply and demand matching graph modelled in energyPro [68].	44
Figure 21: Average outdoor temperature for a yearly period [73].	46
Figure 22: Cyprus solar radiation distribution map [76].	46
Figure 23: Average monthly solar radiation [75].	46
Figure24:Seasonal variation of solar radiation in Cyprus [77].	47
Figure 25: Classification of housing types in Cyprus.	48

Figure 26: Types of domestic heating in Cyprus.	49
Figure 27: Building location on map.	50
Figure 28: Building outside appearance.	50
Figure 29: Oil condensing boiler and equipment.	51
Figure 30: Estimated annual space heating demands as per EPC.	51
Figure 31: Building model geometry.	52
Figure 32: Estimated annual space heating demand profile from ESP-r.	53
Figure 33: Daily space heating demand profile for the 8 th of January.	53
Figure 34: System configuration of a thermosyphon [80].	54
Figure 35: Monthly direct hot water demand from EPC	55
Figure 36: Hourly probability percentage for domestic hot water demand [82].	55
Figure 37: Estimated hourly heating demand profile for domestic hot water.	56
Figure 38: Combined heating demand profile for both space heating and DHW	57
Figure 39: Sustainable heating system schematic and component configuration [83].	58
Figure 40: ASHP schematic with buffer tank supplying DHW and space heating	60
Figure 41: Results file with the yearly SPF variation for the ASHP with a buffer tank.	62
Figure 42: Relationship between COP by varying the heat source and heat sink temperature [87].	62
Figure 43: Heating demand profile on the 8 th of January with potential energy storage capacity.	63
Figure 44: ASHP model schematic with TES and a buffer tank.	64
Figure 45: Yearly SPF variation for the ASHP with a buffer tank and TES.	65
Figure 46: ASHP model schematic with TES, buffer tank and solar thermal collector.	66
Figure 47: Variation in the angle of incident during Summer and Winter [89]	66
Figure 48: Average incident solar radiation vs tilt angle.	67
Figure 49: Results for optimum tilt angle on a seasonal and annual average.	68

Figure 50: Variation of solar energy incident on the collector when the tilt angle is varied as per modelled, annual, and seasonal average values.68

Figure 51: Annual SPF variation for the ASHP with a buffer tank, TES and solar thermal collector.....69

Figure 52: Monthly profile of electrical power consumption.....71

Figure 53: Yearly profile of electrical power consumption.....71

Figure 54: System schematic of the PV array model.....71

Figure 55: Electrical technical drawing of the PV model.....72

Figure 56: Heat pump power consumption vs PV power generation.73

Figure 57: Validation results of PV*Sol vs PV Watts.....73

Figure 58: Overall proposed system model in energyPro.....74

Figure 59: Yearly profile of outdoor temperature generated from energyPro.....75

Figure 60: Yearly profile of annual solar radiation deduced from energyPro.75

Figure 61: ASHP results from energyPro for January the 8th.76

Figure 62: Results from energyPro for PV generation and ASHP consumption.....77

Figure 63: Comparison in the CO₂ emission of heating oil and HP with PV panels.....81

List of Tables

Table 1: Advantages and disadvantages of ammonia and Carbon dioxide [15]..... 18

Table 2: Operational characteristics of flat plate and evacuated tube collectors [45]35

Table 3: Operational parameters of the three types of PV cells.41

Table 4: Seasonal variation factor of domestic hot water demand [81].56

Table 5: Performance characteristics of 3 different models of air source heat pumps.59

Table 6: Percentage difference in total solar energy radiation incident on the collector.....69

Table 8: Main results generated from the complete heating system run in energyPro.....76

Table 9: Total cost of investment for the proposed system.78

Nomenclature

<u>Symbol</u>	<u>Description</u>	<u>Units</u>
$T_{\text{condenser}}$	Temperature of the condenser	$^{\circ}\text{C}$
$T_{\text{evaporator}}$	Temperature of the evaporator	$^{\circ}\text{C}$
m	Mass flow	kg/s
c	Specific heat capacity of water	$\text{kJ/kg}^{\circ}\text{C}$
ΔT	Temperature difference	$^{\circ}\text{C}$
V	Volume	l
$\eta_{\text{compressor}}$	Efficiency of compressor	N/A
ρ	Density	Kg/m^3
Q_{sink}	Heat energy released	kW
W_{net}	Total power input	kWh

ABBREVIATIONS

Abbreviations Description

HP	Heat Pump
ASHP	Air Source Heat Pump
DHW	Direct Hot Water
GWP	Global Warming Potential
HCFCs	Hydrochlorofluorocarbon
HFCs	Hydrofluorocarbon
PV	Photovoltaic
ESP-r	Environmental System Performance-renewable
ODP	Ozone Depletion Potential
GHG	Greenhouse Gasses
CO ₂	Carbon Dioxide
COP	Coefficient of Performance
SPF	Seasonal Performance Factor
SAHPS	Solar Assisted Heat Pump System
DX-SAHPS	Direct Expansion Solar Assisted Heat Pump System
IDX-SAHPS	Indirect Expansion Solar Assisted Heat Pump System
CFCs	Chlorofluorocarbons
EAC	Electrical Authority of Cyprus
TSA	Total Surface area

1.0 Introduction

1.1 Background

Since the evolution of the 20th century, the influence of severe environmental issues such as climate change, earth temperature rise leading to global warming and glacier melt, has caused dramatic consequences on human and ecological life. The uncontrollable release of greenhouse gasses to the environment from human actions such as burning of fossil fuels to produce energy, has led to the urgent need, of drastic measures to be taken in order to tackle these phenomena. According to statistical data, the amounts of CO₂ emitted every year, has rapidly increased over the last 20 years with numbers showing a 45% increase [1]. One of the highest contributors for this rapid percentage increase was the development of industries and the population shift from rural to urban areas. As a result of urbanization, the building sector has faced a significant growth which has led to a massive direct impact to the environment. The building sector on its own according to the International Energy Agency, accounts for almost 40% of the total final energy use with a global consumption in 2020 of 128 exajoules [2].

The vast majority of this amount of energy is consumed by residential buildings for space heating and direct hot water with a final percentage of 22% as shown in figure 1, and according to Aruna they account for 75% of the gross European building floor area. This rapid increase of residential buildings was mainly caused due to urbanization which has directed humans to spend more time in a closed conditioned space (indoors). Nowadays, according to the Environmental Protection Agency

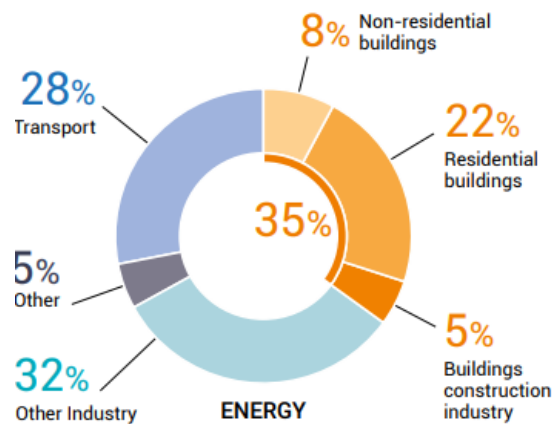


Figure 1: Global share of residential sector in final energy use [3].

(EPA), humans' tend to spend on average 22 hours per day indoors resulting to a percentage of 90% [4]. To achieve thermal comfort conditions in a space, heating and cooling systems should be installed, that will establish stable conditions and hence making the person comfortable. This process requires a lot of energy which according to Brian, in the European Union, the 70% of the heating demand is primarily based on fossil fuels whereas only 10% comes from renewables. This big percentage difference identifies the potential of the decarbonisation of the building sector by implementing technologies like heat pumps which can effectively improve the energy efficiency and achieve carbon neutrality by 2050 with a medial reduction of 55%

by 2030 as proposed by the European Commission [5,6]. The development of low-grade heat technologies could eventually help in the transition from high-grade heat supplied by fossil fuels to carbon neutrality with massive reduction in greenhouse gasses. Therefore, this thesis was conducted, to provide a complete methodological design approach of replacing the current heating systems in the domestic sector with more sustainable, using heat pumps and integration of renewables for clean energy production.

1.2 Aim and Objectives

The overall aim of this thesis was to design and assess the technical and financial aspects of a sustainable heating system for space conditioning (heating only) and direct hot water, using air source heat pump for a residential building in the republic of Cyprus.

The main objectives for this thesis are outlined below as follows:

1. Perform a thorough literature review on air source heat pump systems and emphasise on the innovation in this sector.
2. Examine the current industry practise and current technologies used.
3. Investigate the potential integration of renewable energy generation methods.
4. Construct a reliable methodological approach to be followed by similar projects.
5. Examine the current energy demand in the sector chosen to perform the analysis.
6. Determine the overall heating demands and trends for the selected case study and evaluate the performance of the existing heating systems.
7. Design a proposed heating system and asses its performance by generating models and running simulations in a dynamic energy simulation software.
8. Evaluate and discuss results to be able to conclude and recommend a solution
9. Asses the financial and environmental aspects of the proposed system.

1.3 Thesis plan

The whole thesis is divided into different sections as shown below in order to accomplish the overall aim and objectives of this project.

- Section 1- Brief introduction including background knowledge, thesis aim and objectives.
- Section 2- Thorough literature review on the state of the art of heat pumps and integration to renewables for the generation of thermal energy and electrical power.
- Section 3- Outlines the system design methodology and also an assessment of the appropriate dynamic energy simulation tool to be used.
- Section 4- Case study introduction, data gathering and data processing
- Section 5- Estimation of the current heating demands of the chosen building.
- Section 6- Modell construction and simulation results assessment.
- Section 7- Financial and environmental evaluation based on the complete system.
- Section 8- Discussion and closing remarks.

2.0 Literature review

At the beginning of this section, a brief overview on the heat-pump technology was performed focussing on the working principle, the thermodynamics analysis behind that and the different configurations and types of heat pumps that can be implemented to effectively replace the reliance on fossil fuels for domestic heating. In addition, a specific emphasis was provided on the effect of thermal energy storage connected to a heat pump system including a proper sizing technique based on standards and literature. In the second and third part of this section the possibilities of a hybrid system with renewable power generation and solar energy collectors were analysed to investigate the effectiveness of the overall hybrid system.

2.1 Heat pumps

The principle of operation of heat pumps has been established since the 1800s and forms the foundation for any refrigeration system. A heat pump can be characterised as a heat engine that can operate in reverse cycle to provide heat, instead of removing heat from a conditioned space and was firstly proposed by Lord Kelvin [7]. A heat pump can extract low grade heat from a lower temperature heat source and transfer it to a higher temperature heat sink that can effectively be used for space heating and direct hot water. This statement opposes the Clausius form of the second law of thermodynamics which suggests that thermal energy can spontaneously be transferred from a hot medium to a colder region. In more depth the total entropy of the system will never decrease, it will either increase or stay the same for any spontaneous process [8]. Since thermal energy cannot freely flow from a cold medium to a hot medium, an external energy in the form of electricity or gas should be applied to enable the principle of operation a heat pump. Referring to the heat pump this amount of energy is supplied to the compressor which is responsible for the flow of the refrigerant in the system. A simple example of where the same principle is applied can be found in a household fridge. A schematic with the difference in the principle of operation between the heat pump cycle and the refrigeration cycle is shown in figure 2 to the right.

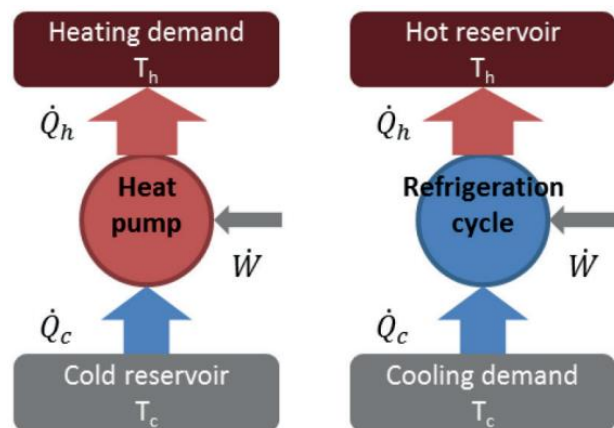


Figure 2: Simple energy flow diagram for refrigeration and heat pump [9]

Heat energy is extracted from the inside of the fridge, and it is dumped to the surroundings. By establishing this process, the overall temperature inside the fridge is maintained at constant level. As previously stated, heat pumps work in the exact opposite cycle. The main advantage of heat pumps is that the total amount of energy required to drive them is much less than the amount of heat energy they can transfer, making them an effective technology in providing space heating and cooling in domestic and commercial buildings. In addition, as of their nature, they do not burn any fossil fuel to transfer the heat hence making them more environmentally friendly [10].

2.1.1 Heat sources and heat pump classification

For any heat pump to operate and transfer heat it requires a specific heat source that can extract energy. The three main heat sources are air, water, and geothermal (ground). Based on the heat source the heat pumps can be classified as either Air source heat pumps, Water source heat pumps or Ground source heat pumps. All these types of heat pumps are able to work both by providing heating or cooling since their principle of operation relies on the vapor-compression (heating mode) and absorption cycle (cooling mode) which are explained in detail below. In addition to the heat source the heat pump can be further separated based on the heat sink as well. Heat source is described as the medium where heat is being extracted whereas heat sink is described as the medium where thermal energy is being transferred to or dumped. The most common are summarised below as follows:

- Air to Air Heat Pumps
- Air to Water Heat Pumps
- Ground to Water Heat Pumps

From the list mentioned above the most cost-effective type of heat pump that is used for domestic and commercial heating since it can operate for both heating and cooling is the Air to Water Heat Pump which is the one chosen for this specific project.

2.1.2 Refrigerants

For any heat pump to be able to transfer heat from the heat source to the heat sink, it requires an appropriate volatile substance or the working fluid that will be responsible for absorbing and releasing the heat which is called refrigerant. The performance of the heat pump is heavily based on the refrigerant therefore an appropriate selection should be established at the beginning of the designing process of a HP system. At the beginning of the evolution of the heat pump applications the most common refrigerants that were used, were the

chlorofluorocarbons (CFCs). Over the decades it was identified that they had a bad influence on the environment since they were highly contributing to the depletion of ozone and thus they were strictly banned in 1987 by the signing of the Montreal Protocol [11]. Hydrofluorocarbons (HFCs) and Hydrochlorofluorocarbons (HCFCs) were the next refrigerant types that replaced the CFCs. The main difference between these two types of refrigerants is that HCFC has chlorine which highly affects the ozone layer. Based on that, the European Union had decided to phase down the use of HCFCs by 2040 [12]. On the other hand, HFCs have the advantage of not containing chlorine making the Ozone Depletion Potential (ODP) reaching a zero value. Some of the most common HFCS refrigerants that are used in heat pump and refrigeration technologies are R 134a, R 410A and R152a which are non-flammable and chemically stable [13]. Nevertheless, HFCS can be characterised as vigorous greenhouse gasses (GHG) with a relatively high Global Warming Potential (GWP). In fact, the average GWP of HFCS are 3,770 times higher than the GWP of CO₂, indicating that it is essential that heat pump manufacturers should replace the existing conventional refrigerants with ones that are natural and more climate friendly and with low GWP. The European Commission based on the F-Gas Regulation suggested different alternatives such as ammonia (R-717) and carbon dioxide (R-744) which are climate friendly and energy-efficient [14]. There are also some drawbacks with the use of such refrigerants. For example, ammonia is a toxic gas and hence it has an increase in the overall cost since health and safety precaution measures should be established to prevent the chance of any leakages. In addition, CO₂ must be pressurised to be able to achieve an optimum performance requiring a higher initial cost.

The following table below summarises the key advantages and disadvantages of the two alternative refrigerants suggested above.

Table 1: Advantages and disadvantages of ammonia and Carbon dioxide [15].

Refrigerant	Advantages	Disadvantages	GWP	ODP
Ammonia (R-717)	<ul style="list-style-type: none"> • 3-7% higher efficiency than CFC'S • Less consumption of electricity • Lower operating costs 	<ul style="list-style-type: none"> • Toxic and poisonous at high concentrations • It's not compatible with copper pipes 	1	0
Carbon Dioxide (R-744)	<ul style="list-style-type: none"> • Non-corrosive • Higher efficiencies at lower temperatures 	<ul style="list-style-type: none"> • Higher initial cost in comparison to ammonia • It requires a two-stage compression 	1	0

From the table it can be concluded that there is not a single refrigerant that can be used for all different types of heat pump technologies since each one has not identical properties. Therefore, when designing any heat pump application things like operating performance, safety, reliability, and environmental acceptability should be considered [16]. The following figure represents a graph for the correct selection of the refrigerant to be used based on two critical aspects for the performance of the heat pump which are temperature and pressure.

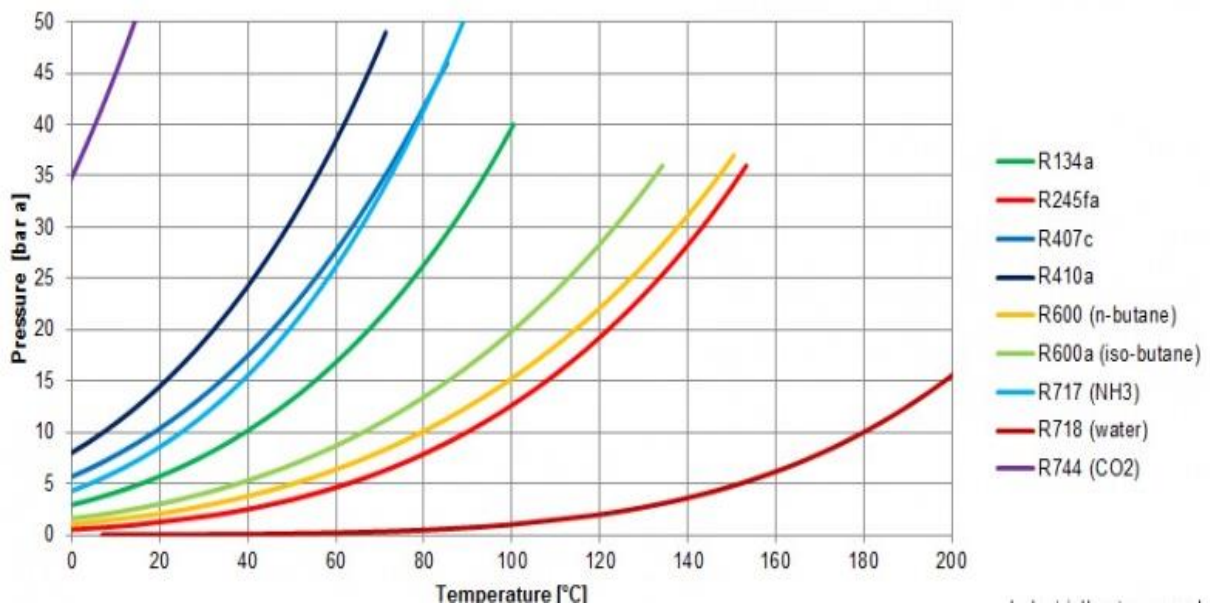


Figure 3: Refrigerant selection graph based on temperature and pressure [17].

2.1.3 Principle of operation- vapour compression cycle

The vapor compression cycle comprises the main cycle of operation for any configuration and type of heat pump technology. The whole system is configured by four main components which are the compressor, the condenser, the expansion/ throttle valve, and the evaporator. Each component has a unique function that when combined it allows the full performance of any heat pump system since they form a close circuit where the refrigerant circulates.

The following figure shows a simple schematic with the four main components of the system with a representation of how heat energy is flowing in the cycle.

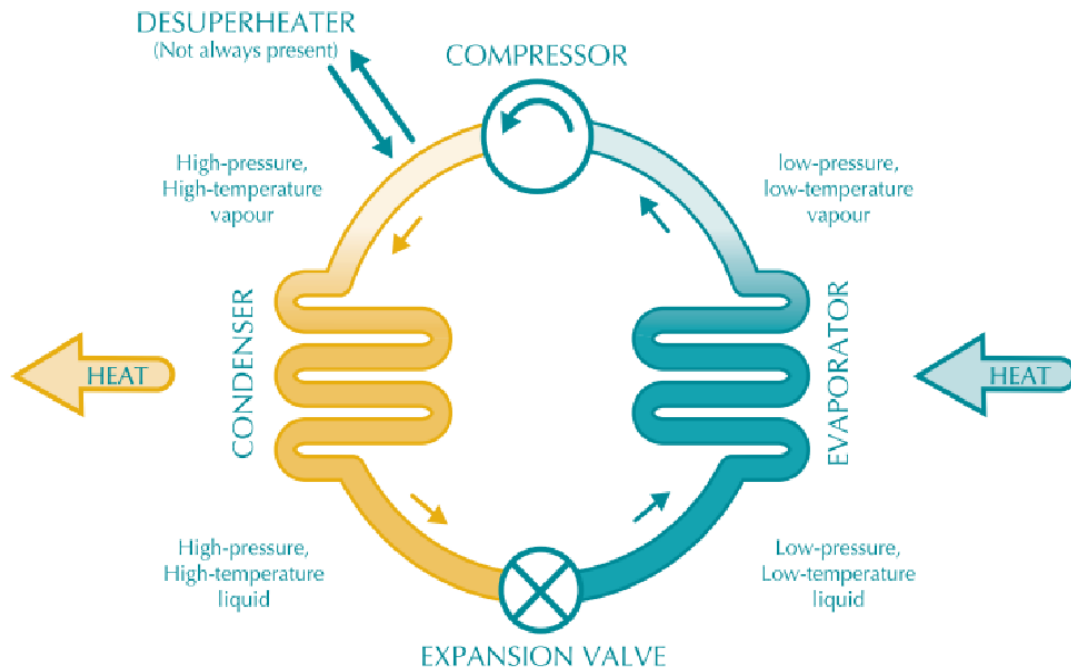


Figure 4: Vapor compression cycle of a heat pump [18]

The role of each component is shortly described below as follows:

- **Compressor:** it is a mechanical device that is used to compress the gaseous refrigerant to increase its overall temperature and pressure.
- **Expansion valve:** it is a pressure differential valve that is responsible for reducing the high pressurised refrigerant leaving the condenser and hence lowering the temperature of the refrigerant close to its boiling point [18].
- **Evaporator:** it acts as a heat exchanger, by allowing the liquid refrigerant to absorb low grade heat energy from the outside medium. In addition, in the evaporator, due to the temperature difference, the refrigerant is then boiled to turn from liquid to vapor.
- **Condenser:** it also acts as another heat exchanger where the high pressurised refrigerant from the compressor releases the heat energy gained to the inside medium, which can be either air or water for space heating, and finally it changes phase to liquid.

2.1.4 Thermodynamics and ideal vapour-compression cycle

The following graphs on figure 5 represent the pressure and temperature enthalpy diagram for an ideal-vapour compression cycle respectively. Both diagrams represent with solid red line the ideal vapour-compression cycle and the actual with dotted red line.

Ideal vapour-compression cycle

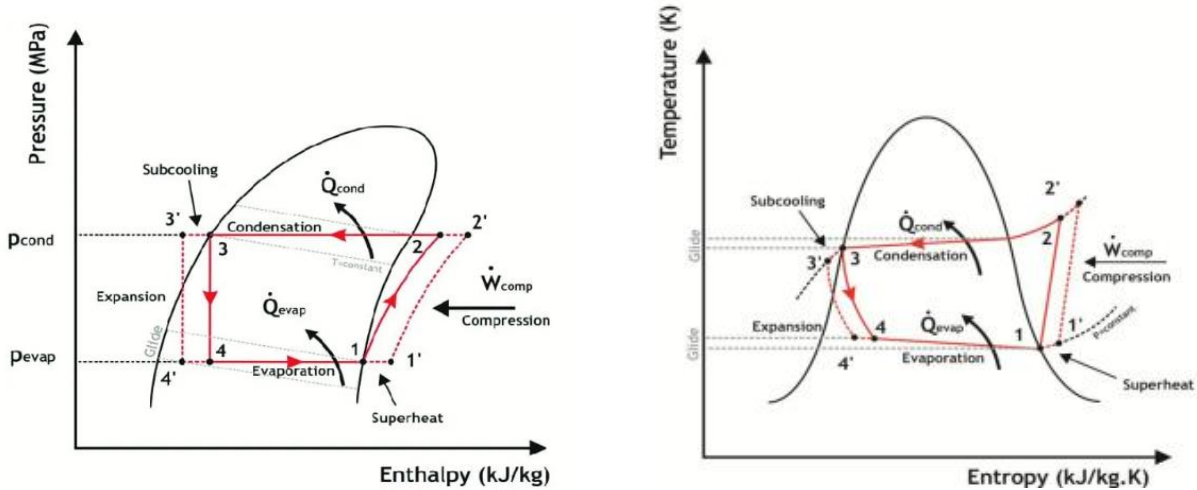


Figure 5: Theoretical and actual vapour-compression cycle.

At point 1 where the refrigerant enters the compressor, it is at low temperature and pressure. The compressor, which is driven by electrical power supply, compresses / forces the refrigerant molecules to increase their pressure and as a result of higher pressure their temperature also increases. According to Clausius statement, this compression process requires an external force (power supply) for heat energy to be able to flow from low to higher temperatures. After the refrigerant is compressed, it becomes a hot gas and enters the condenser. As previously state the condenser acts as a heat exchanger, that is used for the refrigerant to release the heat energy absorbed to the outside medium (space heating or DHW). This process takes place since the temperature of the refrigerant is much higher from the temperature of the heat sink (indoor space) and hence heat flows from the hot to the cold medium and as a result the hot gaseous refrigerant condenses. The condensed now liquid refrigerant enters the expansion valve where a drop in its temperature and pressure is maintained due to the expansion. The final step in the process is the evaporator where the refrigerant enters at a low-pressure and low temperature as a liquid-vapour mixture. The evaporator acts a second heat exchanger where the refrigerant absorbs heat energy from the outside environment (air or water). Because of this effect the working fluid is fully vaporized, becoming a low temperature and low-pressure vapour. Finally, the refrigerant enters again the compressor where the cycle starts from the beginning.

From this short analysis it can be deduced that the operating cycle of a heat pump system can be fully reversible. This indicates that by reversing the role of the evaporator and the condenser, the direction of flow of heat can be reversed providing the opportunity to the heat pump to be used for both cooling and heating purposes. The discussion above represents only the heating mode of the heat pump.

Thermodynamics

The figure below represents a fully annotated temperature entropy diagram with all the thermodynamic process taking place in the whole vapor compression cycle.

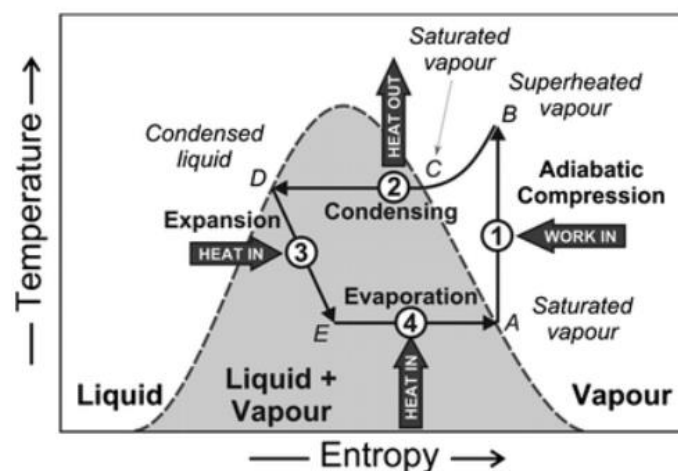


Figure 6: Thermodynamic processes in the ideal vapor compression cycle [19].

From figure 6:

- A to B: An adiabatic/isentropic compression of the working fluid resulting from a saturated vapor to a superheated vapor.
- B to C: The superheated vapor after the compression enters the condenser as saturated vapor.
- C to D: Heat exchange occurring in the condenser. Heat energy is released from the refrigerant to the heat sink (indoor heating and DHW). The whole process is isobaric meaning no change in pressure. The working fluid leaving the condenser is a condensed liquid.
- D to E: An isenthalpic expansion occurring in the throttle valve. There is a temperature and pressure drop causing the condensed liquid refrigerant to become liquid and vapour.
- E to A: An isobaric low pressure and low temperature heat exchange making the working fluid fully vaporised.

Difference between ideal and actual vapour compression cycle

As it can be seen from the two graphs in figure 5 above there is a minor difference between the actual and the theoretical performance of the vapour compression cycle. The two cycles differ mainly because of the following reasons:

- In the pipes that the working fluid is flowing there are some pipe friction losses that are not considered within the ideal cycle resulting to several pressure drops.
- In the ideal cycle the compression is meant to be isentropic but in reality, there are some fluid dynamics losses caused by friction that result to lower coefficient of performance [20]. This occurs because there is heat produced during compression resulting to an increase in the entropy.
- In the actual cycle, the refrigerant leaving the condenser is not a saturated liquid due to the subcooling process which results to a lower enthalpy.

2.1.5 Effectiveness of the system performance

An important parameter that describes the effectiveness of the ideal vapour compression cycle is the Carnot efficiency which is depended on a ratio of the temperature of the evaporator and the condenser. The equation below represents a simple calculation on how the maximum ideal Carnot efficiency can be calculated.

$$\eta_{Carnot} = \frac{T_{condenser}}{T_{condenser} - T_{evaporator}}$$

In real applications of heat pumps this efficiency is not feasible, due to the reason described in the above section, resulting to lower efficiency. In fact, the performance of any heat pump system can be identified by the Coefficient of Performance (COP) which is more accurate parameter in calculating the system performance. The COP takes into account all the energy changes that occur in the heat pump vapour compression cycle such as the heat transferred to the heat sink (Q_{sink}), the work input to drive the compressor (W) and the heat energy absorbed from the heat source (Q_{source}). The following equation can be used to calculate the COP of a heat pump system taking into consideration the energy changes mentioned above as follows:

$$COP = \frac{\text{Heat demands}}{\text{Total power input}} = \frac{Q_{sink}}{W_{net}}$$

The above equation can be described according to literature as a measure on how effectively any heat pump system can utilise electrical energy to transfer heat energy from the cold medium

to the hot medium [21]. The following graph in figure 7 demonstrates the variation in the COP of the heat pump when the temperature of the indoor space is kept constant whereas the outdoor temperature is changing.

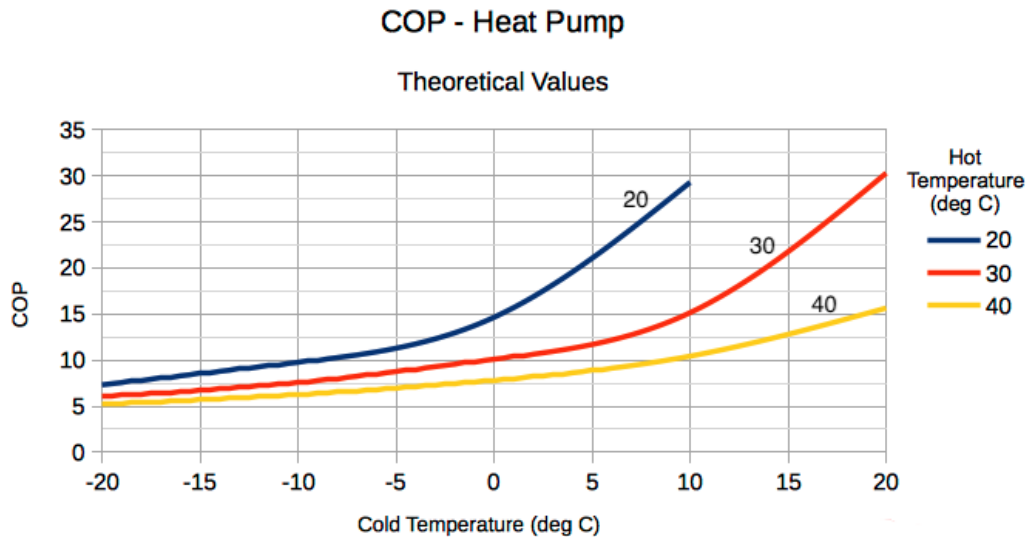


Figure 7: Evaporator and condenser temperature difference on COP[22].

From the results represented on the graph it can be concluded that the highest COP occurs when the temperature difference between the heat source and the heat sink is low.

2.1.6 Seasonal performance factor

In addition to the coefficient of performance there is another important metric that need to be considered when evaluating the system performance of a HP and it is referred to as the Seasonal Performance Factor (SPF). This is an extra parameter that can be expressed as the ratio of the overall annual heating supplied to the conditioned space over the total electrical power supplied to the compressor and any other auxiliary systems such as immersed heating elements over a year period.

$$SPF = \frac{\text{Yearly total heat demand output}}{\text{Yearly power input}}$$

The main difference between the COP and SPF is the fact that COP can provide the efficiency only for the heat pump system whereas the SPF considers any other equipment of the system that also consume electrical energy [23].

2.1.7 Energy Balance and System Efficiency

Figure 8 represents a schematic of a domestic building maintained by an ASHP in heating mode. The symbol Q_i represents the amount of heat energy that is released from the condenser to the internal volume of the house. Similarly, Q_a represents the amount of heat that is absorbed by the heat pump evaporator. For the whole system to be fully functional an external amount of electrical energy should be supplied to the compressor and in this schematic is represent by W .

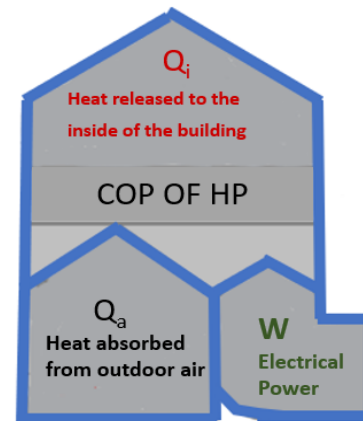


Figure 8: Energy balance schematic on building.

According to the first law of thermodynamics, energy is never created or destroyed; it is just converted from one form to the another. Hence by applying the first law to the building the following energy balance equation can be established:

$$Q_{released\ internally} = W_{compressor} + Q_{absorbed\ from\ ambient\ air}$$

The total work supplied to the compressor can be calculated by knowing the total efficiency of the compressor.

$$W_{compressor} = \frac{W_{total}}{\eta_{compressor}}$$

The Carnot efficiency was described as the maximum theoretical COP. From that value, the actual COP of any heat pump can be calculated by multiplying the Carnot efficiency by the overall system efficiency as follows:

$$COP_{actual\ HP} = \eta_s \times COP_{Carnot\ HP}$$

2.1.8 Heat exchangers in heat pumps

The most essential equipment in any heat pump system are the heat exchangers that are responsible for transferring heat from one medium to the other. In fact, there are two heat exchangers in any heat pump system. One which is responsible for extracting the heat from the outside medium (evaporator) and the other which delivers the heat absorbed from the refrigerant to the water (condenser) circulating around the building providing space heating.

According to literature the most efficient heat exchanger type to be used in such a system is the counter flow shell and tube heat exchanger, where the direction of flow of the two fluids is opposite resulting to an efficient transmission of heat energy [24].

To maintain the conditioned space to a desired temperature, the heat energy absorbed by water from the refrigerant should be transferred to the indoor environment using natural convection. In domestic houses there are two main systems that are used to achieve that, either using radiators which are mounted to the walls of the house or underfloor heating system. Radiators are hollow metal devices with fins at the back that have the ability when hot water is flowing through them to warm the surrounding air using natural air circulation. In fact, as the air around the radiator is heated up it becomes less dense and starts to rise. Then cooler air particles due to their higher density they fall back to take its place. As a result, a rotational current is formed that eventually causes the air in the enclosed space to heat up slowly. The hot water flowing through the inlet valve of the radiator (supply temperature) according to literature should be around 75°C [25]. If we consider the COP of a heat pump, it was stated above that the efficiency increases when the temperature difference is close together. Now if we consider the supply temperature of radiator it can be seen that a heat pump system will have a poor performance when connected to the radiators. Therefore, to be able to lower temperatures without affecting the thermal comfort of the conditioned space, either the total surface area of the radiators should increase or to invest in new technologies such as underfloor central heating systems. Underfloor heating is a new technological and innovative idea that is being used widely over the last decades since it can effectively maintain thermal comfort using lower water supply temperatures. The main advantage of such a system is that the energy losses compared to a heating system with radiators are much less resulting to higher efficiencies and hence the reduction in the operation cost.

From a research analysis performed by a company called Nu-Heat it was identified that underfloor heating system is a cost-effective way of transferring heat since it can save up to 25% of the energy when compared to radiators and also it has the potential to save around 40% of the energy when it is run from a heat pump [26].

2.1.9 Heat pump systems vs conventional boilers

A critical point that was also assessed when undertaking this project was to identify the impact of changing the existing conventional boiler used in domestic buildings for space heating with heat pumps. The following discussion is based on results and conclusion drawn from other

experts that performed different analysis to quantify the positive outcomes from switching to heat pumps. From an analysis performed by Kelly, on the potential saving for replacing a gas condensing boiler with air source heat pump, it was concluded that there is a potential to reduce the CO₂ savings by 12% compared to natural gas boiler [27].

2.2 Thermal energy storage system

Thermal energy storage system is a huge technological accomplishment since it can store energy in different forms and then can be used at a later time for heating or electricity generation applications [28]. Heat pumps as of their nature they heavily rely on electricity directly drawn from the grid which acts as an external force in driving the compressor. Therefore, TES has a significant role to play in cases where the electricity supply is not secure, or it is dependent on renewable energy sources for electricity generation that are influenced by external factors such as weather conditions. In real life application thermal energy storage systems can be separated into three categories based on the thermal mechanism used to store energy and can be classified as sensible and latent heat and thermo-chemical reactions [29]. All three types of heat storage methods can store energy due to the change in internal energy of the material used. Sensible heat storage can be established when a solid or liquid can store energy by increasing its temperature (charging) and release this amount of energy when it is needed by decreasing its temperature (discharging). For this storage method to be efficient the materials used such as water, sand, or molten salts, should have a high heat capacity. According to literature gasses are not so widely used in sensible thermal energy storage because they have relatively low densities. In addition, latent heat storage can be established when a material changes phase e.g. from solid to liquid or from liquid to gas. In more depth, when there is a phase change of a material, there is either energy absorbed or released depending on the process that takes place (melting or freezing). For example, when a material undergoes melting (solid to liquid), the phase transition enables the material to absorb energy. On the other hand, when a material freezes (liquid to solid), it releases an amount of energy. The graph in figure 9 below represents the variations in internal temperatures for both sensible and latent thermal storage methods when undergoing a phase transition.

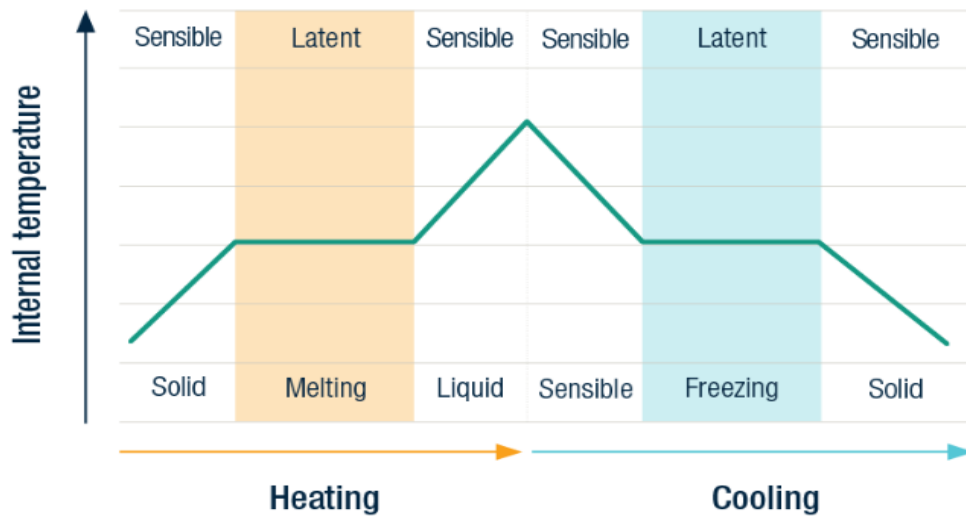


Figure 9: Internal temperature variations while phase change is occurring [30].

From the graph in figure 9, it can be identified that latent heat storage has some advantages compared to sensible heat storage. With latent heat storage it is achievable to store huge amounts of energy with very small temperature differences resulting to a higher storage density. Moreover, the two horizontal lines for melting and freezing represent that the phase transition occurs at a constant temperature making possible the temperature variations to become smoother [31].

The last type of thermal energy storage is the thermo-chemical, where thermal energy is stored in chemical bonds as a result of a reversible chemical reaction. A typical example of such a reaction that is used to store energy is the hydration of salts [32]. For this project the focus is concentrated on sensible thermal energy storage thus the following section introduces the key aspects when considering the use of STES such as the amount of heat, thermal density of the storage medium, thermal stratification, and rate of losses.

2.2.1 Heat capacity

Heat capacity is an important parameter to be calculated when designing any thermal energy storage system since it can provide valuable results for the identification of the specific thermal density of the storage medium to be used [33]. The total capacity of the sensible heat storage can be estimated using the following equation which is a multiplication of the total mass of the storage medium with its specific heat capacity and the temperature difference between the inlet and the outlet.

$$Q = mC_v\Delta T$$

From the equation of density, which is equal to mass over volume, the total mass can be rearranged and be written as:

$$Q = \rho V C_v \Delta T$$

Therefore, from the equation above, the total thermal density of the storage medium can be calculated using the following rearrangement:

$$\frac{Q}{V \Delta T} = \rho C_v$$

As previously state, the thermal density is an important parameter for sizing any sensible thermal energy storage tank since a higher thermal density storage medium will result to the reduction of the total volume of the storage tank. In addition, as seen from the equations above the temperature difference is proportional to the heat capacity of the whole system which implies that the heat capacity can be enlarged by an increase in the temperature difference. The only drawback of such an action is the fact that operating temperatures are highly affected by the implementation and the main heat source. According to a review for the potential materials for sensible thermal energy storage in building application performed by Parfait, it was identified that water is the best storage medium due to various reasons such as overall cost, abundance, thermal density, and environmental impact since it is non-toxic and non-flammable [34].

2.2.2 Thermal stratification

In any building that thermal energy storage system is being used, there is a tank which is usually constructed from stainless steel or copper, and it is used to store water at high temperature. Thermal stratification of the tank is very important in such an application since it can minimize the heat loses. The thermal stratification of the storage medium in the tank (fluid), can be described as a natural process where due the different densities of the fluid molecules in the tank there is a stratification occurring [35]. The molecules that have a higher temperature are less dense than colder ones resulting in the separation of the tank with hot molecules at the top and cold at the bottom. This flow of molecules with different temperatures generates a zone in the middle which acts as a boundary layer in separating the top heated layer with the lower unheated layer and it is called the thermocline. The following figure 10, shows different variations in the total level of stratification of storage tanks.

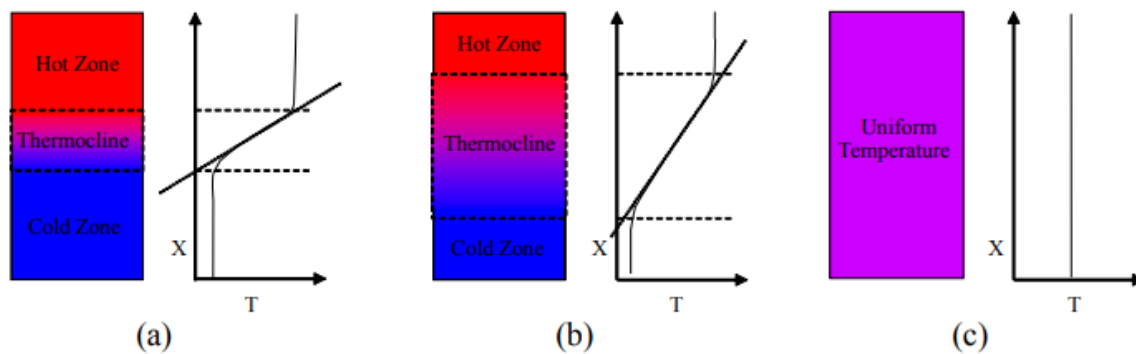


Figure 10: Variation in the thermal stratification based on temperature difference [35].

From the three graphs illustrated above there are two points of interest that determine the level of thermal stratification in the tank which are the temperature gradient and the total thickness of the thermocline region. When the temperature gradient is not so high as shown in diagram (a) the thermocline region is smaller and hence the thermal stratification is higher. On the other hand, when there is no temperature gradient there is no thermocline region being formed hence no thermal stratification. Therefore for a storage tank to be fully stratified the temperature gradient and thermocline region should be as small as possible.

2.2.3 Rate of heat loss

Another important aspect that needs to be considered when designing a thermal energy storage system for domestic buildings is the rate of heat loss from the storage tank. The average heat loss from the storage medium should be minimal so that the overall performance of the thermal energy storage system will not be minimized. To be able to calculate the heat loss from the hot storage medium, the product of the heat loss coefficient, the total surface area of the tank and the temperature difference can be calculated as follows:

$$q_{rate\ of\ heat\ loss} = TSA \times U \times \Delta T$$

Where:

- U is equal to the heat loss coefficient and is calculated using conduction and convection equations with specific thermal conductivities and overall thickness of the materials.
- ΔT is calculated from the difference between the temperature of the hot storage medium and the temperature of the surroundings.

In addition to the transmission losses from the hot storage medium, there are important heat losses occurring from the thermal bridges in insulation. Usually, they are caused from the effect of bad level of insulation or even due to the relatively small thickness. Lastly, another important source of heat loss is the piping and the coupling connections to the storage tank. To eliminate the losses due to piping it is advised that the connections to the tank should be placed at the lower part of the tank to avoid the internal circulation in the piping that would result to a higher heat loss. Moreover, the heat loss from the pipe connections at the upper part of the tank are higher and hence a method of piping called heat trap should be constructed to reduce the losses as much as possible [65]. The heat trap is represented in figure 11 below, which shows the difference in the circulation of the cold water when heat trap is applied and not applied. The heat trap piping system is mainly used to avoid the thermosiphoning (circulation of water due to natural convection) of water that causes the energy losses when there is no charging or discharging of the thermal energy store.

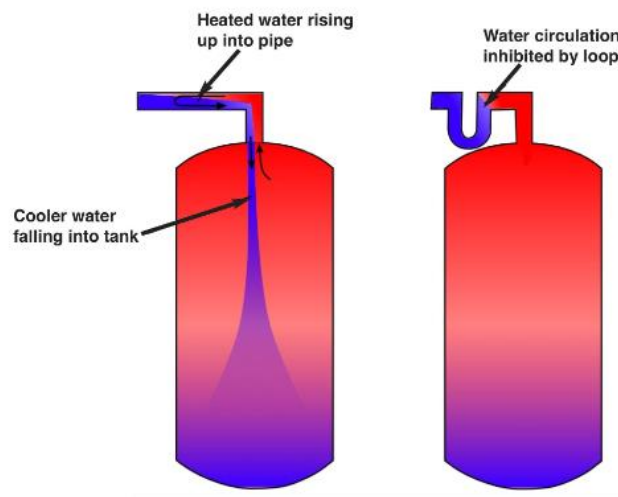


Figure 11: Heat trap piping schematic [35].

2.2.4 Importance of TES implementation with air source heat pumps

The transition to the electrification of heating using heat pump systems can dramatically increase the total electricity demand and hence thermal energy storage technologies are a viable solution in mitigating the impact on the electricity network. This can be managed through a demand management strategy that would be responsible for controlling the time at which electricity is drawn from the network and the time that heat will be supplied to the buildings. Therefore, thermal energy storage is capable for shifting the power demand from peak times to off-peak hours [37]. In addition, the thermal energy storage has several other advantages when coupled with any heat pump system and are summarised below as follows:

- Have the capability to increase the overall energy efficiency since the temperature difference will be smaller resulting to a higher coefficient of performance of the heat pump system.
- TES can effectively reduce costs since the charging of the thermal store will be performed during off-peak times when electricity prices are lower.

2.3 Integration of renewables

As of their nature, heat pump systems to be fully operatable they require some external energy in the form of electricity to be able to drive the compressor and transfer energy from the outside medium to the conditioned space. With the decarbonization of the domestic heating sector it is expected that the power consumption will increase significantly. Therefore, alternative more sustainable technologies for reducing the power consumption of heat pumps and increase efficiency should be established to be able to reduce the reliance on the grid. For that reason, this project focusses on solar assisted heat pump system for both the production of thermal energy and renewable power.

2.3.1 Renewable thermal energy production

In addition to thermal energy storage, another important technology that may be used to enhance the overall efficiency of any domestic heat pump system, can be achieved by coupling it with a solar thermal collector and creating the so called solar assisted hybrid system. This system can be described as a dual source since it can combine two technologies by integrating the heat pump technology and the solar thermal collectors in one hybrid system providing both hot water for use and space heating. The main difference of a SAHP is that the low-grade heat source is solar energy rather than water or air. Ambient air or water both have a lower-temperature energy source in comparison with solar energy thus making the SAHP having a higher operational performance [38]. The solar radiation has the capability of elevating the temperature of the evaporator resulting to a higher COP since the temperature difference is lower.

2.3.1.1 SAHPS components

There are different ways in which this type of system can be configured using five components which are: solar thermal collectors, the evaporator, the compressor, the thermal expansion valve, and a storage tank. From the components mentioned above the only new component that is not included in a normal heat pump vapour compression cycle is the solar thermal

collectors, hence the following sections provides a detailed analysis on the performance, different types, and configuration of solar thermal collectors in a SAHP system.

2.3.1.2 Solar thermal collectors

Solar thermal collectors work by utilizing the solar energy from the sun and transferring it to the fluid which circulates inside the pipes of the collector. The collectors can effectively act as a heat exchanger where the energy captured from the sun can be transferred either for water heating or for direct space heating. The solar collectors can be classified as non-concentrating and concentrating collectors and their implication is selected based on the temperature requirement of the system. The main difference among the two types of collectors is the size of area of the interceptor and the absorber [39]. The interceptor or otherwise called the aperture area is the area where solar radiation enters the collector [40]. In a concentrating collector the interceptor area is higher than the absorber area whereas in the non-concentrating both interceptor and absorber have the same area. Based on that, the two types of collectors can achieve different temperature outputs with the concentrating and non-concentrating collector reaching temperatures of 400 °C and 100 °C respectively [41]. For domestic applications which is the main scope of this project the most appropriate solar thermal collectors are the non-concentrating one due to the temperatures they can achieve and hence the following section focuses on the different types of non-concentrating collectors.

2.3.1.2.1 Flat plate collectors

Flat plate solar collectors are one of the most widely used solar thermal systems and can achieve a heat temperature output in the range from 30 °C to 80 °C with the potential in some newer type of collectors reaching a higher temperature close to 100 °C [42]. The picture on figure 12 represents a labeled schematic of a typical flat plate collector including the different components.

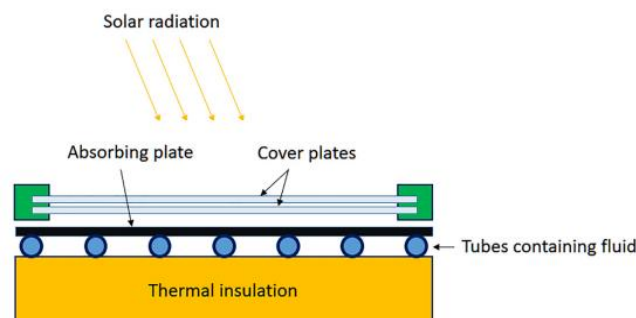


Figure 12: Flat plate collector system schematic and component configuration [43].

When solar radiation is incident to the surface of the collector, it is absorbed by the absorbing plate which is a dark surface. The role of the absorbing plate is to convert the solar radiation from the sun into thermal energy. This amount of energy is then transferred to the fluid flowing through the tubes that are attached to the absorbing plate. For the heat transfer mechanism to take place, suitable materials with relatively high thermal conductivity such as copper or steel which are painted in a dark colour, are used to make the absorption plate and the tubes. Above the absorbing plate there are some cover plates which usually are made from glass and their main function is to allow the high frequency solar radiation to reach the surface of the absorbing plate and to prevent the thermal radiation of low frequency from the absorbing plate escaping. In addition, it forbids any cool air to interfere with the absorbing plate that would result in the reduction of the performance of the collector. Lastly to enhance the performance and avoid heat loss, an insulating material which can be either mineral wool or fiberglass is placed around the absorbing plate.

2.3.1.2.2 Evacuated tube collectors

Evacuated tube solar thermal collectors are another technological achievement since it was developed based on the main disadvantage of flat plate collectors. In fact, the position of the flat plate collectors and as the name suggests ‘flat’, affects the overall efficiency of the collector since maximum efficiency can only be achieved when the sun rays are perpendicular to the collector and this effect only occurs during midday. Therefore, in 1965 an engineer called Speyer introduced to the market the first development of an evacuated tube collector [44]. The schematic below represents a simple representation of an evacuated tube collector with its main components.

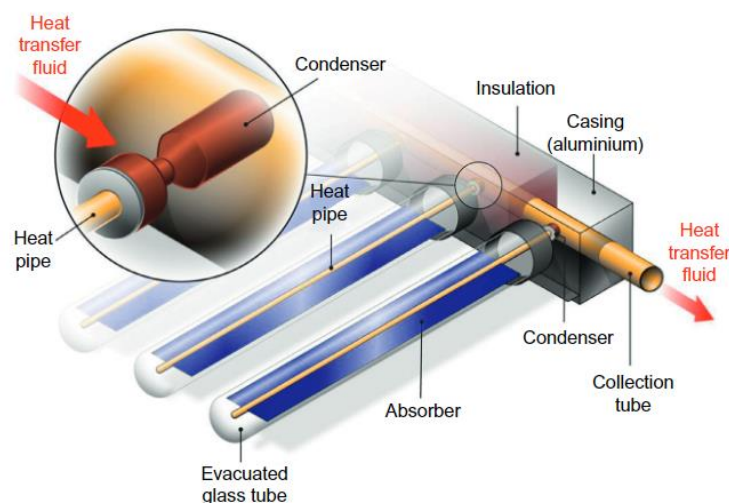


Figure 13: Evacuated tube collector system schematic and components configuration [45].

As seen from the schematic, the collector has several parallel rows which are called evacuated glass tubes and they are made from a transparent material usually glass and they are all connected to a primary perpendicular header tube. The evacuated glass tubes have a cylindrical shape and that's the main difference from the flat plate collector and therefore the solar radiation reaching the surface of the tubes is always perpendicular enhancing the overall system performance. In addition, another main difference between the two collectors is that in the evacuated tube collector, the water in the pipe is not heated directly. The tubes are enclosed in a thick glass tube where air is being removed forming a vacuum space. The vacuum space can effectively act as an insulator minimizing heat losses through convection and radiation and hence it enhances the efficiency of the collector. Based on that, the tube collectors are able to generate higher thermal temperatures in the fluid flowing inside. From the diagram it can also be seen that there is a fin attached to the heat pipe which is called an absorber plate and usually it is manufactured from copper or steel. The role of this fin is to absorb the thermal energy from the evacuated tube and transfer it to the heat pipe. Lastly, evacuated tube collectors have the ability to extract energy from the ambient air surrounding the tube and thus the operation of such a collector is not limited to only the times when there is direct sunlight.

2.3.1.3 Thermal efficiency of solar thermal collectors

Thermal efficiency of a solar collector is a very important parameter in evaluating the system performance. It is described as the ratio of the useful energy that can be extracted from the fluid passing through the heat pipes over the total solar energy incident directly on the surface of the collector. The solar radiation incident on the collector consists of both beam and diffuse solar radiation and need to be considered in addition with the ambient and inlet fluid temperature to be able to assess the thermal performance of the collector according to ASHRAE standards 93. The following table represents the performance characteristics of the two different collectors describes above.

Table 2: Operational characteristics of flat plate and evacuated tube collectors [46]

Collector type	Conversion factor	Thermal loss factor [kW/m ² °C]	Operating Temperature Difference [°C]
<i>Flat Plate Collector</i>	0.66-0.83	2.9-5.3	20-80
<i>Evacuated Tube Collector</i>	0.62-0.84	0.7-2.0	50-120

From the data represented above it's obvious that evacuated tube collectors have a higher performance than flat plate collectors since they have a lower thermal loss factor with a wider range of operating temperature.

2.3.2 SAHP system configuration

The coupling of any solar thermal collector/evaporator to any heat pump system integrating it to a SAHP, is a crucial step since based on the system configuration, the overall system efficiency can vary. For that reason, there are two main categories that SAHP are classified to, as being the direct and indirect expansion and are described briefly below. The hierarchy tree in figure 13 below, represents the full classification of SAHP system.

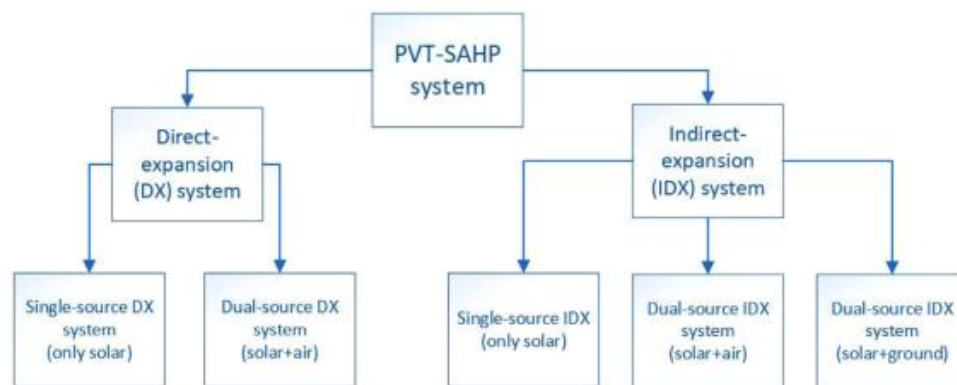


Figure 14: Different system configurations of SAHP systems.

2.3.2.1 Direct expansion

Direct expansion SAHP (DX-SAHP), was the earliest design of SAHP system which was proposed by Sporn and Ambrose in the early fifty's, with their aim to expand the technology of solar thermal system with the coupling to a heat pump system [47]. In a DX-SAHP, one of the two types of solar thermal collectors described above were integrated to replace the evaporator of a normal heat pump system and perform the same task. The main role of the collector-evaporator is to vaporise the working fluid passing through the collector by transferring the solar energy captured. The following figure represents the schematic of a typical ASHP and DX-SAHP.

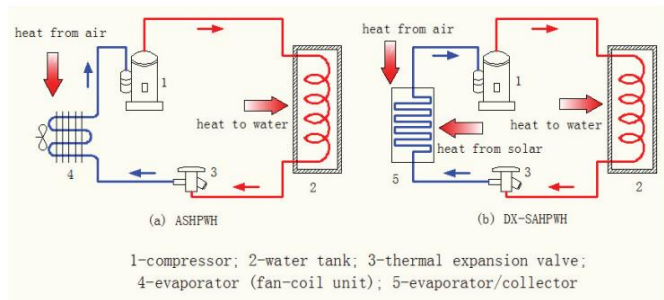


Figure 15: System configuration difference of ASHP and DX-SAHP[48].

AS it can be seen from the figure above the two cycles have the same principle of operation since they both function based on the vapour compression cycle with the only difference being the heat source. The ASHP uses the ambient air as a heat source whereas the DX-SAHP uses solar energy. Based on literature the system performance of the DX-SAHP will be better, since the evaporating temperature will be higher [49-51].

Extended research on DX-SAHP have shown that the performance is highly affected by the solar radiation at the specific time, since the working fluid passes directly through the collectors [52]. Due to the limitations of such a system, an engineer draw his attention on how to overcome the high dependence on solar radiation by designing a newer type of system called indirect expansion SAHP (IDX-SAHP) which is described in the next section.

2.3.2.2 Indirect expansion

The main difference between a DX-SAHP and an IDX-SAHP is the presents of a type of a heat exchanger which in most cases is a water tank. This type of system configuration is further broken done into three different categories: the serial system, a parallel system and a more complicated one, the complex system. The figure below represents the three categories system schematic diagram.

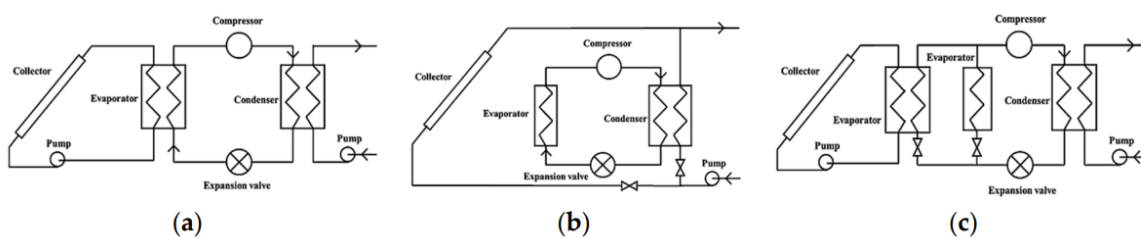


Figure 16: (a)Serial;(b) Parallel; and (c)Complex configurations [53]

In the series system configuration, the solar thermal collectors are connected in series with the heat pump evaporator and hence the heat source of the evaporator is supplied from the solar thermal collectors. The only disadvantage of such a system is that it is heavily depended on the solar radiation incident on the collector. The parallel system came in to play, to mitigate this by connecting the evaporator of the heat pump in parallel with the solar thermal collectors. By doing so the two system can be described as independent and therefore both can assist the heating demands of the application that the system was designed for. The parallel system's main advantage is that at times when solar radiation is high the heat pump system could stop operation and the heating supply will be, primarily maintained from the collectors. As a result, no need to consume electrical power to drive the compressor, hence enabling a higher COP for the system. In addition, the complex system is different from the two other categories described before since it can have two heat sources enabling the replenishment of each other at times when the first heat source overcome the other. To sum up, the most widely used system for any domestic heating system is the parallel system and according to literature it accounts for almost 60% of the market [54].

2.3.3 Renewable electrical power generation

One of the most rapidly expanding renewable power generation technology in the domestic sector, is the utilisation of the energy from the sun by converting it to electrical power with the use of solar photovoltaic panels. According to Statista the total worldwide installed capacity in 2019 was 633.7 GW with a rapid percentage increase of 22% in 2020 resulting to an installed capacity of 773.2 GW [55]. In addition, from an analysis performed by the IEA, it was estimated that the annual additions of installed capacity in the residential sector are supposed to accelerate rapidly due to the implementation cost reduction and the enhancement and support from the governments incentive schemes. In fact, the annual installations in the residential sector for 2021 were found to be 15GW and by the end of 2022 it is expected that there will a 28.5% increase reaching a value of 21GW [56]. From the statistics presented above, it is obvious from its market penetration that photovoltaics will be the dominant technology going forward.

2.3.3.1 Mode of operation of solar cells

The technology dates back to 1839 when Edmond Becquerel who was a physicist discovered the so-called photovoltaic effect which is a process that generates voltage or a current when subject to light [57]. The photovoltaic effect is the process that take place inside a solar panel, and this is how the cells can convert light from the sun to electrical voltage.

The solar cells which are found in a solar panel are manufactured from two specific semiconducting materials which are the p-type and the n-type respectively and together they form the p-n junction as shown in figure 16. When the two semiconducting materials are joined together, an electric field is generated due to the charge difference of the two materials. The electrons from the n-type material move towards

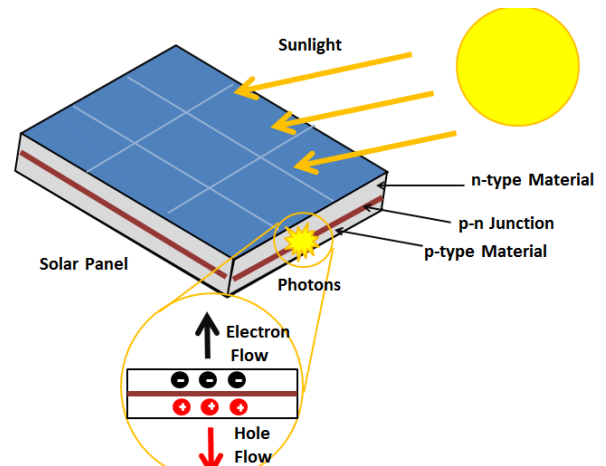


Figure 17: Photovoltaic effect on solar cell [58].

the p-type material and the electron holes move to the n-type material. This movement of the charge particles (electrons and electron holes) creates an electric field. The duty of the sun plays a crucial role in initiating this movement of electrons. In more depth, the solar energy from the sun consists of photons which when incident on the surface of the solar cell, they cause the excitation of electrons from the atoms of the semiconducting material. This process makes the electrons to jump in a higher energy level which according to the wavelength of the incident ray, the higher the excitation which result to greater amount of energy generated [59].

2.3.3.2 Importance of semi-conducting materials

The efficiency of the photovoltaic solar cells is heavily related to the band gap which is determined by the material properties. Conductors, semi-conductors, and insulators each one has it is own equivalent band gap with their corresponding benefits and limitations. For example, insulators have a very large energy band gap between the valence and conduction band which implies that a big amount of energy will be required to excite the electrons and according to literature the photons incident on the surface do not contain this amount. On the other hand, semi-conductor has a band gap which is much less than the insulators. As a result, the incident photons can effectively excite the electrons making the generation of electricity achievable. Moreover, when considering conductors, there is no band gap between the valence

and the conduction band, there is just the conduction band. As previously stated, for the photovoltaic cells to be able to generate electricity (flow of electrons), an electric field should be induced which can only be formed when semi-conducting materials are combined to form the p-n junction. Inside the p-n junction the electrons and the electron holes attempt to blend together but with the existence of the electric field they can't, and hence the constant flow of electrons can generate electricity. Finally, conductors and insulators do not form an equivalent p-n junction hence no electric field, which suggests that these types of materials cannot be used for the manufacturing of PV cells.

2.3.3.3 Solar PV cell types

In the previous chapter, it was briefly outline that the material to be used in the manufacturing of solar cells should be a semi-conductor and thus the most widely used is silicon which is non-toxic and relatively cheap since it's the 2nd most abundant element found in the earth's crust [60]. In the market, there are three main categories of PV cell types, and these include the monocrystalline silicon, the polycrystalline silicon and the thin film. Figure 17 to the right represents the three different types of PV cells.

The monocrystalline cells are the most efficient cells from the 3 types, and their solar cells are manufactured from single crystalline silicon and as result the cells composition is purer since they are cut from a single piece of silicon. In addition, they can perform better even when the operating conditions are not ideal, and they can produce

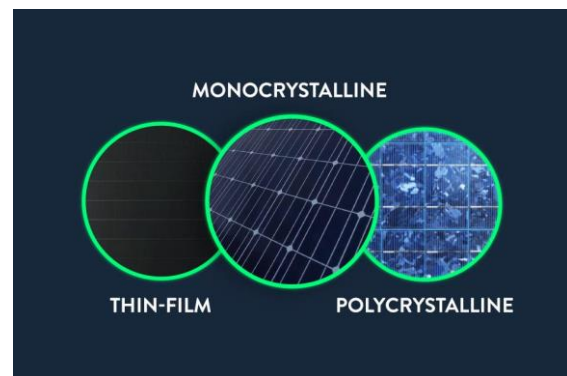


Figure 18: Solar PV cell types solar [61].

almost the same output voltage. The polycrystalline cells are the initial type of cells invented at the beginning of solar capture technology and thus their efficiencies are not so good. The major difference between the two that directly affects their performance is the manufacturing method. The monocrystalline cells are extruded as a single pure ingot whereas the polycrystalline cells are formed by the formation of cubes from melting the fragments in an oven and then cutting them into very thin wafers [62]. On the other hand, thin film solar cells are composed from micron-thick photon-absorbing material such as cadmium telluride, which is placed above a specific substrate and can be polymer materials with a multilayer

configuration [63]. The following table summarises some of the key performance indicators of the three PV cells described above.

Table 3: Operational parameters of the three types of PV cells.

PV CELL TYPE	EFFICIENCY [%]	RATED OUTPUT [W]
Monocrystalline	20	275-400
Polycrystalline	13 -16	320-375
Thin film	4-12	250

2.3.3.4 Solar PV system configurations

The way of connecting a PV system with different power sources, is a crucial aspect to be considered at the beginning of the design. The system components and their configuration should be established based on the functionality and the operational specification of the system to be implemented. In real life applications there are different types of PV system configurations that can be operated both as standalone systems or grid-connected. The following schematic in figure 18 represents the different PV system divisions.

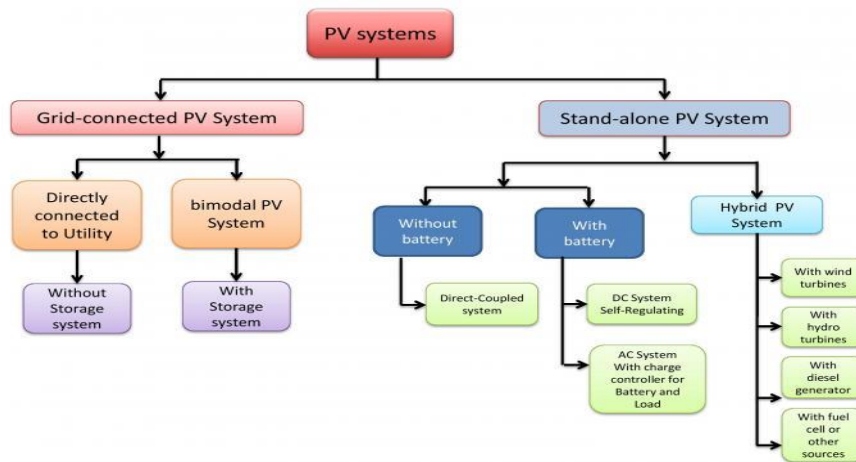


Figure 19: Classification of solar PV system types [64].

3.0 System Design Methodology

The system design and implementation of any sustainable heating system for domestic applications is a complicated procedure that requires a correct strategical approach for the system to be fully functionable and for it to operate at maximum efficiency. A multifaceted engineering design approach using engineering tools and software simulation packages should be evaluated at the beginning of the project. Therefore, the generation of a project methodology was a crucial step for this thesis, as it can act as a guidance for other engineers who deal with similar designs in the field of sustainable heating systems for domestic applications. The following figure represents the main steps undertaken to execute the scope of the project.



The first section of this thesis introduced a thorough literature review on all aspects concerning heat pump systems and their operation in addition with a brief overview on how to enhance their performance by coupling them with photovoltaic and solar thermal collectors. In addition, to assure that the proposed system design is suitable, an experimental analysis using simulation software will be carried out, to assess the system at different stages in order to deduce the final

one with the maximum efficiency. Therefore, software evaluation is critical step in the design approach and hence reference from online journals will be used as a guidance for the correct selection of engineering software package.

3.1 Software Assessment and Selection

The technical specifications of any new system design are the most important aspects that need to be assessed and evaluated carefully before actually implementing the design. This can also be supported from various engineering software packages that help with simulating the performance of the proposed system. Therefore, the proper selection of software will lead to more accurate and reliable results and that's the main reason why this process should be carried at the beginning of the design stage.

The performance of the air source heat pump can be assessed using various modelling software which were designed to simulate heating systems like the proposed one. An example of such a software is Geo T*SOL which was developed by a company called Valentin Software based in Germany [65]. It is a comprehensible software, that can effectively be used for the design and modelling of the performance of any heat pump system. It also has the ability to integrate heat pump systems with solar thermal systems and after a dynamic simulation of a minute interval is run, results such as electrical consumption, heat losses, COP and SPF can be established. In addition, a more sophisticated and advanced software is energyPro which was developed by EMD International and can analyse complex energy systems that combine both electrical power and thermal energy [66]. The main advantage of energyPro over Geo T*SOL is the fact that it can automatically generate both technical and economic reports providing a comprehensive overview of the system to be modelled. From the short description outlined above, it was concluded that for the scope of this project a combination of the modelling tools will be used to analyse the performance of the heat pump system.

From the literature review it was briefly discussed how the overall heat pump system performance can be enhanced by introducing renewable sources such a photovoltaic module to produce electricity and solar assisted thermal systems for harnessing the energy from the sun and transferring it to water that can be directly used as hot water for use or space heating. Therefore, a variety of engineering simulation tools can be used to evaluate the performance of these types of systems and thus provide a reliable estimation of their contribution to the overall heating system. The globally used PV simulation package is PV_{SYST} which can be effectively used for array sizing, simulating results and analysing system performance [67].

The software has built-in a Meteo Database which contains data gathered from online meteorological sources. The main advantage of PVsyst over other available software package is that it's an open-source software that can effectively be used for the exact system sizing whereas other software such as HelioScope can only simulate and estimate the electricity generation. HelioScope is a simpler software that takes advantage of satellite data from Google Maps and all the weather data associated with the specific location chosen in order to be able to model the photovoltaic modules energy generation. In addition, ESP-r which was selected as the whole building energy simulation program to estimate heating demands, can also be used for analysing the potential of renewable power generation providing more robust results since it considers more aspects such as thermal heat gains and moisture content from air. Finally, PV*Sol is another online modelling software for photovoltaic systems assessment that could be used, since it includes a detailed shading analysis which the pre-mentioned software does not.

Being able to match the supply with demand is crucial step in the design process of the proposed heating system. The total electrical power generation from the photovoltaics should be compared to the heat pump electrical demand to be able to draw valid conclusions of the reliability of the system. The same thing occurs when trying to integrate a thermal energy storage to the system to identify the amount of energy that can be covered from the store rather than consuming electrical power to produce energy. For supply and demand matching assessment, there are a few software packages available which include energyPro. EnergyPro which was discussed above, it can generate technical reports with graphical representation on the performance of the system including systems that cover both the supply and demand. Therefore, an in-depth investigation can be performed in order to optimize the system components size and capacity so that the final results could be reliable, and the final system will be operating at maximum efficiency. The graph on figure 19 represents an example of a supply and demand match graph generated using energyPro, for a heating system.

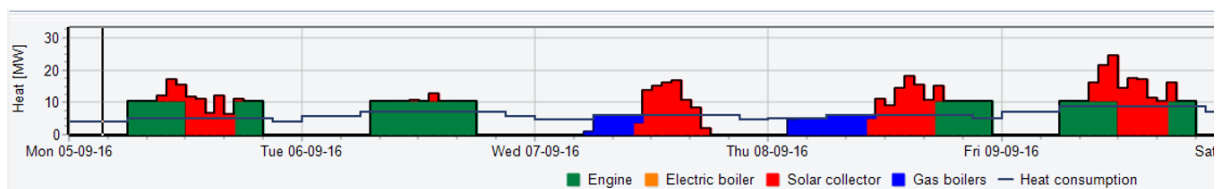


Figure 20: Example of supply and demand matching graph modelled in energyPro [68].

4.0 Case Study Description: Cyprus

For this project, an island in the Mediterranean Sea called Cyprus, was selected as the location to design a sustainable domestic heating system since its primary source of energy for domestic heating comes from fossil fuels which release greenhouse emissions when burned. According to World Population Review, Cyprus has a population of 1.2 million and an estimate projected Gross Domestic Product for 2022 of 24.8 billion USD [69-70]. Cyprus is the third largest island in the Mediterranean Sea, and it is found on the north-east hemisphere with longitude and latitude coordinates of 33.2E and 35.1N respectively covering around 9,250 km² of land [71]. The following figure represents the map of Cyprus with the main cities annotated on it.



Figure 20: Cyprus map with main cities annotated on it [72].

4.1 Climate

4.1.1 Temperature

Cyprus due to its geographical location which is close to equator it has a Mediterranean climate with long hot and dry summers that begin from May until September, and mild cool rainy winters from November till February. The following graph demonstrates the average maximum and minimum temperatures recorded per month from a 20-year period analysed by the Meteorological Service of the island.

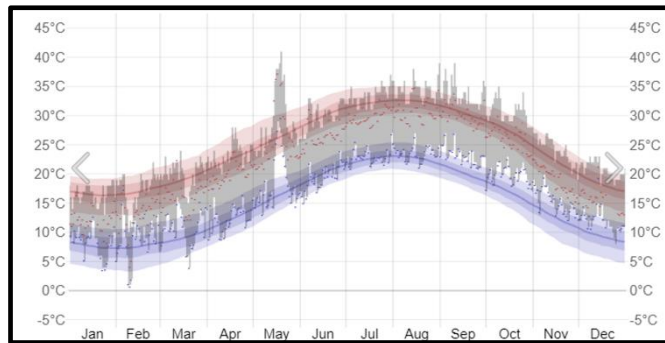


Figure 21: Average outdoor temperature for a yearly period [73].

It is very important to evaluate the thermal properties of the heat source when designing a heat pump system in order to be able to assess the suitability and performance of the designed space and water heating systems. From the graph above it can be clearly seen that during the winter period the average temperature ranges from 7 to 9 °C. According to the COP of a heat pump, it will result to a higher efficiency since the temperature difference (evaporator and condenser) will be lower than other countries with colder winters and lower outside temperatures.

4.1.2 Solar radiation

Another parameter which is of great importance for the Republic of Cyprus, is the daily amounts of solar radiation that it receives. Solar radiation in Cyprus, is the indigenous main natural source of energy and according to the Meteorological Service it receives a daily global horizontal radiation of around 5.4 kWh/m² with average hours of sunshine ranging from 5.5 to 12.5 per day in winter and summer respectively [74]. The two figures below represent the solar radiation map of Cyprus with a graph summarising the average daily solar radiation per month.

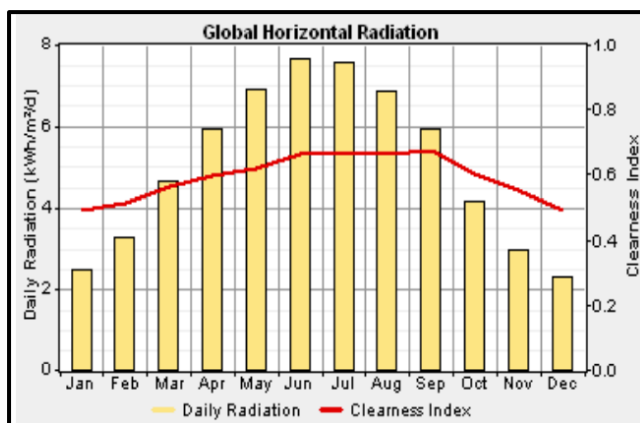


Figure 23: Average monthly solar radiation [75].

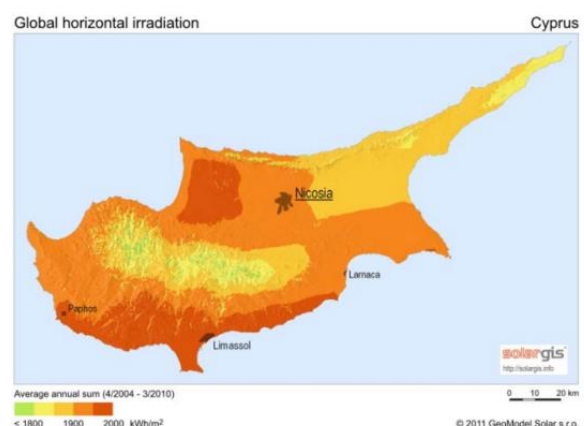


Figure 22: Cyprus solar radiation distribution map [76].

From the graph above it can be deduced that the average solar radiation in the winter period, which is the point of interest of this project, varies from 2.3 to 3.4 kWh/m² with an average clearness index of 0.5. Moreover, the global horizontal radiation reaching the surface of the

earth can be split into direct and diffuse solar radiation and a graph representing the seasonal variation based on data from the Meteorological Agency are represent in figure 24.

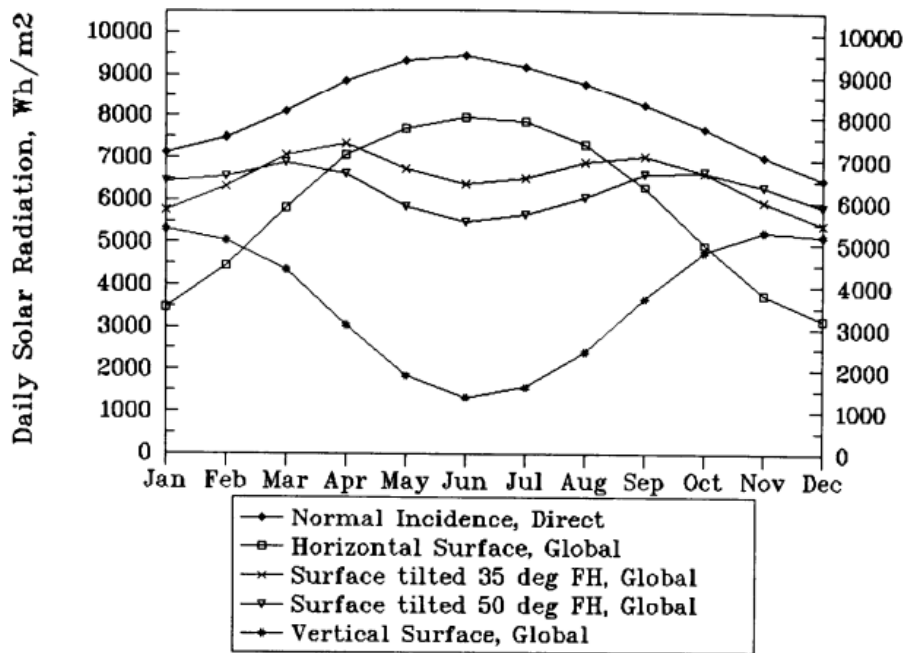


Figure24:Seasonal variation of solar radiation in Cyprus [77].

From the results surprisingly, during the winter period which as expected the energy consumption for heating purposes is at a higher value, the amount of normal incident direct solar radiation is much higher than the summer month. This makes solar radiation a suitable renewable source to introduce to heat pump system since it can be harnessed for two main functions: 1) heating water for use in space heating system and DHW and 2) in the renewable energy production for electrical power supply for the heat pump device. As a result, less amount of electricity will be needed to be drawn from the national grid to raise the temperature of the water, and hence making a more sustainable heating system since it will be primarily based on the energy from the sun.

4.2 Energy provider

The main energy providers on the island are the Electricity Authority of Cyprus (EAC) which supply electrical power and other oil companies that provide fuels for both transport and heating. From a statistical analysis performed by Our World in Data it was concluded that the main source of energy for consumption was oil reaching a percentage of 92.90% in 2020 [78].

4.3 Housing Stock in Cyprus

The domestic housing sector in Cyprus consist of different types of buildings and they are described as follows:

- Single house
- Semidetached or duplex
- Row house
- Backyard house
- Multi-family apartment blocks

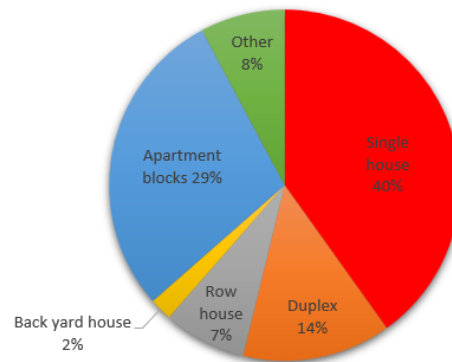


Figure 25: Classification of housing types in Cyprus.

The pie chart on figure 25 was able to be deduced from the data gathered from the Statistical Service of Cyprus in order to identify the percentage of population living in each specific classification of housing. From the results, it was found out that the majority of the people are living in single house and apartment blocks with percentages of 40 and 29 % respectively. Therefore, for the scope of this project the focus will be primarily based on the single house category since it has the highest percentage and hence a bigger contribution to the heating consumption of the country.

4.4 Current Heating Systems

The current heating systems on the island vary from central heating systems using underfloor heating or radiators which are mainly powered from boilers that consume either kerosene or natural gas (LPG), up to storage heaters. By gathering information from the CENSUS of Population and Housing that was conducted in 2021, the graph in figure 26 representing the existing heating systems and their percentage coverage for a single housing classification was able to be produced. Each colour on the bar chart represents a different source of energy as per the key at the top of the graph.

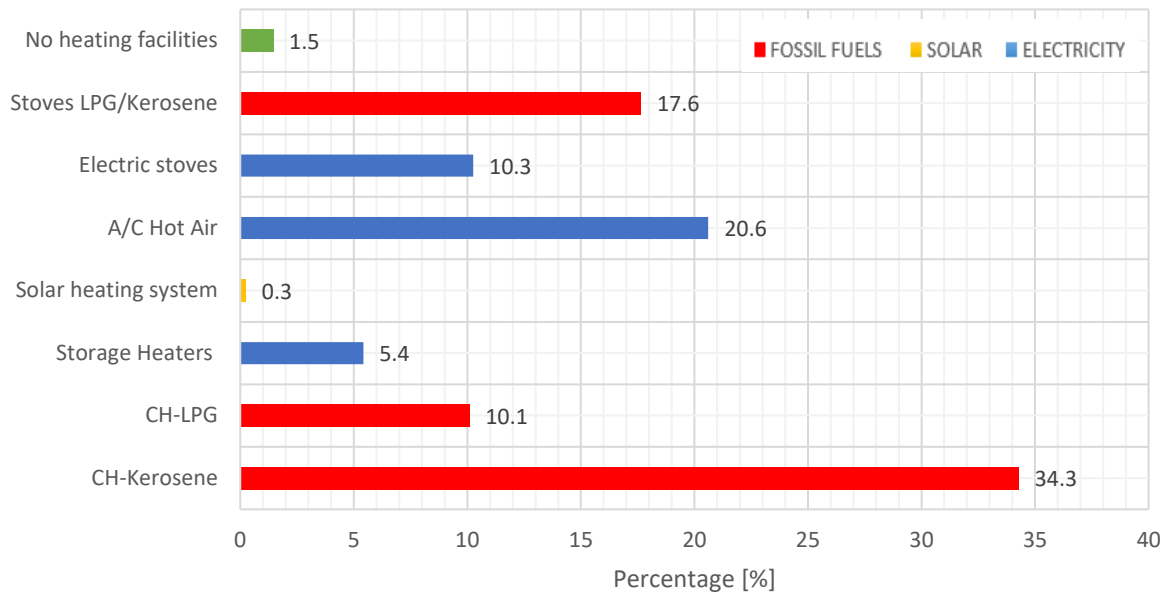


Figure 26: Types of domestic heating in Cyprus.

From figure 28 above it can be concluded that the predominant type of single housing heating consumption is met by systems that consume fossil fuels as their main source of energy. In addition, there are systems that consume electrical power in providing the space heating conditioning which according to literature they are less efficient which consequently mean higher consumption of electricity. It's worth mentioning that the only electricity provider on the island is EAC, which their main source of energy for the production of electricity is heavy fuel oil and since Cyprus has no primary sources of energy, it is entirely imported [79]. As a result, the electrical power drawn from the grid it cannot be characterised as green energy.

Furthermore, the percentage of single type houses, that uses solar energy as their source of energy for heating, is very low and in fact it does not even reach 1%. In the previous section regarding solar energy, it was briefly outlined that: energy from the sun is the most promising source to be utilised in a future sustainable heating system since according to research papers Cyprus is the top list of the countries in the world that receives the highest amount of solar radiation. Therefore, based on the poor performance of the current heating systems on the island and the heavy reliance on fossil fuels for the production of heat, Cyprus and especial the capital, Nicosia, was chosen as the case study to analyse and propose a more sustainable heating system.

4.5 Site Selection

The overall scope of this project was to design and assess the performance of a sustainable heating system for a residential building in Cyprus, that uses fossil fuels as its main source of energy to provide space heating. Therefore, the first step was to choose a specific residential building on the island, to analyse and generate results. In the Greek-Cypriot site of the country there are mainly five cities which are Nicosia, Limassol, Larnaca, Paphos, and Famagusta. The building selected to perform the analysis was chosen based on several factors such as the accessibility of data, background knowledge and ability for site visits. After taking into consideration all the important factors, a single-story family residential building located in Nicosia, the capital of the island, has been selected as the feasibility study of this project. The building location and outside appearance are shown in figure 28 and 27 below.



Figure 28: Building outside appearance.



Figure 27: Building location on map.

The building is a double story house with kitchen and living room at the ground level, and 4 main bedrooms at the first floor. It has a total floor area of 383.05 m², and all the floor plans and elevations can be found in the Appendix 2. The house was built in 2012 and the construction was complete based on the building regulations and standards of the country. A sample of the composition of the walls and configuration of the windows with their corresponding values can also be found in the Appendix 3, gathered from the energy performance certificated (EPC) of the building.

5.0 Existing heating system

The current heating system in the building consist of a central heating system powered from oil in a condensing boiler configuration. The system has a capacity of 28 kW and the thermal energy produced from the boiler it is being transfer to the inside of the building through

underfloor heating. The picture below represents the plant room of the house with the boiler and connections installed.



Figure 29: Oil condensing boiler and equipment.

Since the main source of energy for the boiler is oil, there are greenhouse emissions associated with it and hence the importance of replacing the current one with a more sustainable.

5.1 Heating Demands

5.1.1 Space Heating

The heating demands of the house including both space heating and domestic hot water were the predominant source of data gathered from the EPC. As it can be seen from the graph in figure 30 the heating demands are divided into monthly periods according to the data provided by the EPC which can be found in the appendix 1.

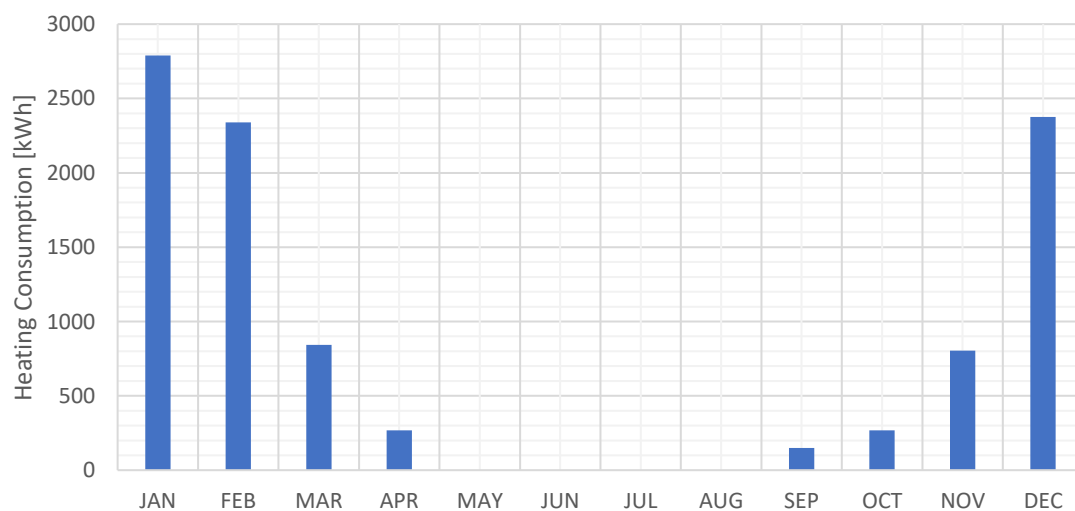


Figure 30: Estimated annual space heating demands as per EPC.

As it can be seen from the chart, the higher heating demand occurs between December and February which was as expect since, during the winter period, the outdoor temperature drops significantly.

From the EPC, the data were divided in monthly time steps with the limitation of not providing an in depth into daily and hourly trends and data, introducing an inaccuracy and unreliability to the system design sizing and capacity. Therefore, to generate more accurate results for the designed system an energy management software was used to provide a reasonable approximation of the hourly heating demands in one year period. One of this type of tools include the ESP-r software, which was developed by the University of Strathclyde and can effectively model different functions that consume energy in a building including things like heating, cooling, and electricity demand. In addition, the software is capable in simulating results in one-minute timestep which increases the reliability even further and hence making it suitable for generating the specific energy profiles needed.

Model Geometry

The model geometry was constructed based on dimensions from the floorplans and elevations of the building, which can be found in the appendix 2. The model geometry constructed is shown in figure 31.

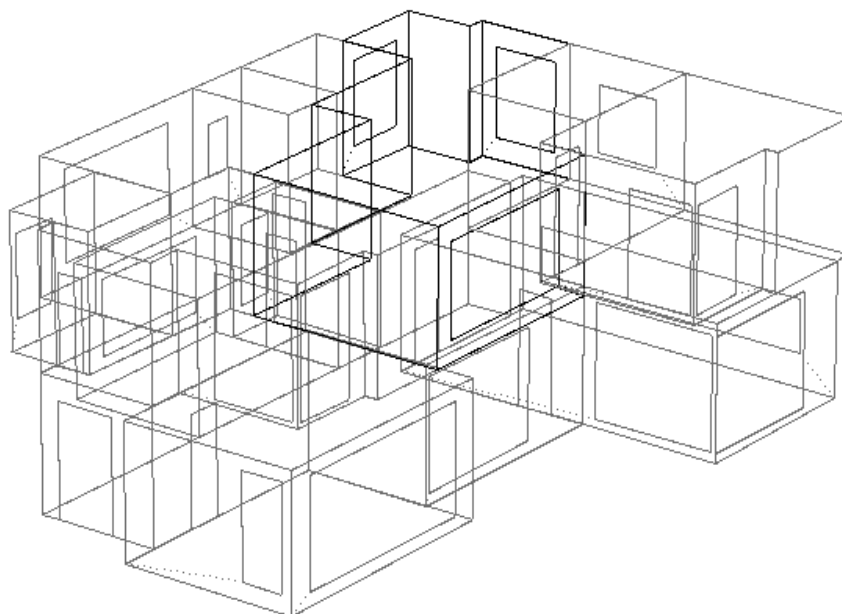


Figure 31: Building model geometry.

The building geometry has a total floor area of 383.05m² and it was divided into 13 thermal zones in order to be able to model and simulate the heating demand of the building in 1 minute time step. The materials and layer composition of the constructions used in the model were assigned as per the tables given from the EPC and from a site visit. Lastly the operational parameters such as infiltration, ventilation, heat gains and heating set points were set as per the Building Regulations of Cyprus and European standards. After assigning the model correctly, the simulation was run in one minute time step, in order to deduce the annual heating demand as it can be seen from the graph in figure 32.

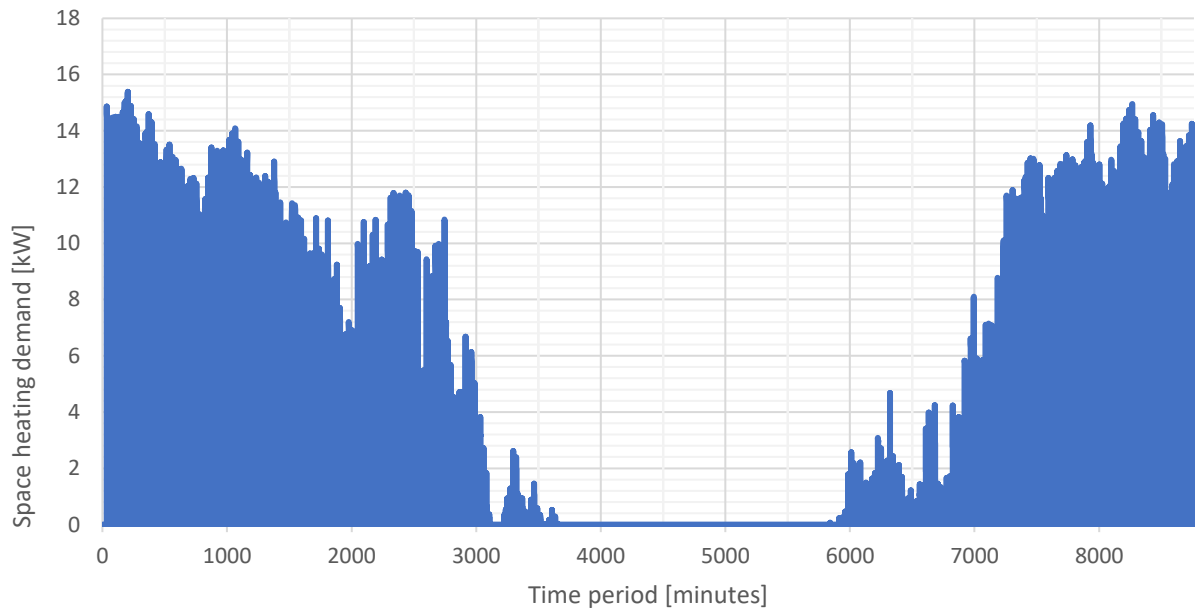


Figure 32: Estimated annual space heating demand profile from ESP-r.

From the results represented on the graph above, it was identified that the highest space heating demand occurred in January the 8th, with the daily profile of that period shown in figure 33.

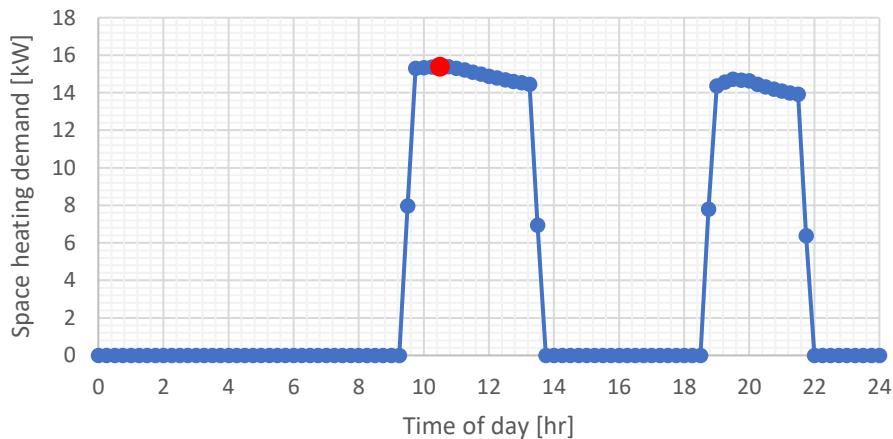


Figure 33: Daily space heating demand profile for the 8th of January.

From the data provided by the EPC of the building the following monthly hot water demand was established as shown in figure 35.



Figure 35: Monthly direct hot water demand from EPC

From the results gathered from the EPC, it was found out that the highest demand occurred during the months of December until March, and that was as expected since, the outside temperature drops significantly. To be able to obtain more accurate results regarding the hourly hot water demand, a probabilistic analysis was performed using reference from literature. According to Papakostas and Papageorgiou analysis, they identified the average hourly and daily hot water demand patterns based on data collected from a sample of 210 houses in Athens, the capital of Greece [82]. From their analysis they were able to calculate a specific probability (%) of the total daily demand for every hour in a single day. Their findings are shown in figure 36 below and they were used as a guidance to accurately deduce the hourly hot water demand of the current building.

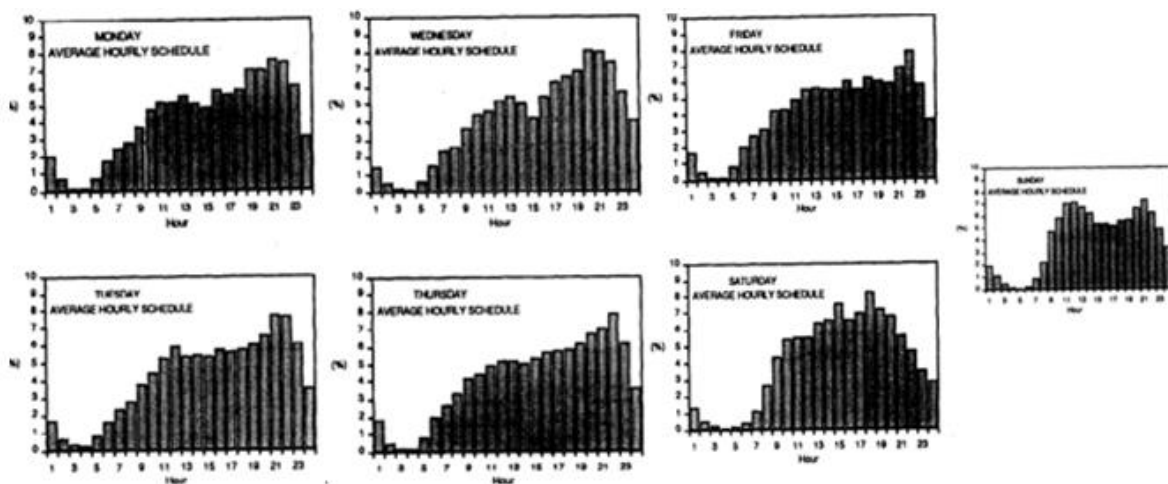


Figure 36: Hourly probability percentage for domestic hot water demand [82].

In addition, to the hourly probability of hot water demand, a seasonal variation factor according to the government’s Standard Assessment Procedure for Energy Rating of Dwellings as shown on table 4 was also applied to the model to be able to accurately estimate the hourly DHW demands.

Table 4: Seasonal variation factor of domestic hot water demand [82].

Month	JAN	FEB	MAR	APR	MAY	JUN	JUL	AUG	SEP	OCT	NOV	DEC
Variation Factor	1.10	1.06	1.02	0.98	0.94	0.90	0.90	0.94	0.98	1.02	1.06	1.10

All the data were processed using MATLAB and Excel software and the results for the hourly direct hot water demand are represented by the energy profile in figure 37.

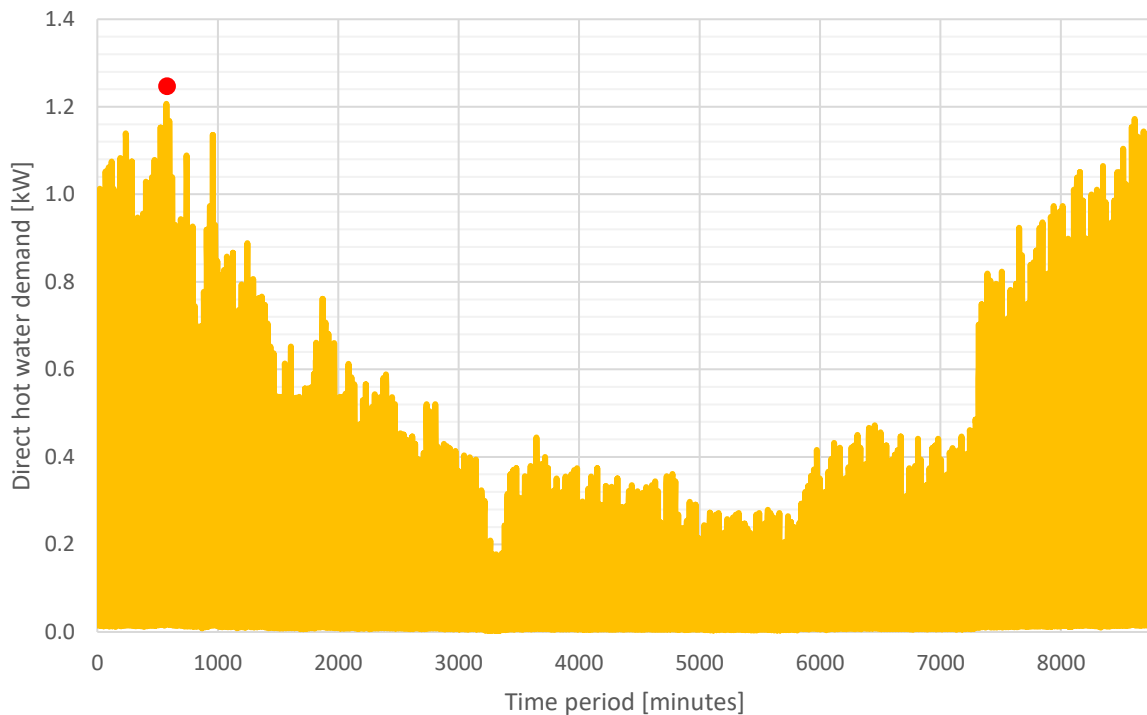


Figure 37: Estimated hourly heating demand profile for domestic hot water.

5.1.3 Overall estimate heating demands

The final total annual heating demand for space heating and direct hot water was calculated by combining the two graphs in figures 31 and 36 respectively into a single annual energy profile as shown in figure 38 below.

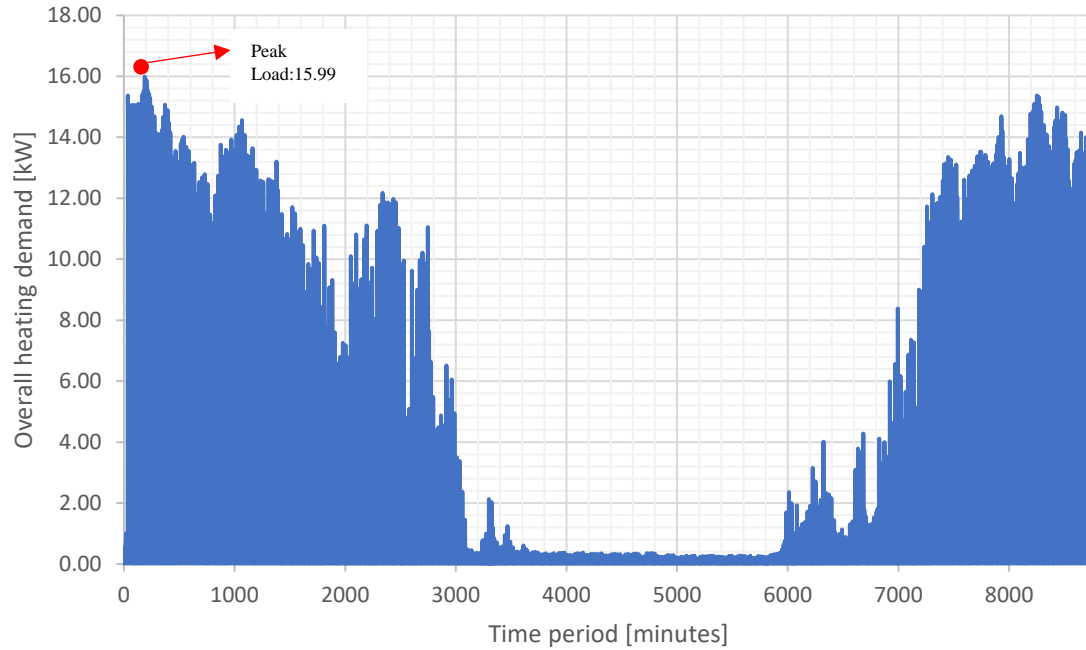


Figure 38: Combined heating demand profile for both space heating and DHW

From the graph above, the hourly peak demand of 15.99 kW was recorded occurring on the 8th of January. The peak value found was then used to accurately identify the capacity of the heat pump that can effectively supply the building with heat at the highest maximum efficiency. Incorrectly sizing a heat pump by oversizing or under sizing the heat pumps capacity can result to a minimized operating performance. Hence the methodology described above in identifying the hourly demands was a crucial step in the methodological approach of the project since it enhanced the system reliability and accuracy.

6.0 System Technology Design

The purpose of the project was to design a sustainable heating system that can mainly cover the heating demands of the site selected and thus become suitable in replacing the current oil condensing boiler which releases greenhouse gasses when it is operating. Hence to properly selected the appropriate heat pump system, an analysis on the current energy performance of the building was performed as shown in section five above, to be able to establish the daily heating demands. The current heating distribution inside the house is maintained by circulating water through circuit loops which are found underneath the finished floor (underfloor heating). Therefore, the heat pump system chosen to evaluate its performance and suitability was an air to water heat pump system that can provide both space heating and direct hot water for domestic use. In addition to enhance the overall performance of the system a thermal energy storage tank was incorporated to account for the daily peak loads. From the literature section of this report,

it was identified that by assisting any heat pump system with a solar thermal system can increase the overall performance. Hence the system was updated with a solar thermal collector and an extra buffer tank in which both can effectively raise the temperature of the water before entering the heat pump system. Lastly as of their nature heat pumps require electrical power to drive the compressor and this amount of energy is usually consumed from the grid. The production of electricity in Cyprus as previously stated comes from fossil fuels which are not a clean form of energy, hence the implementation of photovoltaic modules was another essential technology that was considered when designing the proposed system. By doing so most of the electrical power consumed by the heat pump will be generated from the PV module resulting to zero CO₂ emissions.

The proposed system schematic with its main components and system configuration is shown in figure 39 below.

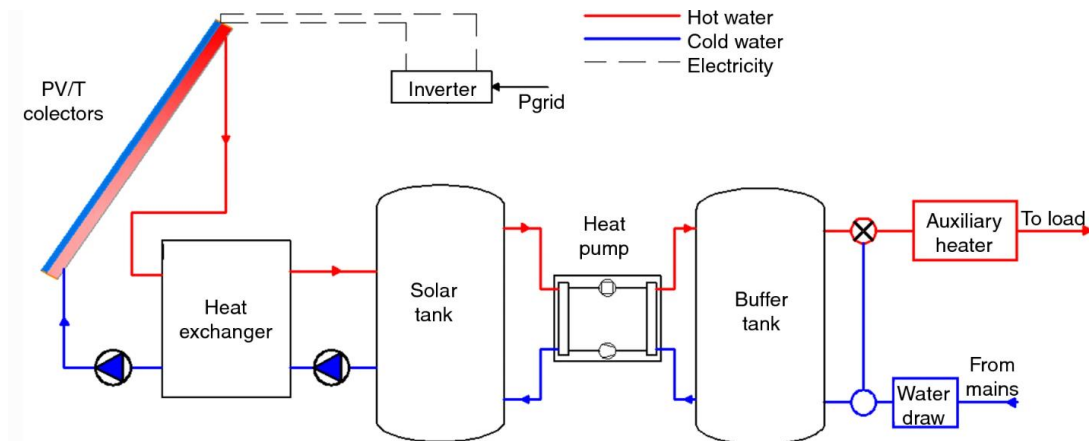


Figure 39: Sustainable heating system schematic and component configuration [83].

The solar thermal collector shown in the diagram is responsible for capturing the energy from the sun and transferring it to the water which circulates in the system. The hot water is then transferred to the solar tank which acts as a thermal store and thus it can supply the heat pump system with water at higher temperature resulting to maximum efficiency. The heat pump system is also connected to a PV module where energy from the sun is converted to electricity through the use of an inverter. To validate the performance of the proposed system, individual analysis and modelling simulation were carried out to estimate the overall performance of the complete system.

6.1 System Capacity

The system capacity was estimated based on the peak hourly heating demand deduced when space heating and direct hot water demand were combined in a single energy profile. The daily peak load as shown in figure 37 was equal to 15.99 kW representing the maximum heating demand occurred in the yearly period monitored. Therefore, a market research analysis was performed to identify an air source heat pump with a heating capacity close to 16kW so that it can efficiently supply the dwelling. From the analysis different manufacturers with several heat pump models have been assessed with their system characteristics and performance parameters shown on table 5 below.

Table 5: Performance characteristics of 3 different models of air source heat pumps.

	Mitsubishi Ecodan HWM140V	Daikin Altherma 3 EDLQ016CV3	Samsung EHS Mono AE160JXYDEH
Heating Capacity [kW]	14.0	16.0	16
Heating COP	2.45	4.20	4.21
Input Power [kW]	5.71	4.56	3.7
Refrigerant	R-32	R-32	R-410A

The performance values and heating capacities of the heat pumps mentioned in the table above, would only be met under the standard conditions set by the manufacturer and EN 14511 ($T_{\text{evap}}=2.0\text{ }^{\circ}\text{C}$ and $T_{\text{cond}}=35.0\text{ }^{\circ}\text{C}$). From the three models of air source heat pumps that were examined, the two more suitable are the Samsung and Daikin which both have a nominal heating capacity of 16.0 kW and COP around 4.20. The fact that the Daikin model uses R-32 as a refrigerant is its advantage over the Samsung since R-32 has a GWP of 675 which is on average 30% lower in regard to R-410a. Hence the air source heat pump model used to evaluate and simulate its performance is Daikin Altherma V3.

From the technical specifications, the Carnot COP of the heat pump and the volumetric efficiency of the system was found to be 4.20 and 85% respectively. Hence a simple analysis with varying the temperature of the heat source and the delivery temperature was performed to establish the optimum temperatures that will result to the higher maximum possible efficiency. The graph below summarises the variation in COP.

7.0 Results and Discussion

7.1 Performance Evaluation of ASHP

Simulating the operating performance of the air source heat pump was the key feature of this project in order to be able to assess the feasibility of replacing the current heating system with the proposed described in section 5. At the beginning, a simple model with an air source heat pump powered from the grid was constructed in GeoT*Sol as shown in figure 40. The location selected from the software to capture the weather data was Athalassa which located 15km from the actual location of the house.

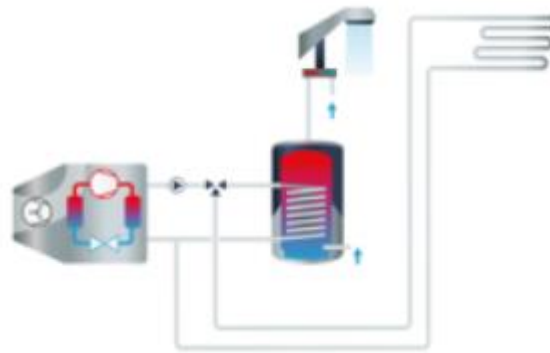


Figure 40: ASHP schematic with buffer tank supplying DHW and space heating

The model consists of an air source heat pump system and a buffer tank which are used to supply the heating demands for both space conditioning and domestic hot water for use. The hot water produced from the heat pump is transferred to the buffer tank which acts as a heat exchanger to combine the HP system with the indoor heating demands [84]. In addition, the buffer tank can effectively minimize the short cycling of the heat pump system by stabilizing the temperature of the water inside the tank when there are fluctuations in the outdoor temperature. Hence the incorporation of a buffer tank is essential for an overall optimized system performance.

After the proper selection of the system schematic, the model was assigned with several parameters to be able to run the simulation and generate results. From the heating demand estimation analysis performed in section 5.1, it was found out that the highest hourly demand was 15.99kW which suggests that the heat pump system to be chosen should have a heating capacity of 16kW. Geo T*Sol has a pre-defined database which contains around 4,000 heat pumps from different manufacturers with each one having specific performance specifications

listed. Based on the heating capacity mentioned above the heat pump that was selected, was a Diakin model ALTHERMA V3 16kW with a COP of 4.20 and a nominal heating power of 6.9kW. The full specification and technical data can be found in the appendix 3 According to literature there are various types of heat pumps that can be either single or variable speed heat pumps with the main difference being in the energy efficiency [85]. The seasonal variation of temperature makes the heat pump work at different speeds to meet the demand. For example, during winter period the speed is much higher than in summer due to the temperatures which are lower. For the scope of this project the heat pump was assigned to be single speed for simplicity reasons.

The current heat distribution network as mentioned in section 6.0 above, is achieved by underfloor heating. This type of distribution network can be characterised as a low temperature heating loop and thus the system was set as 100% low grade heat. The supply and return temperature of the heat pump were set to be 40°C and 28 °C respectively as per the technical data provided by the manufacturer with a target indoor temperature set to 21°C. In addition, for the model to run, it required the correct sizing of the buffer tank for space heating. The heating capacity of the heat pump was found to be 16kW. According to reference from literature a good ‘rule of thumb’ for sizing a buffer tank is that it can maintain around 15 litres per 1kW of the HP’s capacity [86]. Therefore, the buffer tank size was calculated and set to be 240 litres. From the existing database of buffer tanks in the software the most suitable was found to be a Vokera model AQUAFLOWTWIN250 with total volume of 250 litres.

The second function of the heat pump was to be able to provide direct hot water for use and thus an estimation of the average daily hot water demand in litres was established. From the DHW demand estimation analysis it was found that, the total annual demand was 3.8MWh which corresponds to an average daily consumption of 235 litres. Therefore, the hot water supply was set to be 50 °C according to the Health and Safety Executive (HSE), and the cold-water supply to the heat pump was assigned to be calculated entirely based on the climate data.

By assigning the model with all the parameters and technical data, the simulation was run to deduce the performance of the heat pump system over a year period. The graph in figure 41 below represents the results of the simulation.

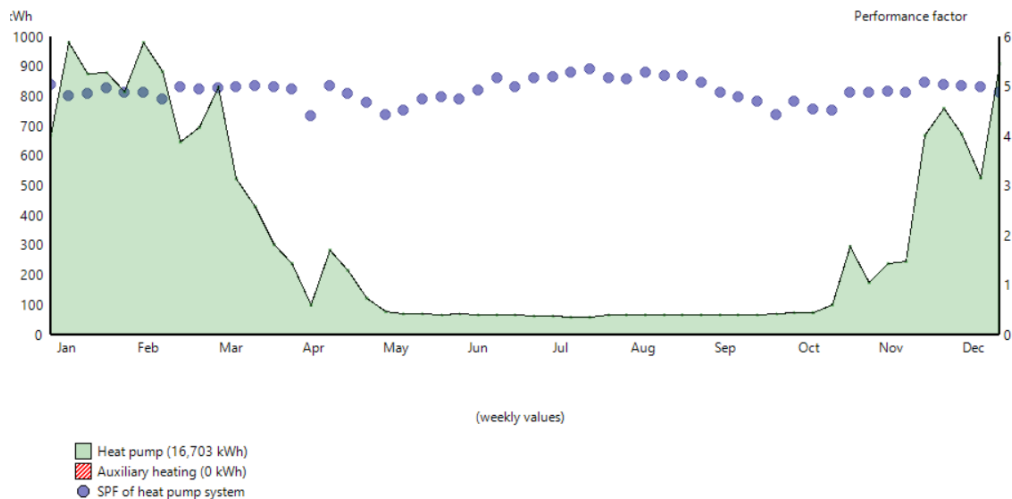


Figure 41: Results file with the yearly SPF variation for the ASHP with a buffer tank.

On the graph above the area shaded in green represents the heat production from the heat pump and the blue dots demonstrates the change in the COP according to the heat demands. The average SPF deduced from the variation in the COP of the heat pump was found to be 4.48. Figure 42 below represents the expected COP of the heat pump to be achieved by various heat source and heat supply temperatures according to Janne and Kai who performed an analysis on a sample of 100 houses.

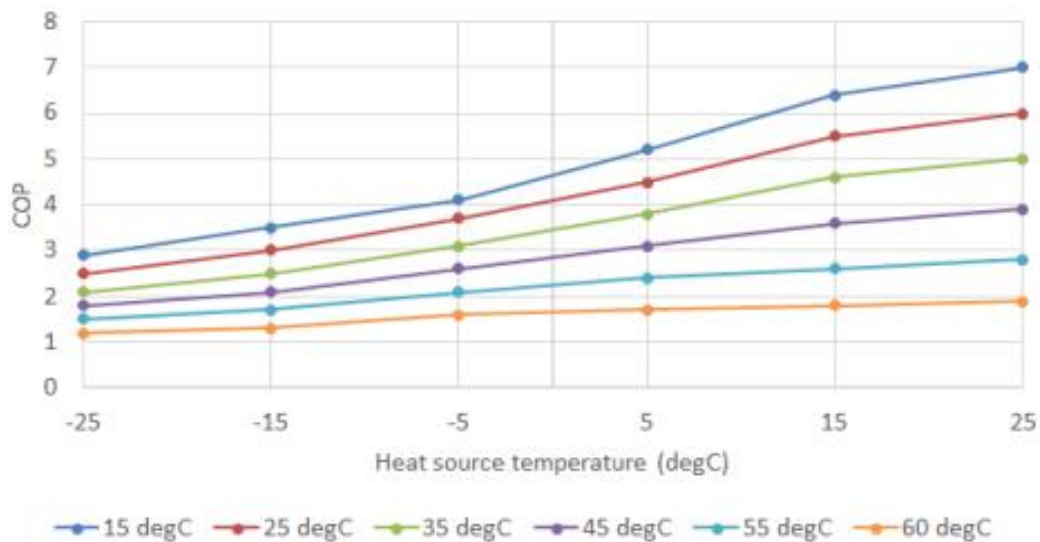


Figure 42: Relationship between COP by varying the heat source and heat sink temperature [87].

In the system modelled, the average heat source temperature was calculated and found to be 10.2°C and the heat supply temperature as previously stated was set as 40°C. Therefore, the predicted COP based on the graph will be around 4.7 and hence if it's compared with the SPF

deduced from the simulation it can be concluded that the simulation results are reasonable and can effectively provide a reliable prediction of performance of the heat pump system.

In addition, from the simulation It was also found that 10% of the overall demand couldn't be met by the heat pump system and hence optimization to the current design should be established to account for this difference.

7.2 Enhancing Performance

7.2.1 Introducing a TES

The initial results from the simulation have shown that with the system design set up as shown in figure 39, the entire heating demand could not be 100% met by the heat pump. Therefore, the first optimisation method that was discussed in literature was the implementation of a thermal energy storage tank. For the scope of this project a sensible TES was chosen to be analysed and modelled with water as the storage medium.

The most important parameter when incorporating a TES to the system, is to establish the optimum size required that can effectively decrease the peak load. From the graph of annual heating demand for both space heating and DHW shown in figure 37, it was found that the peak demand occurred during January the 8th with a total value of 15.99kW. For that reason, a daily profile was generated to monitor exactly the hours of peak demand as shown in figure 43.

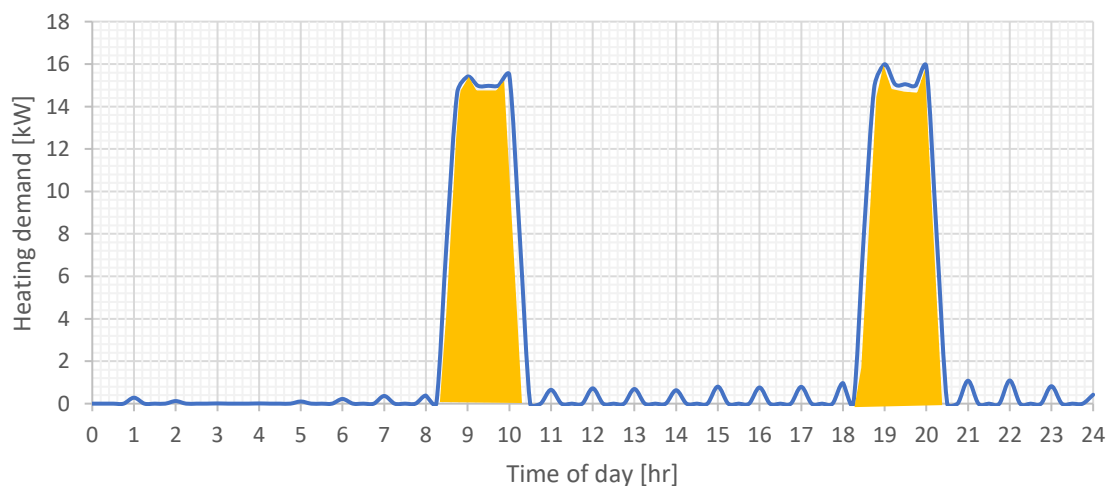


Figure 43: Heating demand profile on the 8th of January with potential energy storage capacity.

During the day there are two main peaks which are indicated with the yellow shade area, one in the morning and one in the evening time. The TES to be sized, should accommodate for this specific heat capacity and thus the total demand that will need to be supplied by the TES was

calculated and found to be 51.5kWh. Therefore, the size of the tank was determined using the following equation according to BG 7/2009 [88]:

$$V = \frac{Q \times 3600}{c \times \Delta T}$$

Where:

V: volume of stores water in tank [L]

Q: heat capacity [kWh]

c: specific heat capacity of water [kJ/kgC]

ΔT : difference of flow and return temperature [$^{\circ}\text{C}$]

To be able to estimate the volume of the TES tank it was assumed that the temperature difference between the inlet and outlet will be equal to 30°C and thus the total volume was found to be 1478.5 litres.

The final step after deducing the TES volume was to update the model with a TES tank as shown in figure 44 in order to be able to run the simulation.

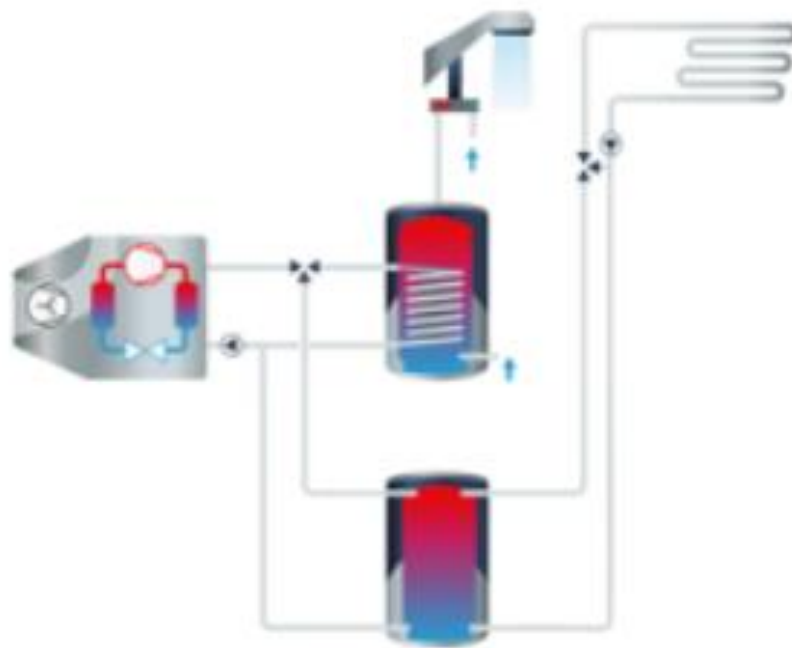


Figure 44: ASHP model schematic with TES and a buffer tank..

The TES tank model was selected from the pre-defined library on the software, and it was assigned to have a volume of 1500 litres with accounted thermal losses of 3.83kWh/d.

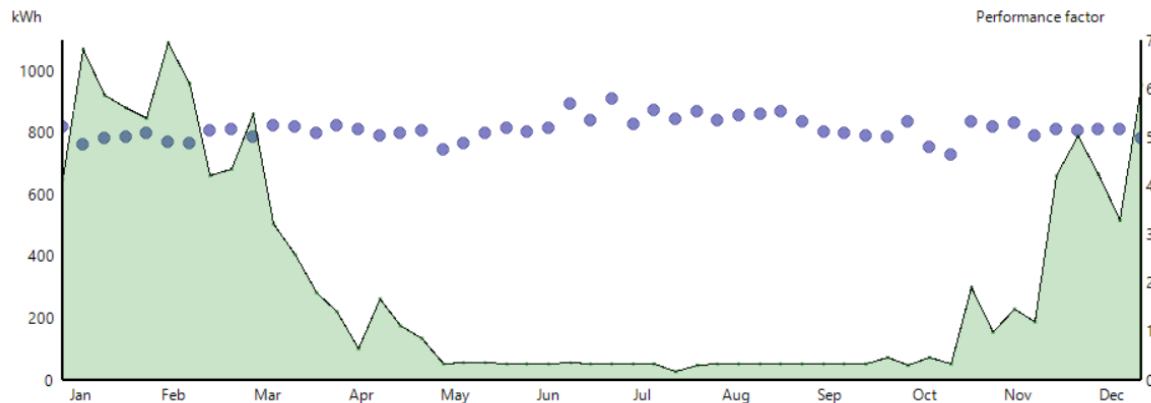


Figure 45: Yearly SPF variation for the ASHP with a buffer tank and TES.

The results from this simulation are represented on the graph above. By introducing the thermal energy storage, the SPF was escalated from 4.48 in the previous simulation to 5.1. This was mainly due to reason that the variation in the COP for the whole year was not varying as much as in the model with no TES which implies that the system will be performing much better because the daily peak demand was mitigated using TES. Additionally, the percentage of the space heating demand that couldn't be met with the previous system design was reduced to 3% suggesting the importance of TES.

7.2.2 Solar Assisted Heat Pump Modelling

The performance of the heat pump system as briefly discussed by the literature section of this report, it can be reinforced by assisting the system design with solar thermal collectors in a SAHP system configuration. A system schematic as the one shown in figure 46 was used to simulate the performance of the proposed SAHP system.

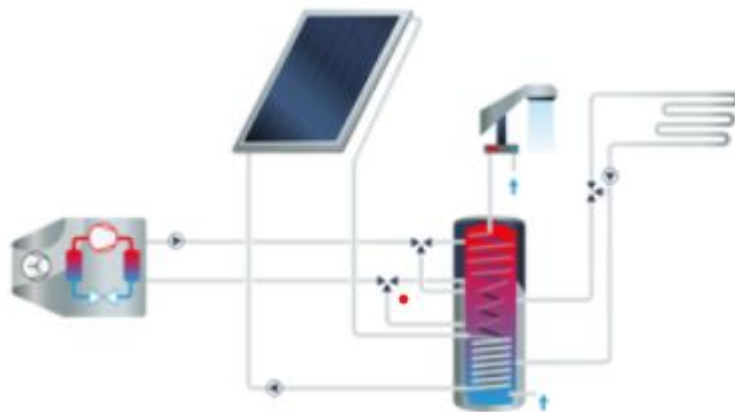


Figure 46: ASHP model schematic with TES, buffer tank and solar thermal collector.

For this simulation the solar thermal collector chosen was a flat plate type collector with an efficiency of 80%. The orientation was set to be 180° facing the South since according to studies performed in the same field, South facing solar thermal collectors can absorb higher percentages of solar radiation compared to other orientations. Additionally, another important parameter that must be considered when incorporating a solar thermal collector to a heat pump system is the inclination. From the schematic on figure 46 it can be seen that the angle of incidence of solar radiation on the solar panels is higher during the summer months and lower during the winter months.

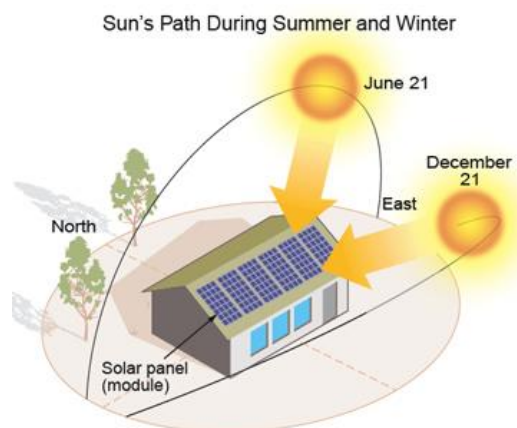


Figure 47: Variation in the angle of incident during Summer and Winter [89].

This effect occurs due to the earth's tilt of 23.5° and hence as it moves away from the sun, the angle of incidence changes. Therefore, to be able to have the maximum utilisation of solar radiation the collectors should be placed in a tilt angle that the incident radiation reaching the surface is almost perpendicular. In real life situation the change in the tilt of the collectors according to the position of the sun can be established by installing a solar tracking system. The system will be responsible for altering the tilt of the collectors based on the time of the

year and the position of the sun. The whole monitoring and actuating system described above was outside the scope of the project hence it was not considered.

To increase the validity of the simulation by generating more accurate results a simple mathematical model set up in Excel and executed in Matlab was used, to monitor the solar radiation reaching the surface of the collector every day for a complete one year by varying the inclination. Parameters such as hourly solar radiation, latitude, longitude, declination, and hour angles were used to calculate the values for beam, diffuse and ground reflected radiation on the inclined solar thermal collector. For every day of the year the tilt of the collector was varied from 0 to 90° and for every change, an estimated value of the total solar radiation on the surface was calculated to deduce the one with the highest solar energy absorbed. Each line in figure 48 shows the average daily solar radiation incident on the surface of the collector at varying tilt angles, for a given month.

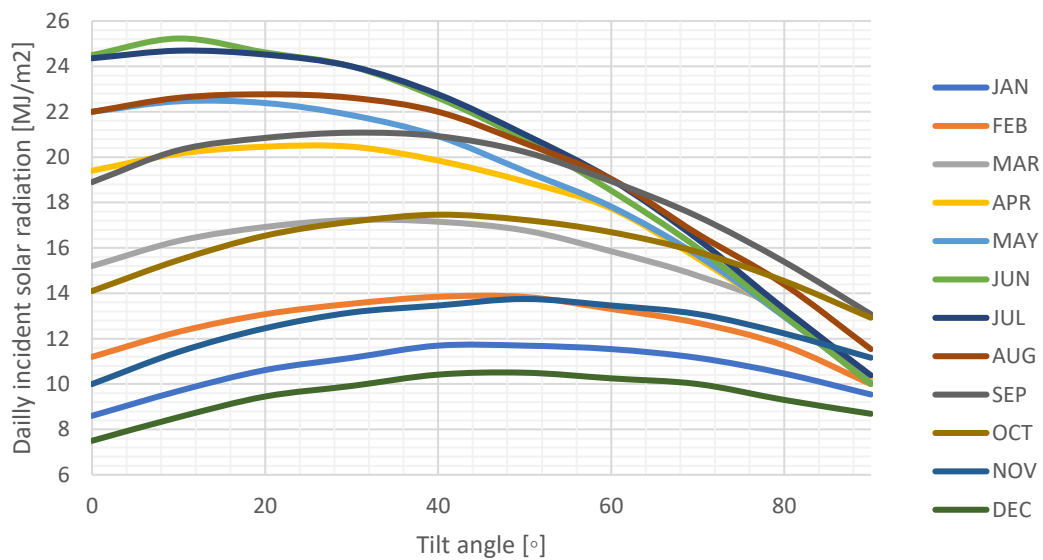


Figure 48: Average incident solar radiation vs tilt angle.

From the results of the above analysis the optimum tilt angle for each month was deduced, allowing for seasonal and annual average values to be calculated, as shown in figure 49.

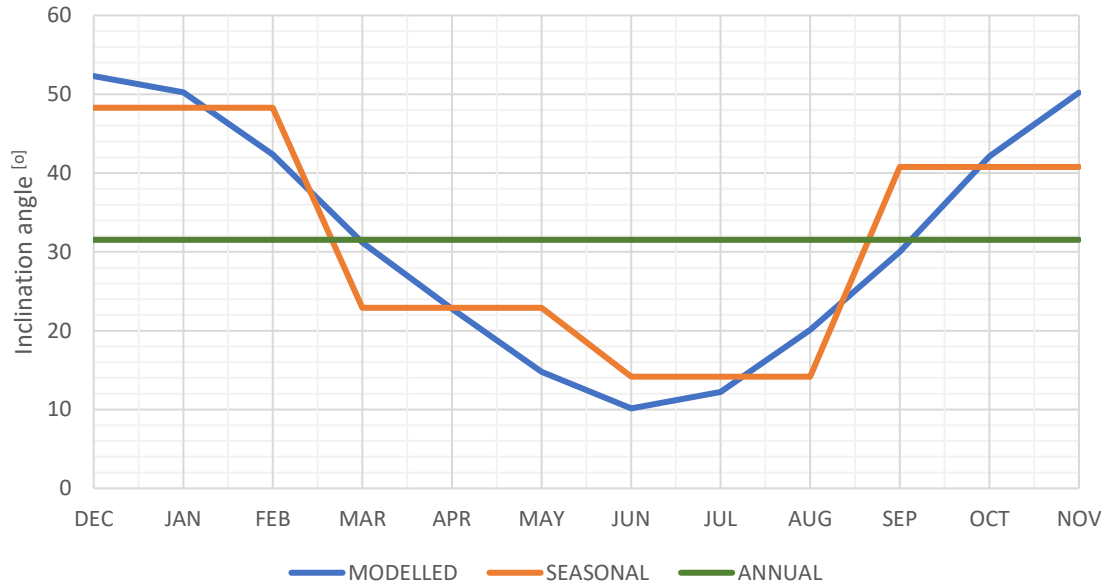


Figure 49: Results for optimum tilt angle on a seasonal and annual average.

In the summer and winter season the optimum angles were found to be 14.2 and 48.3 degrees respectively. The annual average value of optimum tilt angle represented by the green line, was calculated by combining the results from each month of the year and it was found to be 31.5 degrees.

By gathering information from the above graph regarding the seasonal, annual, and modelled results, a verification examination on the total solar energy incident on the collector was established. The results are shown in the bar chart in figure 50.

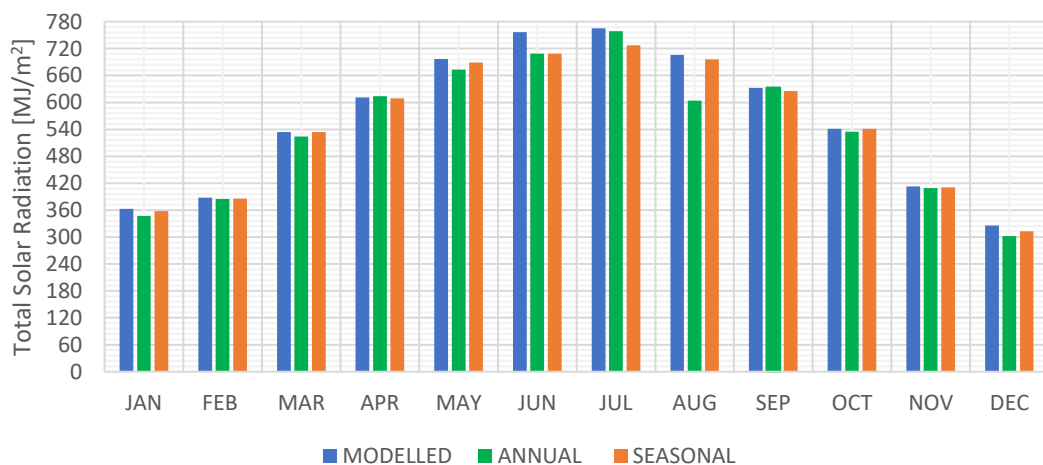


Figure 50: Variation of solar energy incident on the collector when the tilt angle is varied as per modelled, annual, and seasonal average values.

The variation in the energy absorbed by the collector, as can be seen from the figure above, is minor. In fact, the yearly totals from the three sets of data were added together to calculate the percentage error as follows:

Table 6: Percentage difference in total solar energy radiation incident on the collector.

	TOTAL INCIDENT RADIATION [MJ/m² per year]	PERCENTAGE DIFFERENCE [%]
MODELLED	6732	N/A
ANNUAL	6494	3.53
SEASONAL	6598	1.99

From the results generated, it is obvious that the percentage difference for both the annual and seasonal values of optimum tilt angle is negligible and hence for the scope of this model the selected angle was set as 31.5 degrees for every month of the year.

The system to be modelled as shown in figure 45 was amended with the key parameters deduced above, and the simulation was run to monitor the performance of the proposed system. The graph in figure 51 summarises the annual performance of the heat pump system in addition with the assistance form the solar thermal loop.

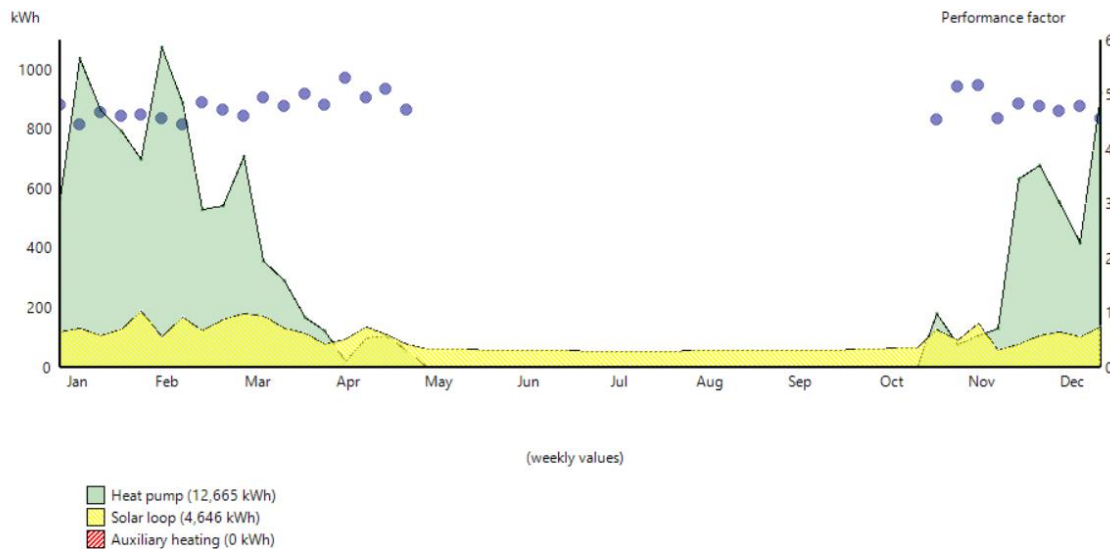


Figure 51: Annual SPF variation for the ASHP with a buffer tank, TES and solar thermal collector.

The shaded area with yellow represents the thermal energy produced by the solar thermal collector and the green the energy supplied from the heat pump. As it can be seen from the beginning of April until the end of October the heating demands of the house can be primarily met by the solar thermal system with minor assistance from the heat pump. As a result, the SPF of the whole system was escalated from 5.1 in the previous simulation to 6.15 demonstrating that the efficiency of the system had gradually increased. With the existing system design which includes both a thermal energy storage and a solar loop the overall heating demand of the building can be fulfilled. This suggests that the system can now operate at maximum performance and be reliable in replacing the current oil condensing boiler existing in the building.

7.3 PV Electricity Generation

For any heat pump system to operate and generate thermal energy, it requires an external source of energy in the form of electrical power to drive the compressor. On the island, as previously mentioned, the electricity supply is delivered from the national grid on where the electrical power is produced by burning fossil fuels. This is not a clean method of producing electricity and thus a more environmentally friendly method to produce electricity on site should be established.

According to the location of the building and weather conditions the most promising renewable energy production method to be implemented is by installing a solar photovoltaic module. Therefore, to evaluate the performance of the PV module on the existing building, a model was set up in PV*Sol and run to generate results and help in the appropriate sizing of the photovoltaic module.

The first step was to estimate the electrical power that the heat pump will consume based on the current COP and the estimated heat demands generated in section 4.1. The equation of the COP of a heat pump states that:

$$COP_{HP} = \frac{Q}{W_{NET}} \quad \longrightarrow \quad W_{NET} = \frac{Q}{COP_{HP}}$$

Therefore, to be able to calculate the annual electrical power of the heat pump, the following equation was used:

$$\text{Annual electrical power} = \sum_{h=1}^{8760} \frac{Q_h}{COP_{HP}}$$

An estimated hourly electrical power consumption was established as in figure 53 and then everything was summed up to form the monthly electrical profile shown in figure 54.

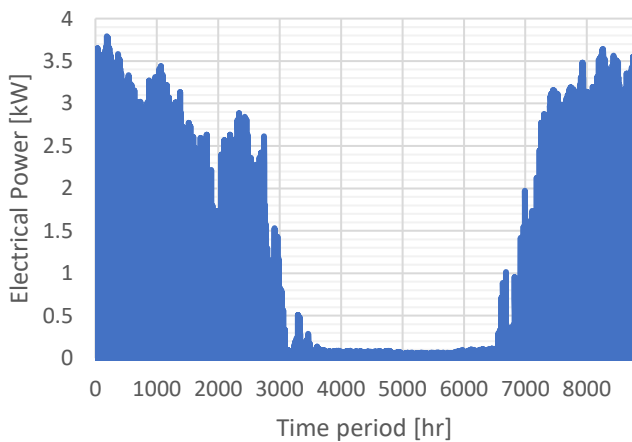


Figure 53: Yearly profile of electrical power consumption.

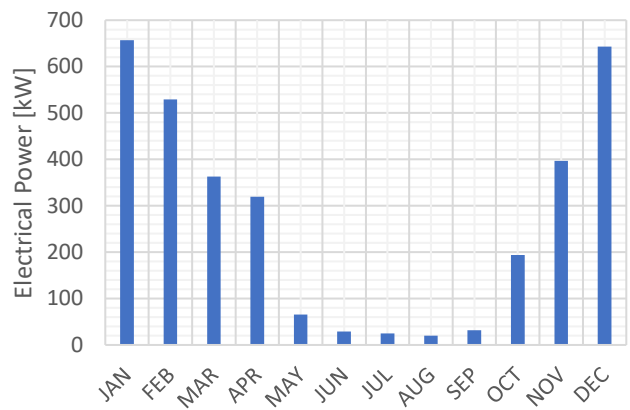


Figure 52: Monthly profile of electrical power consumption.

By combining the results from the two graphs above the average annual electrical power consumption of the heat pump system was found to be 3.3 MWh with peak load on the 8th of January of 3.79kW.

The overall photovoltaic array with the appropriate number of panels and selection of the inverter was based on the peak load and the estimated annual consumption mentioned above. The system schematic of the designed model and energy flow diagram are shown below in figure 54.

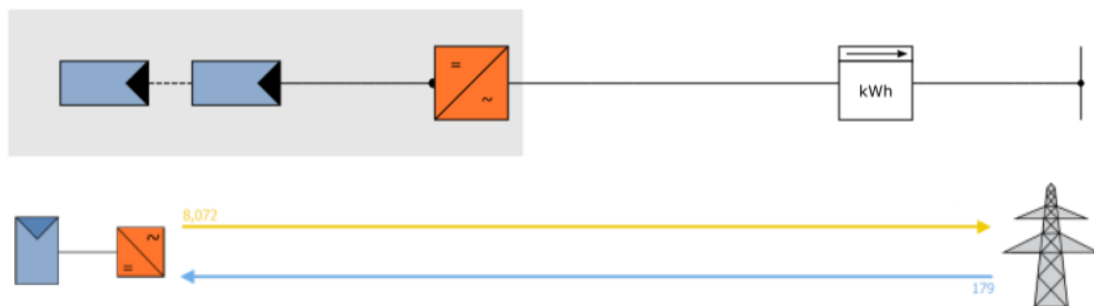


Figure 54: System schematic of the PV array model.

The system chosen is grid connected and thus at times when demand cannot be met by the PV array, electricity can be drawn from the grid to account for this difference.

The initial step for this simulation was to identify an appropriate PV panel for the system design. From market research analysis the panel chosen to be assigned to the model had a power output of 410-425W with an efficiency of 21.2% manufactured by Sunpower.

The exact number of panels were calculated based on the peak load and the rated output of the selected panel. The peak load was escalated to 4kW by considering the heat and transmission losses that are accounted by the software as 5 and 1% respectively.

By determining the revised peak load, the number of panels to be used were also being calculated as:

$$No_{panels} = \frac{Peak\ load}{Panel\ rated\ output\ power} = \frac{4.0kW}{410W} = 9.76 \therefore 10\ panels$$

The roof space that the panels will require when installed, based on their dimensions provided by the technical sheet, was found to be approximately 20m². The tilt angles of the PV panels were assigned as 31 degrees according to the analysis performed above for the optimum tilt angle. Lastly, before the simulation was run an appropriate inverter was selected based on the nominal power output of the PV module. The estimated power output was set to 4kW hence a Sunsynk hybrid inverter of maximum power of 5kW was chosen, accounting for any irreversibility in the system.

The system schematic was set as in figure 55, on where there are two series connections consisting of 5 panels each and then both connected in parallel with the inverter.

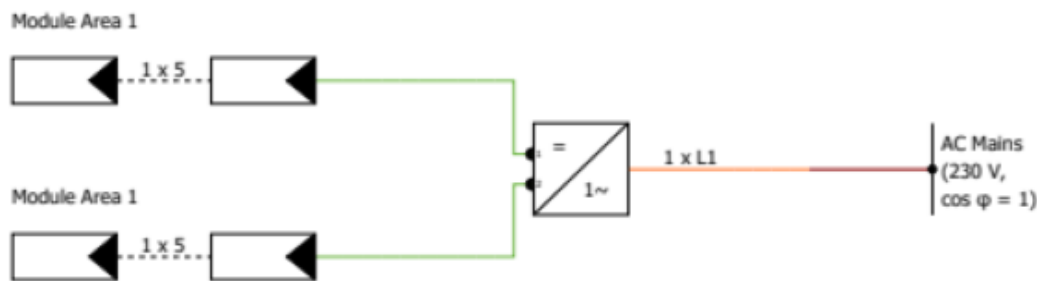


Figure 55: Electrical technical drawing of the PV model.

All the technical data discussed previously were assigned to the model to be able to estimate the monthly electricity production and compare it with the power demand of the heat pump as shown in figure 56 below.

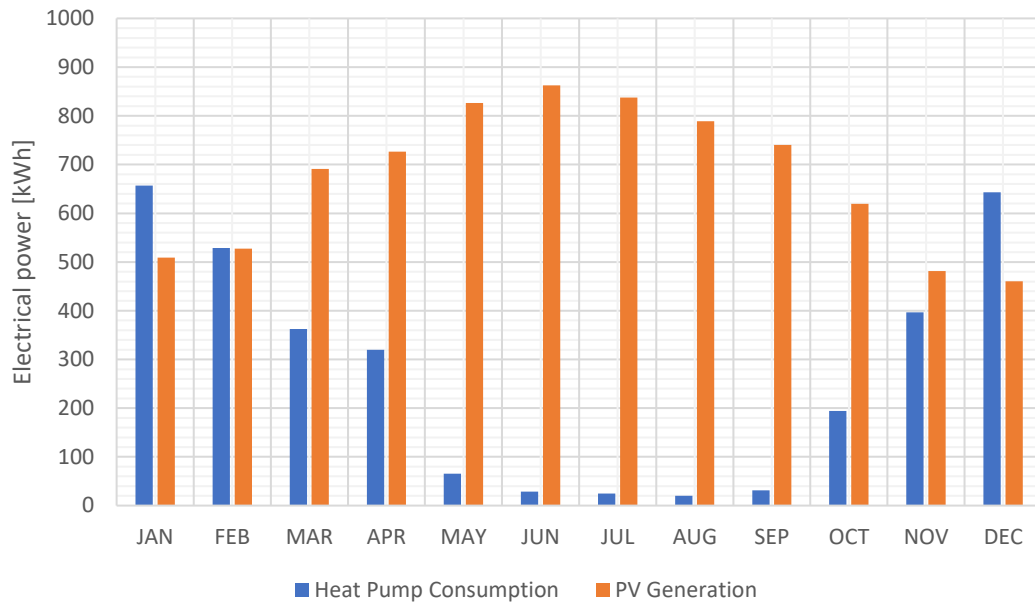


Figure 56: Heat pump power consumption vs PV power generation.

The total estimated yearly electricity generation from the PV array was found to be 8072.2 kWh which can effectively power the heat pump except the months of January and December on where the consumption is higher than production. To validate the results a simple model was set up in PV Watts, which is an online calculator for grid connected PV systems. The graph shows the validation results generated from the PV*Sol and PV Watts.

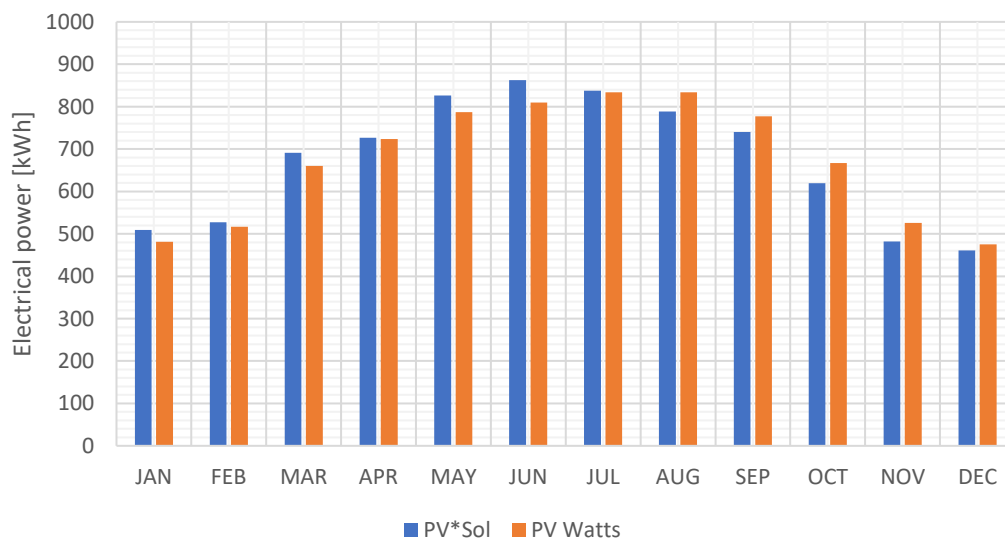


Figure 57: Validation results of PV*Sol vs PV Watts.

The yearly total was estimated from PV*Sol and PV Watts as 8072.2 and 8092 kWh respectively. An annual percentage difference was calculated, and it was deduced as 0.25%, which implies that the results from PV*Sol are accurate and thus it can effectively provide a reasonable approximation of the final results.

Overall, from the evaluation performed, it can be concluded that PV array can effectively generate electrical power to assist a heat pump system if the location of the case study to be assessed has solar radiation abundance. For the power demand that cannot be met especially in January and December, an external investigation could be carried out in analysing the effect of implementing a battery system. The system can supply the heat pump with power at the times of the year when solar irradiance is not sufficient. This investigation was not carried out because it was outside the scope of the project and hence it was excluded.

OVERALL SYSTEM PERFORMANCE EVALUATION

Finally, to assess the overall performance and feasibility of the proposed complete system, a model was set up, including every assessed element described above such as thermal energy storage, photovoltaic arrays, and solar thermal collectors. The overall system model was designed in energyPro, to assess the feasibility and reliability of the proposed system. The system schematic is shown in figure 58.

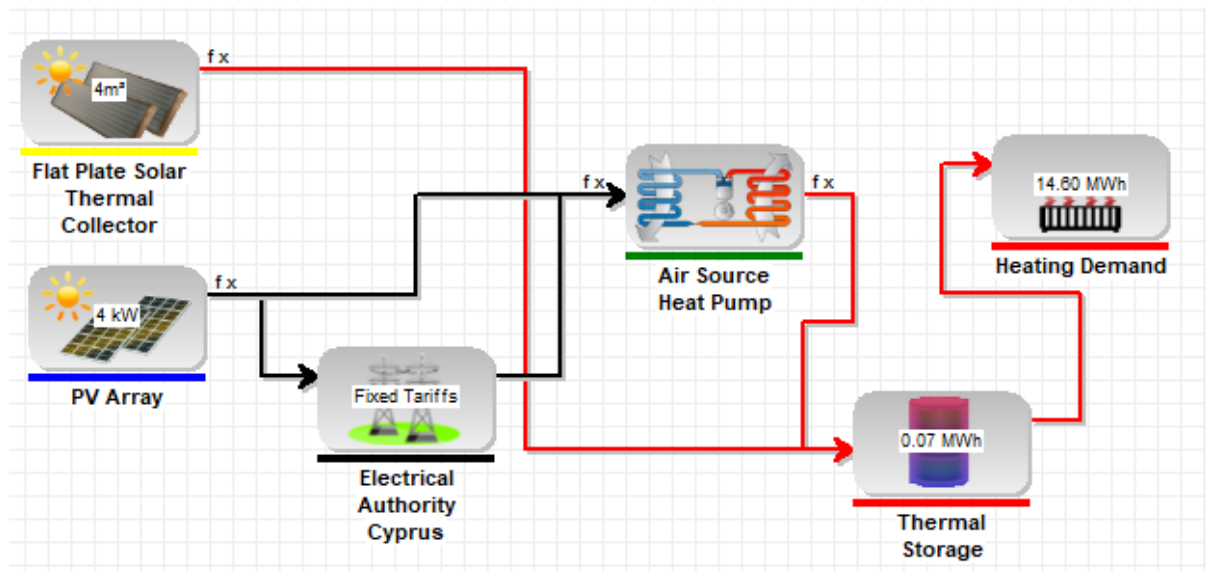


Figure 58: Overall proposed system model in energyPro.

The technical data and specifications of each component in the system were assigned based on the results generated from the above simulations. The software has pre-installed weather files for all the countries around the world and hence the appropriate one was used for this model.

For example, the two figures below show the variation in the outdoor temperature and solar radiation for a yearly period as generated by the software which were both added to the model as a time series function.

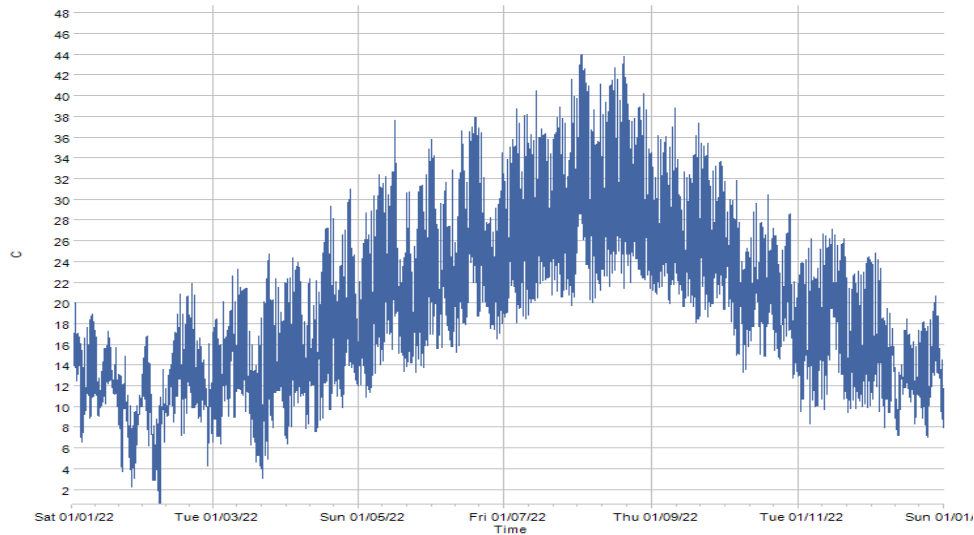


Figure 59: Yearly profile of outdoor temperature generated from energyPro

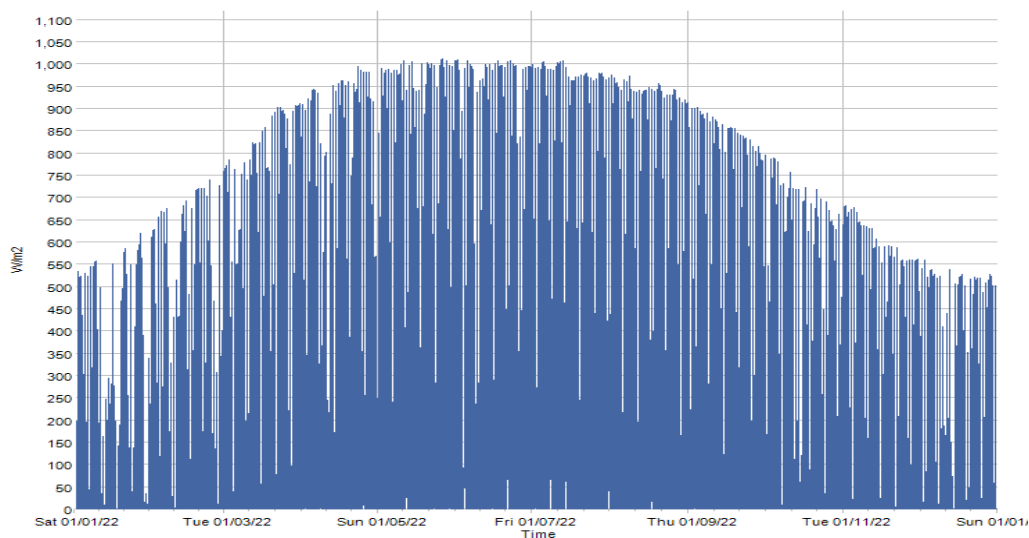


Figure 60: Yearly profile of annual solar radiation deduced from energyPro.

In addition, the annual estimated heat demand including both space heating and direct hot water for use was input to the model as a time series. The data were exported from the combine load graph generated earlier as shown in figure 38. From the different analysis performed on individual systems in previous simulation, it was found out that heat demands should be revised by the addition of an extra 4% which accounts for the extra losses not considered in the earlier models. Finally, the heat capacity of the heat pump, the sizing volume of the thermal store, the size of the solar thermal collector and the electrical properties of the PV module were

entered into to the model from the results deduced in the simulations described above. The table below summarises the some of the technical data and specifications assigned to the model.

The simulation was run to establish the full results which are shown summarised below in table 8.

Table 7: Main results generated from the complete heating system run in energyPro.

Overall space heating and hot water demand	14.60 MWh
Accounted losses in the system	0.6 MWh
Annual heat pump electrical power consumption	3.5 MWh
Annual electricity generation from Photovoltaic module	7.95 MWh

From the results generated from the software it was concluded that the annual heating demand of the building was entirely met by the air source heat pump system in addition with the thermal energy supplied from the thermal storage and the solar thermal collectors. The following graph in figure 61 represents the performance of the proposed system for the 8th of January which was recorded from previous stages in this thesis as being the day with the peak load.

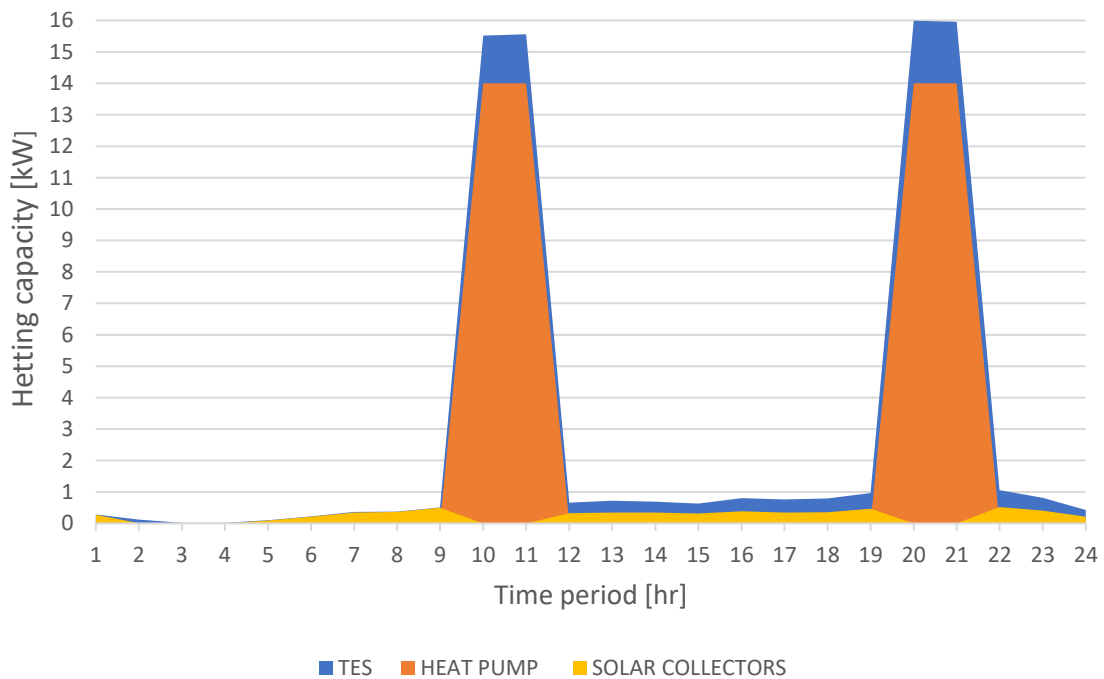


Figure 61: ASHP results from energyPro for January the 8th . .

From the figure above it can be seen that the heat produced from the heat pump can meet to a great extent the heat demand of the building with minor assistance from the thermal store and the solar thermal system installed. Moreover, when calibrating the model, it was set that the maximum heat produced by the heat pump will be 14kW since from the heating demand analysis performed above it was found that only 5% of the hourly heat demand was found to be above 14kW. Hence when demand is above 14kW thermal energy is being supplied to the building from the thermal energy storage and also from the solar thermal collectors. The thermal storage system installed in the proposed design as it can be deduced from the graph in figure 60, plays a crucial role in minimizing the operation of the heat pump at part load which is inefficient. The solar collectors can entirely meet the hot water demand without the need of operation of the heat pump.

The last evaluation analysis performed on the model, was to assess the performance of the photovoltaic module if it can effectively supply the heat pump system with electrical power. The graph below represents the power consumption of the heat pump on the 8th of January with the estimated electricity produced from the photovoltaic panels.

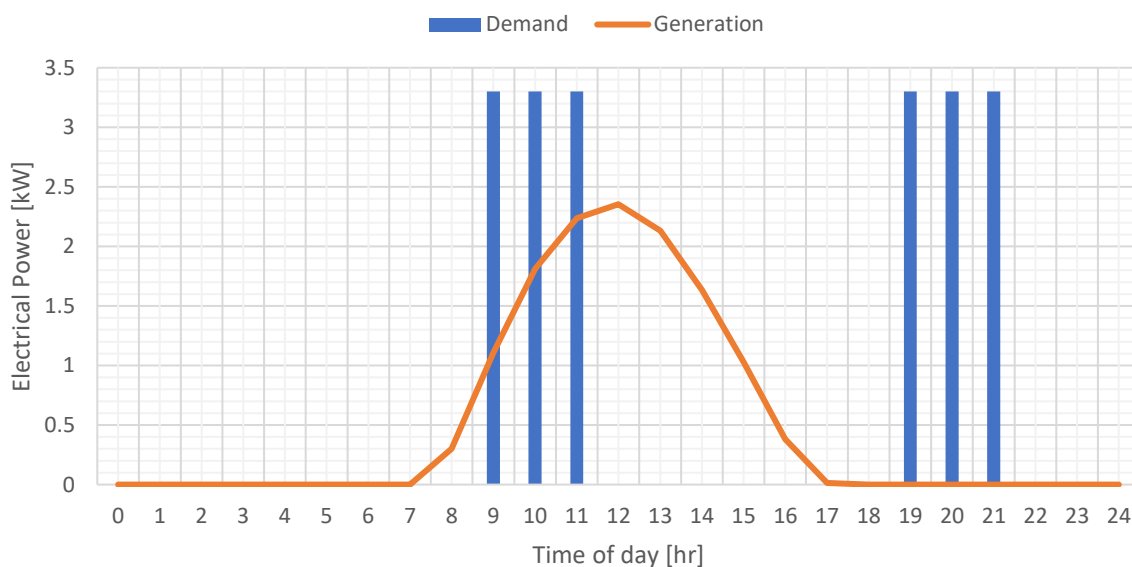


Figure 62: Results from energyPro for PV generation and ASHP consumption.

The power consumption of the heat pump and the electrical power produced from the photovoltaics do not directly associate with each other, but also it was found out that the energy produced on a daily basis especially during winter period is much less than the power consumed. Moreover, the majority generation occur at times in the day where consumption is minimal, hence an appropriate battery should be designed that can store this amount of energy

produced and supply it when there is power demand. In the short-term photovoltaics seem to be not so favourable for the designed system but when considered in longer the annual production is much higher than the annual consumption which implies that with the proper selection of battery system the whole heating system could become a standalone fully sustainable system. To sum up, the proposed system modelled in energyPro was assessed, and it was established that it can effectively supply with thermal energy the overall heating demands of the building.

8.0 Financial Evaluation

To fully assess the feasibility and reliability of any project, a financial analysis should always be executed, to ensure that the proposed design will have a future benefit to the user by its development. Therefore, an appropriate selection of some economic parameters such as initial investment (CAPEX), annual savings, payback period and the cash flows over the years should be estimated, to be able to judge the feasibility of the project.

8.1 Capex

The initial investment cost, which is also known as CAPEX, is total amount of money need to be spent at the beginning of the implementation of the project in buying equipment such as heat pump, photovoltaic panels, inverter, solar thermal collectors, TES and overall piping. The following table summarises the equipment prices and overall cost of the proposed system. The labour price is included in the prices of each specific equipment.

Table 8: Total cost of investment for the proposed system.

Component	Quantity	Price per single unit [£/unit]	Total Cost [£]
16kW Heat pump	1	5 537.50 [90]	5 537.50
Thermal energy storage tank	1500 l	2.7 per litre [91]	4050
Buffer tank (240l)	240 l	2.7 per litre	650
Photovoltaic Panel	10	268 [92]	2680
4kW Inverter	1	1155	1155
Solar charge controller	1	386 [93]	386
Piping	25m	5.66	141.5

The total investment cost was calculated from the individual prices of each component, and it was found to be £14,600.

8.2 Total Savings

The total savings achieved every year were estimated based on the amount of money saved by the production of electrical power from photovoltaic panels in contrast to the amount of money spent when the primary source of energy was oil for the boiler. The total heating demand for the yearly period was found to be 14.56 MWh.

According to Statista.com the average price per kWh of heating oil in Cyprus was 23.04-euro cents [94] which corresponds to 13.62-pound pence. Hence:

$$Total\ Cost_{natural\ gas} = 0.136 \times 14,560 = 19.35 \times = \text{£ } 1983.1$$

The supply tariff from EAC for Cyprus is 0.22-pound sterling per kWh of electrical power consumed [95]. Therefore, the total cost of operating the heat pump only consuming power from the grid and no assistance by the PV panels electricity generation will be:

$$Total\ Cost_{heat\ pump} = 0.22 \times 3300 = \text{£ } 726$$

Therefore, by determining the two values above for one year operation the potential savings can be simply calculated by:

$$Potential\ Savings = Cost_{natural\ gas} - Cost_{heat\ pump} = 1983.1 - 726 = \text{£ } 1257.1$$

The system has also installed PV panels for the potential generation of renewable power from the sun. According to the EAC the price which electrical power can be sold to the grid is 6.2-pound sterling per kWh sold [94]. Thus, the potential savings that can be established in one year period by selling electricity back to the grid can be calculated as:

$$Savings_{grid} = Total_{generation} \times price = 8092kWh \times 0.062 = \text{£ } 486$$

*In Cyprus all the energy generated from PV panels is entirely exported to the grid, there is no self-consumption that's why the total generated power is used above.

The yearly savings that could be established by simply replacing the current oil boiler with the proposed heating system are calculated as:

$$Yearly_{savings} = 1257.1 + 486 = \text{£}1742.6$$

8.3 Payback Period

The payback period was established by simply dividing the total investment cost over the potential savings per year as deduced from the calculations above. Therefore:

$$Payback\ period = \frac{14600}{1742.6} = 8.4\ years$$

8.4 Return on Investment

The final key performance indicator that was calculated from the potential profits was the return on investment which was calculated by dividing the net savings with the initial capex of the design system.

$$ROI = \frac{1742.6}{14600} \times 100 = 11.9\%$$

The potential payback for the complete proposed system with both the photovoltaic panels and the heat pump system was estimated as 8.4 years and the ROI was found to be 11.9%. According to a study performed by a company called Purerenewables, a typical payback period and ROI (on average) should be around 10 years and 10% respectively [96]. This suggests that the economic results deduced above are reliable and accurate.

9.0 Environmental Analysis

The final key performance indicator was to assess the environmental feasibility of the proposed sustainable heating system by analysing the potential CO₂ savings when the old oil condensing boiler is replaced with an air source heat pump system and solar PV panels. To be able to perform this investigation several emission factors for heating oil and electricity from the grid were used. According to the technical annex from the EU Covenant Mayors for Climate and Energy, the emission factors for both heating oil and electricity from the grid for the republic of Cyprus were found to be 0.267 and 0.874 tonnes of CO₂ released when 1 MWh is consumed respectively [97]. Hence a simple calculation was performed to deduce the amount of CO₂ that can be saved when replacing the current heating system with the proposed design discussed in the whole thesis.

9.1 CO₂ Savings

Heating oil CO₂ emissions:

$$\begin{aligned} CO_2 \text{ released} &= \text{Heating Demand} \times \text{Emission Factor} = \\ &= 14.60 \times 0.267 = 3.9 \text{ tonnes} \end{aligned}$$

Electricity consumption for HP CO₂ emissions:

$$\begin{aligned} CO_2 \text{ released} &= (\text{Electrical power consumed from grid} - \text{PV generation}) \times \text{Emission Factor} = \\ &= (3.5 - 2.2) \times 0.874 = 1.57 \text{ tonnes} \end{aligned}$$

The graph in figure 63 below summarises the percentage decrease in the CO₂ emissions that could be achieved by replacing the current domestic heating system with the proposed sustainable heating system.

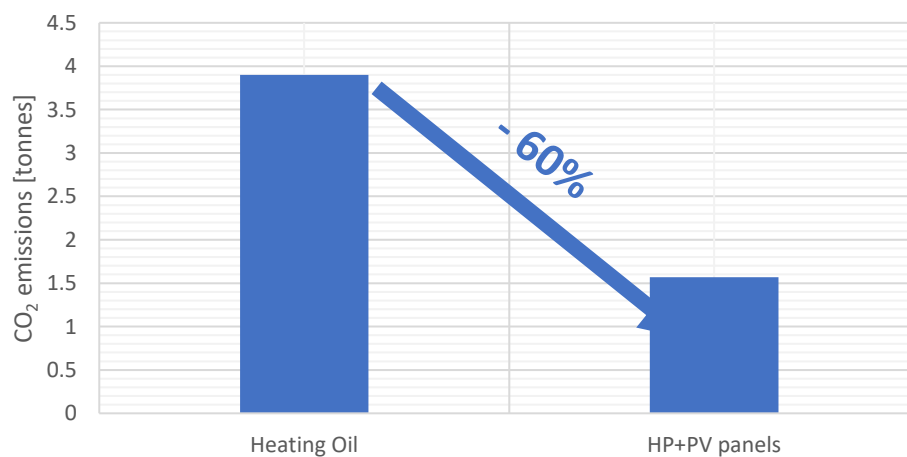


Figure 63: Comparison in the CO₂ emission of heating oil and HP with PV panels.

10.0 Conclusion

To sum up the, the whole thesis aim was to design and assess the technical and economic performance of an air source heat pump for the decarbonisation of heating in the domestic sector. At the beginning of the thesis a thorough literature review was performed to identify the state of the art in the current sustainable heating systems. Furthermore, the potential to enhance the overall system performance by implementing a thermal energy storage and the integration to renewables for the production of electrical and thermal energy was also evaluated. A robust methodological approach with the use of a residential building in the republic of Cyprus as a case study was able to be constructed so that it can be used further from other engineers who tackle similar projects like this.

The building modelled had an annual heating and direct hot water demand of 14.60MWh. The proposed system was tested on the specific building in order to be able to assess its

performance. From the heating demands deduced, a 16KW air to water heat pump system was used to generate models and run simulations. The initial results when only the heat pump system was tested, has shown an annual SPF of 4.48 and 10% of the whole demand was not able to be covered by the heat pump. Therefore, the system was upgraded by the implementation of a 1500l TES, which had effectively proven its importance in decreasing the overall heating capacity of the heat pump. In addition, the integration of renewables was achieved by utilising the energy from the sun for the production of thermal energy using solar thermal collectors and electrical power using PV panels. By doing so, the total heating demands of the house were able to be met 100%, resulting to a fully functionable and effectively operating sustainable heating system.

To conclude, the technical evaluation of the proposed system using different dynamic energy simulation software, indicated the reliability of an air source heat pump in fulfilling the heating demands of a residential building in Cyprus. Taking into consideration the financial analysis, it was deduced that the whole system has a relatively low cost of around £15,000 and an estimated payback period of 8.5 years. The major benefit of implementing such a heating system as proven by the environmental analysis, is the fact that there is a potential of 60% reduction in the overall CO₂ emissions which was one of the main key performance indicators of this thesis to reduce emission and mitigate the effect of global warming and climate change. Overall the whole thesis was successful in addressing it's objectives, since a robust methodological design approach and process flow diagram was able to be constructed for the replication of the design steps of a sustainable heating system to be implemented in other residential buildings.

11.0 Future Work

The current project can serve as a springboard for further investigation into the development of sustainable heating systems. Therefore, the project outcomes could be widened by analysing and evaluating several aspects that were not considered in depth. To begin with, a more sophisticated simulation tool with more functions can be used such as TRNSYS, in order to have more accurate estimations on the final performance of the system. In addition, an in-depth investigation on solar tracking systems for better utilisation of the energy from the sun could be established, to increase the potential of powering a heating system from only renewable sources. Moreover, a proper data collection method must be achieved since the data gathered

were only from the EPC of the building and a rough estimation was generated from ESP-r. Lastly the full system could be further optimized with an analysis in implementing a control system that would be able to operate the system based on technologically advanced system using smart building heating demand management.

12.0 References

[1] H. Ritchie, M. Roser and P. Rosado, "CO₂ and Greenhouse Gas Emissions", *Our World in Data*, 2022. Available: <https://ourworldindata.org/co2-emissions> . [Accessed 20 May 2022].

[2] IEA, *2019 Global Status Report for Buildings and Construction*, 2019. Available: https://iea.blob.core.windows.net/assets/3da9daf9-ef75-4a37-b3da-a09224e299dc/2019_Global_Status_Report_for_Buildings_and_Construction.pdf . [Accessed 20 May 2022].

[3] United Nations Environment Programme, *2020 Global Status Report for Buildings and Construction: Towards a Zero-emission, Efficient and Resilient Buildings and Construction Sector*. Nairobi. 2020.

[4] EPA, "What are the trends in indoor air quality and their effects on human health?", *US EPA*, 2021. Available: <https://www.epa.gov/report-environment/indoor-air-quality>. [Accessed 22 May 2022].

[5] N. Bertelsen and B. Mathiesen, "EU-28 Residential Heat Supply and Consumption: Historical Development and Status", *Energies*, vol. 13, pp. 1-21, 2020. Available: 10.3390/en13081894 [Accessed 23 May 2022].

[6] European Commission, "Revision for phase 4 (2021-2030)", *Climate Action*, 2022. . Available: https://ec.europa.eu/clima/eu-action/eu-emissions-trading-system-eu-ets/revision-phase-4-2021-2030_en. [Accessed 24 May 2022].

[7] I. Dincer and M. Rosen, "Exergy Analysis of Heating, Refrigerating and Air Conditioning", *Heat Pump Systems*, pp. 131-168, 2015. Available: <https://www.sciencedirect.com/science/article/pii/B9780124172036000041> . [Accessed 25 May 2022].

[8] R. Sekerka, "Thermal Physics", *Second Law of Thermodynamics*, pp. 31-48, 2015. Available: <https://www.sciencedirect.com/science/article/pii/B978012803304300003X> . [Accessed 26 May 2022].

- [9] T. Deckmym and V. Eetvelde, *Thermodynamic principle of heat pump and refrigeration cycle*. 2014.
- [10] A. Gagneja and S. Pundihr, "Heat Pumps and Its Applications", *Advances in Chemical Engg., & Biological Sciences*, vol. 3, no. 1, pp. 117-120, 2016. Available: <https://iicbe.org/upload/1922U0516203.pdf> . [Accessed 27 May 2022].
- [11] B. Editors of Encyclopaedia, "Montreal Protocol on Substances that Deplete the Ozone Layer", *Montreal Protocol*, 2022. Available: <https://www.britannica.com/event/Montreal-Protocol> . [Accessed 28 May 2022].
- [12] Linde, "HCFC Phase-Out Legislation", *Linde Gas*, 2022. Available: https://www.linde-gas.com/en/products_and_supply/refrigerants/environment_and_legislation/ozone_depletion_legislation/hcfc_phase-out_legislation/index.html . [Accessed: 29 May 2022].
- [13] K. Rogers, "HFC", *Encyclopedia Britannica*, 2019. Available: <https://www.britannica.com/science/hydrofluorocarbon> . [Accessed 30 May 2022].
- [14] European Commission, 2015. *EU legislation to control F-gases*. Available: https://ec.europa.eu/clima/eu-action/fluorinated-greenhouse-gases/climate-friendly-alternatives-hfcs_en. [Accessed 31 May 2022].
- [15] Goodway, "Ammonia As a Refrigerant: Pros and Cons", *Green Buildings and Green Technology*, 2022. Available: <https://www.goodway.com/hvac-blog/2009/08/ammonia-as-a-refrigerant-pros-and-cons/>. [Accessed 4 June 2022].
- [16] S. Gopalnarayana, "Choosing the Right Refrigerant", *Mechanical Engineering*, vol. 120, no. 10, 1998. Available: <https://doi.org/10.1115/1.1998-OCT-6> . [Accessed 5 June 2022].
- [17] D. Kleijin, *Temperature of evaporation as a function of pressure for several commonly used refrigerants*. 2022.
- [18] S. Badiali and S. Colombo, "Dynamic Modelling of Mechanical Heat Pumps for Comfort Heating", MSc, Politecnico di Milano, 2010.
- [19] I. Staffell, D. Brett, N. Brandon and A. Hawkes, *Temperature-entropy diagram showing the ideal vapour compression cycle for a heat pump*. 2012.

- [20] C. HVACR GUY, "Comparison of Actual and Theoretical Vapor Compression Cycle", *HVACR GUY*, 2022. Available: <https://hvacguy.com/comparison-of-actual-and-theoretical-vapor-compression-cycle/> . [Accessed: 8 June May 2022].
- [21] "Coefficient of Performance Explained", *AirConditionerLab*, 2022. Available: <https://airconditionerlab.com/coefficient-of-performance/> . [Accessed: 8 June 2022].
- [22] Engineering ToolBox, Heat Pumps - Performance and Efficiency Ratings. 2008
- [23] D. Chwieduk, "Advances in Solar Heating and Cooling", *Active solar space heating*, pp. 151-202, 2016. Available: <https://doi.org/10.1016/B978-0-08-100301-5.00008-4> . [Accessed 10 June 2022].
- [24] ALFA LAVAL, "HEATPUMPS", *Alfalaval.com*, 2019. Available: https://www.alfalaval.com/globalassets/documents/microsites/heating-and-cooling-hub/alfa_laval_heating_and_cooling_hub_heat_pumps_brochure.pdf. [Accessed 12 June 2022].
- [25] VIESMANN, "What temperature should a condensing boiler be set at?", *Viessmann.co.uk*, 2022. Available: <https://www.viessmann.co.uk/heating-advice/what-temperature-to-set-condensing-boiler> . [Accessed: 14 June 2022].
- [26] NU-HEAT, "Underfloor Heating vs Radiators – Which is the Best Option?", *Underfloor heating*, 2022. Available: <https://www.nu-heat.co.uk/blog/underfloor-heating-vs-radiators/> . [Accessed 16 June 2022].
- [27] N. Kelly and J. Cockroft, "Analysis of retrofit air source heat pump performance: Results from detailed simulations and comparison to field trial data", *Energy and Buildings*, vol. 43, no. 1, pp. 239-245, 2011. Available: 10.1016/j.enbuild.2010.09.018 [Accessed 17 June 2022].
- [28] I. Sarbu and C. Sebarchievici, "A Comprehensive Review of Thermal Energy Storage", *Sustainability*, vol. 10, no. 1, p. 191, 2018. Available: <https://doi.org/10.3390/su10010191> [Accessed 18 June 2022].
- [29] celsius, *Thermal Energy Storage*, 2020. Available: <https://celsiuscity.eu/thermal-energy-storage/> . [Accessed 20 June 2022].
- [30] CRODA Energy Technologies, *The difference between sensible heat and latent heat*. 2022.

- [31] S. Sharma and K. Sagara, "Latent Heat Storage Materials and Systems: A Review", *International Journal of Green Energy*, vol. 2, no. 1, pp. 1-56, 2007. Available: <https://www.tandfonline.com/doi/citedby/10.1081/GE-200051299?scroll=top&needAccess=true> . [Accessed 22 June 2022].
- [32] E. Barbour, "Thermal Energy Storage", *Energy storage technologies information*, 2022. Available: <http://www.eseslab.com/ESsensePages/TES-page> . [Accessed 23 June 2022].
- [33] S. Wu, "Heat energy storage and cooling in buildings", pp. 101-126, 2010. Available: 10.1533/9781845699277.1.101 [Accessed 23 June 2022].
- [34] P. Tatidjodoung, N. Le Pierres and L. Luo, "A review of potential materials for thermal energy storage in building applications", *Renewable and Sustainable Energy Reviews*, vol. 18, pp. 327-349, 2013. Available: <https://doi.org/10.1016/j.rser.2012.10.025> . [Accessed 26 June 2022].
- [35] M. Abdoly, "Thermal Stratification in Storage Tanks", vol. 42, no. 6, p. 2409, 1981. Available: <https://ui.adsabs.harvard.edu/abs/1981PhDT.....38A/abstract#>. [Accessed 27 June 2022].
- [36] S. Furbo, "Using water for heat storage in thermal energy storage (TES) systems", *Advances in Thermal Energy Storage Systems*, pp. 31-47, 2015. Available: <https://doi.org/10.1533/9781782420965.1.31> . [Accessed 28 June 2022].
- [37] A. Arteconi, N. Hewitt and F. Polonara, "State of the art of thermal storage for demand-side management", *Applied Energy*, vol. 93, pp. 371-389, 2012. Available: <https://doi.org/10.1016/j.apenergy.2011.12.045> . [Accessed 29 June 2022].
- [38] A. Redko, O. Redko and R. DiPippo, "Low-Temperature Energy Systems with Applications of Renewable Energy", *Hybrid systems with renewable energy sources*, pp. 289-328, 2020. Available: <https://doi.org/10.1016/B978-0-12-816249-1.00008-X> . [Accessed 30 June 2022].
- [39] GREENMATCH, "Solar Collectors", *What Are Solar Collectors?*, 2022. Available: <https://www.greenmatch.co.uk/solar-energy/solar-thermal/solar-collectors>. [Accessed 30 June 2022].

- [40] G. Barone, A. Buonomano, C. Forzano and A. Palombo, "Solar thermal collectors", *Solar Hydrogen Production*, pp. 151-178, 2019. Available: <https://doi.org/10.1016/B978-0-12-814853-2.00006-0>. [Accessed 2 July 2022].
- [41] S. Qazi, "Standalone Photovoltaic (PV) Systems for Disaster Relief and Remote Areas", *Solar Thermal Electricity and Solar Insolation*, pp. 203-237, 2017. Available: <https://doi.org/10.1016/B978-0-12-803022-6.00007-1>. [Accessed 4 July 2022].
- [42] S. Kalogirou, "Prediction of flat-plate collector performance parameters using artificial neural networks", *Solar Energy*, vol. 80, no. 3, pp. 248-259, 2022. Available: <https://doi.org/10.1016/j.solener.2005.03.003>. [Accessed 5 July 2022].
- [43] R. Dobriyal, P. Negi, N. Sengar and D. Singh, *Schematic diagram of a flat plate collector showing its different components*. 2020.
- [44] Speyer, E., 1965. Solar energy collection with evacuated tubes. *J. Eng. Power* 86, 270–276
- [45] K. Hudon, *Evacuated tube collector system components schematic*. 2014.
- [46] M. Alghoul, "Review of materials for solar thermal collectors", *Anti-Corrosion Methods and Materials*, vol. 52, no. 4, pp. 199-206, 2005. Available: 10.1108/00035590510603210 [Accessed 6 July 2022].
- [47] Sporn P, Ambrose E. The heat pump and solar energy. Proc of the world symposium on applied solar energy phoenix, US1955
- [48] X. Sun, Y. Dai, V. Novakovic, J. Wu and R. Wang, *Schematic diagram of a typical ASHPWH and DX-SAHPWH system*. 2015.
- [49] P. Sporn, E.R. Ambrose. The heat pump and solar energy. Proceedings of the World Symposium on Applied Solar Energy. Phoenix, Ariz; November 1–5, 1955
- [50] O. Ozgener, A. Hepbasli. A review on the energy and exergy analysis of solar assisted heat pump systems. *Renewable and Sustainable Energy Reviews*; 2007; 11: 482–496
- [51] Xiaolin Sun, Jingyi Wu. Experimental study on roll-bond collector/evaporator with optimized channel used in direct expansion solar assisted heat pump water heating system. *Applied Thermal Engineering*; 2014; 66: 571-579

- [52] L. Tagliafico, F. Scarpa and F. Valsuani, "Direct expansion solar assisted heat pumps – A clean steady state approach for overall performance analysis", *Applied Thermal Engineering*, vol. 66, no. 1-2, pp. 216-226, 2014. Available: <https://doi.org/10.1016/j.applthermaleng.2014.02.016>. [Accessed 7 July 2022].
- [53] C. Huan, S. Li, F. Wang and L. Liu, *System component configuration for indirect-expansion solar-assisted heat pump*. 2019.
- [54] Ruschenburg, J.; Herkel, S.; Henning, H.-M. A statistical analysis on market-available solar thermal heat pump systems. *Sol. Energy* 2013, 95, 79–89.
- [55] Statista, "Cumulative installed solar PV capacity worldwide from 2000 to 2020", *Energy & Environment*, 2022. Available: <https://www.statista.com/statistics/280220/global-cumulative-installed-solar-pv-capacity/#>. [Accessed 10 July 2022].
- [56] IEA, "Analysis and forecast to 2025", *Renewables 2020*, p. 38, 2020. Available: https://iea.blob.core.windows.net/assets/1a24f1fe-c971-4c25-964a-57d0f31eb97b/Renewables_2020-PDF.pdf. [Accessed 11 July 2022].
- [57] E. Chu and L. Tarzano, "A Brief History of Solar Panels", *Smithsonian*, 2022.
- [58] ENERGY EDUCATION, *Schematic representing the photovoltaic effect*. 2015.
- [59] P. Electrons and A. Tutorials, "Photovoltaic Solar Cell Turns Photons into Electrons", *Alternative Energy Tutorials*, 2022. Available: <https://www.alternative-energy-tutorials.com/photovoltaics/photovoltaics-turn-photons-into-electrons.html#>. [Accessed 12 July 2022].
- [60] HAVENHILL, "why is silicon used in making solar panels?", *havenhillsynergy*, 2022. Available: <https://havenhillsynergy.com/silicon-used-making-solar-panels/>. [Accessed: 13 July 2022].
- [61] DEEGE SOLAR, *The main types of PV solar panels*. 2020.
- [62] L. Wallender and S. Allen, "Monocrystalline vs Polycrystalline Solar Panels: What's The Difference?", *ForbesADVISOR*, 2022.
- [63] D. Burgess, "thin-film solar cell", *Encyclopedia Britannica*, 2020. Available: <https://www.britannica.com/technology/thin-film-solar-cell>. [Accessed 16 July 2022].
- [64] AE 868: Commercial Solar Electric Systems, *Main types of systems for solar PV*. 2022.

- [65] N. Rosenkranz, *Geo T*Sol*. Germany: Valentin Software GmbH, 2021.
- [66] D. Burgess, "thin-film solar cell", *Encyclopedia Britannica*, 2020. Available: <https://www.britannica.com/technology/thin-film-solar-cell> . [Accessed 16 July 2022].
- [67] M. Susten, "Limitations in PVsyst Simulation Encountered while Evaluation of PV Energy Prediction", *PV Energy prediction*, 2017. Available: <https://www.mahindrasusten.com/blog/pv-system-design-mahindra-susten/> . [Accessed 17 July 2022].
- [68] EMD International, *Demand and supply matching results graphical representation example 2022*.
- [69] ["Cyprus Population 2022 (Demographics, Maps, Graphs)", *Worldpopulationreview.com*, 2022. Available: <https://worldpopulationreview.com/countries/cyprus-population> . [Accessed: 18 July 2022].
- [70] TRADING ECONOMICS, "Cyprus GDP - 2022 Data - 2023 Forecast - 1975-2021 Historical - Chart - News", *Tradingeconomics.com*, 2022. Available: <https://tradingeconomics.com/cyprus/gdp#> . [Accessed 19 July 2022].
- [71] "Where is Cyprus on Map Lat Long Coordinates", *Latlong.net*, 2022. Available: <https://www.latlong.net/place/cyprus-12396.html>. [Accessed: 20 July 2022].
- [72] A. Farmaki, *Map of Cyprus*. 2012.
- [73] Weather Spark, *Average yearly temperature. 2020*.
- [74] M. Hastunc, "OPTIMIZING RESIDENTIAL RENEWABLE ENERGY UTILIZATION IN NORTH CYPRUS: CASE STUDY OF SOLAR ENERGY", 2018. Available: https://www.researchgate.net/publication/325224511_OPTIMIZING_RESIDENTIAL_RENEWABLE_ENERGY_UTILIZATION_IN_NORTH_CYPRUS_CASE_STUDY_OF_SOLAR_ENERGY . [Accessed 21 July 2022].
- [75] A. Yasli and E. Soujeri, *Average solar radiation in Cyprus*. 2012.
- [76] M. Hastunc, *Average solar irradiation Map of Cyprus*. 2018.
- [77] J. Michaelides, D. Wilson and P. Votsis, *Mean dailysolar radiation Cyprus*. 1991.

- [78] H. Ritchie, M. Roser and P. Rosado, "Energy", *Our World in Data*, 2020. Available: <https://ourworldindata.org/energy/country/cyprus>. [Accessed 22 July 2022].
- [79] "Pages - PowerStation Capacity", *Eac.com.cy*, 2022. Available: <https://www.eac.com.cy/EN/RegulatedActivities/Generation/powerstationcapacity/Pages/default.aspx> . [Accessed 23 July 2022].
- [80] "Hot Water Solar Systems - Suxeed Solar - Solar Energy Systems Cyprus", *Suxeed Solar - Solar Energy Systems Cyprus*, 2022. Available: <https://www.suxeed-solar.com.cy/hot-water-solar-systems/> . [Accessed 24 July 2022].
- [81] N. Abas, N. Khan and A. Haider, *System schematic of thermosyphon*. 2017.
- [82] K. Papakostas, N. Papageorgiou and B. Sotiropoulos, "Residential hot water use patterns in Greece", *Solar Energy*, vol. 54, no. 6, pp. 369-374, 1995. Available: [https://doi.org/10.1016/0038-092X\(95\)00014-I](https://doi.org/10.1016/0038-092X(95)00014-I) . [Accessed 25 July 2022].
- [83] M. Ozturk, O. Calisir and G. Genc, *System scematic of SAHP system*. 2021.
- [84] F. Asdrubali and U. Desideri, "High Efficiency Plants and Building Integrated Renewable Energy Systems", *Handbook of Energy Efficiency in Buildings*, pp. 441-595, 2019. Available: <https://doi.org/10.1016/B978-0-12-812817-6.00040-1> . [Accessed 26 July 2022].
- [85] "WHAT IS A BUFFER TANK AND HOW DOES IT WORK WITH A HEAT PUMP?", *Thermalearth.co.uk*, 2022. . Available: <https://www.thermalearth.co.uk/blog/what-is-a-buffer-tank#:~:text=HOW%20BIG%20IS%20A%20BUFFER,sized%20at%20approx%20150%20litres> . [Accessed 27 July 2022].
- [86] H. Cheung and J. Braun, "Performance comparisons for variable-speed ductless and single-speed ducted residential heat pumps", *International Journal of Refrigeration*, vol. 47, pp. 15-25, 2014. Available: <https://doi.org/10.1016/j.ijrefrig.2014.07.019> . [Accessed 28 July 2022].
- [87] J. Hirvonen and K. Siren, *COP of the water-to-water heat pump with different load-side inlet temperatures. Based on model NIBE-F1345*. 2017.
- [88] "Heat Pumps - A Guidance document for designers (BG 7/2009), Brown R, 9780860226864", *Bsria.com*, 2009. Available:

https://www.bsria.com/uk/product/jnEAnX/heat_pumps_a_guidance_document_for_designers_bg_72009_a15d25e1/ . [Accessed 30 July 2022].

[89] R. Krishnamurthy, *Charting The Sun's Motion In Relation To Your Home And Permaculture Site*. 2015.

[90] D. A++, "Daikin EDLA16D3V3 Altherma 3 Monoblock Air to Water Heat Pump 16Kw/54000Btu A++", *OrionAirSales: Commercial Products Sales*, 2022. Available: <https://www.orionairsales.co.uk/daikin-edla16d3v3-altherma-3-monoblock-air-to-water-heat-pump-16kw54000btu-a-14904-p.asp> . [Accessed 31 July 2022].

[91] T. Direct, "1500 Litre GRP Hot Water Tank, Insulated 50mm", *Tanks Direct*, 2022. Available: <https://www.tanks-direct.co.uk/1500-litre-grp-hot-water-tank-insulated-50mm/p4317> . [Accessed 31 July 2022].

[92] "Sunpower solar panel mono 410W power", *Todoensolar.com*, 2022. Available: <https://www.todoensolar.com/Solar-Panel-from-410W-to-415W-SunPower-Performance-P3-and-P19> . [Accessed 2 August 2022].

[93] "Victron Solar charge controller - SmartSolar MPPT 150/45-MC4", *Europe-solarstore.com*, 2022. Available: <https://www.europe-solarstore.com/victron-solar-charge-controller-smartsolar-mppt-150-45-mc4.html> . [Accessed 2 August 2022].

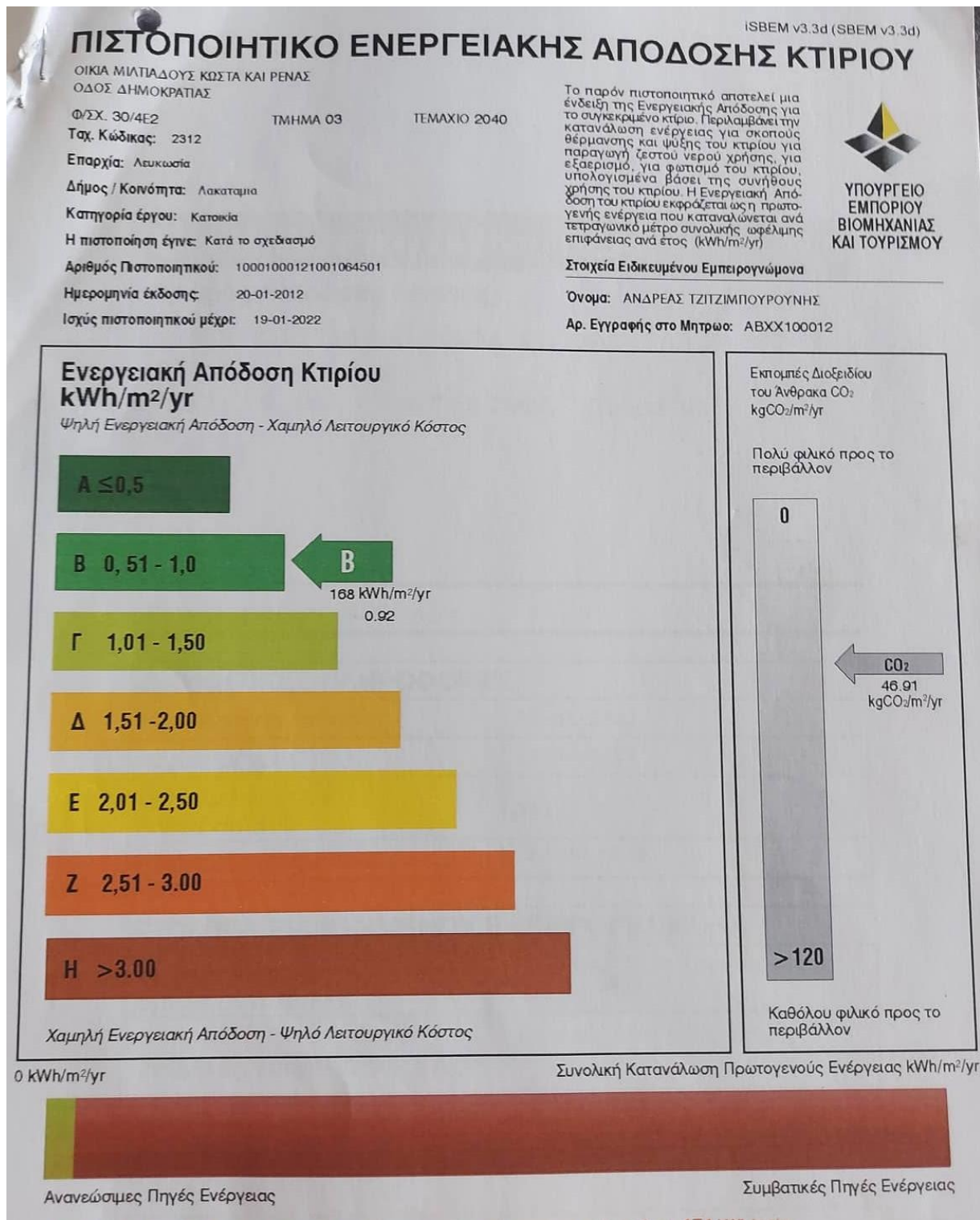
[94] "Energy Cost Comparison", *Nottingham Energy Partnership*, 2020. Available: <https://nottenergy.com/resources/energy-cost-comparison/>. [Accessed 3 August 2022].

[95] "Cyprus electricity prices, December 2021 | GlobalPetrolPrices.com", *GlobalPetrolPrices.com*, 2022. Available: https://www.globalpetrolprices.com/Cyprus/electricity_prices/. [Accessed 3 August 2022].

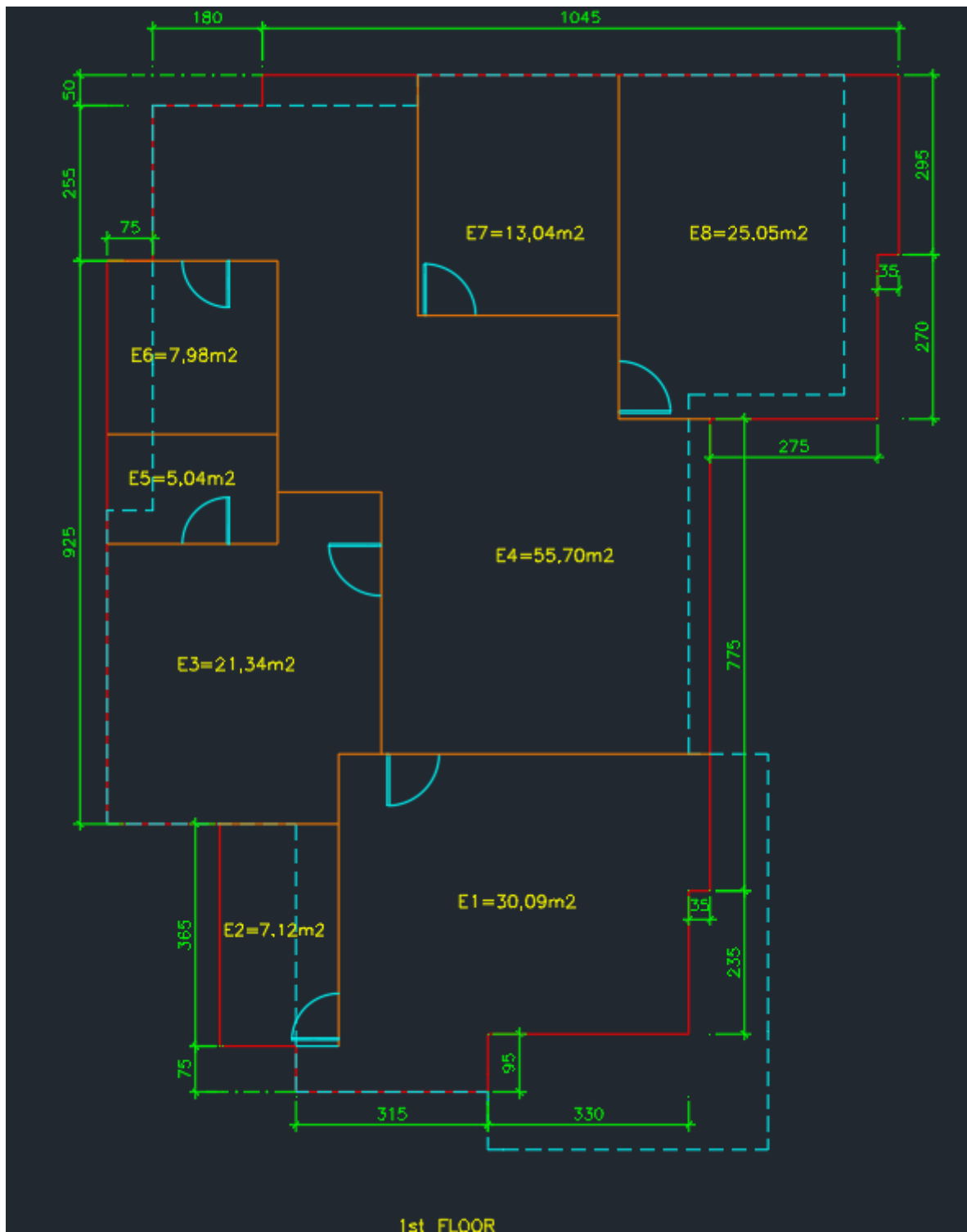
[96] "Air Source Heat Pump - Pure Renewables", *Pure Renewables*, 2022. Available: <https://purerenewables.co.uk/energy-solutions/air-source-heat-pump/>. [Accessed 4 August 2022].

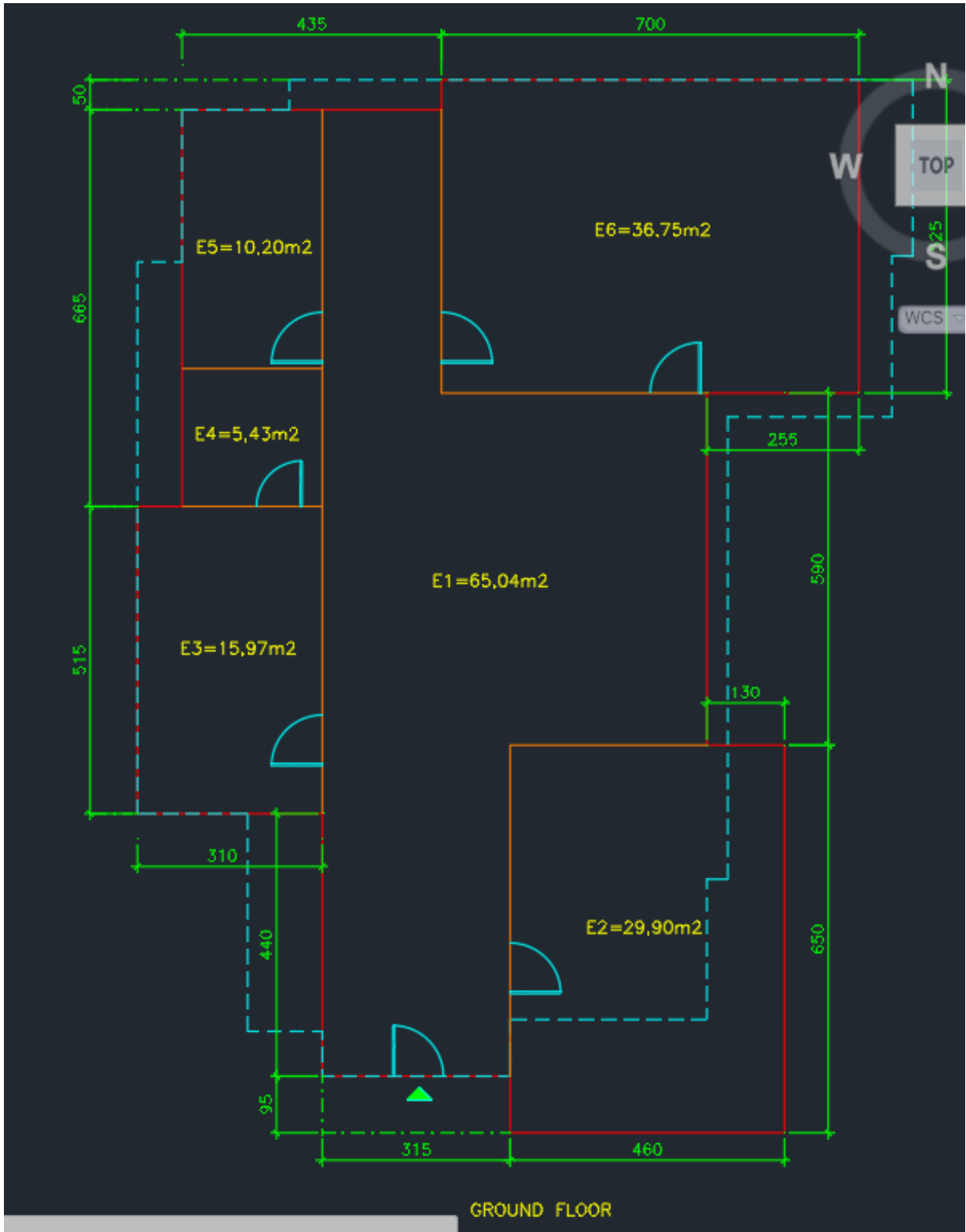
[97] 2022. Available: https://www.covenantofmayors.eu/IMG/pdf/technical_annex_en.pdf . [Accessed 05 August 2022].

APPENDIX 1- ENERGY PERFORMANCE CERTIFICATE OF BUILDING



APPENDIX 2- FLOOR PLAN OF CURRENT BUILDING





APPENDIX 3- SAMPLE CONFIGURATION OF WALL AND WINDOW COMPOSITIONS

A/A	Περιγραφή υλικού	Πάχος d(m)	λ W/(mK)	ρ kg/m ³	Cp kJ/(kgK)	R m ² K/W	Cm kJ/m ² K	Τυπική σχεδιαστική λεπτομέρεια - 0.3m		
1	Άμμος και Τσιμέντο	0.025	1	1800	1	0.025	45			
2	Τούβλα αργιλικά - 200x300x100	0.25	0.4	1000	1	0.625	250			
3	Άμμος και Τσιμέντο	0.025	1	1800	1	0.025	45			
Ροή θερμότητας								Rsi	Rse	Συντελεστής θερμοπερατότητας U (W/m ² K)
Οριζόντια								0.13	0.13	1.07
Αποτελεσματική θερμοχωρητικότητα κατασκευής - Στρώσεις {1,2} Cm (kJ/m ² K)										120

A/A	Περιγραφή υλικού	Πάχος d(m)	λ W/(mK)	ρ kg/m ³	Cp kJ/(kgK)	R m ² K/W	Cm kJ/m ² K	Τυπική σχεδιαστική λεπτομέρεια - 0.485m		
1	Άμμος και Τσιμέντο	0.025	1	1800	1	0.025	45			
2	Τούβλα αργιλικά - 200x300x100	0.35	0.4	1000	1	0.875	350			
3	Εξηλασμένη πολυστερίνη	0.08	0.03	20	0.1	2.667	0.16			
4	Άμμος και Τσιμέντο	0.01	1	1800	1	0.01	18			
5	HPL	0.02	0.3	0.001	0.001	0.067	0			
Ροή θερμότητας								Rsi	Rse	Συντελεστής θερμοπερατότητας U (W/m ² K)
Οριζόντια								0.13	0.04	0.262
Αποτελεσματική θερμοχωρητικότητα κατασκευής - Στρώσεις {1,2} Cm (kJ/m ² K)										120

Σημείωση για το U value: Για να ικανοποιείτε η απαίτηση του διατάγματος, θα πρέπει ο μέγιστος μέσος συντελεστής των τοίχων και στοιχείων της φέρουσας κατασκευής να είναι $U \leq 0.4 \text{ W/m}^2\text{K}$

APPENDIX 3- HEAT PUMP ALTHERMA V3 MODEL SPECIFICATIONS

EAVH-D6V(G)/D9W(G) + EPGA-DV3



BLUEEVOLUTION

Daikin Altherma 3 heating only models

Floor standing air to water heat pump for heating and hot water, ideal for low energy houses

- › Integrated stainless steel domestic hot water tank of 180 or 230L
- › PCB board and hydraulic components are located in the front for easy access
- › Small installation footprint of 595 x 600 mm
- › Integrated back-up heater choice of 6 or 9 kW
- › Outdoor unit extracts heat from the outdoor air, even at -28°C



Efficiency data		EAVH + EPGA	16518D6V(G)/D9W(G) + 11DV	16523D6V(G)/D9W(G) + 11DV	16518D6V(G)/D9W(G) + 14DV	16523D6V(G)/D9W(G) + 14DV	16518D6V(G)/D9W(G) + 16DV	16523D6V(G)/D9W(G) + 16DV
Heating capacity	Norm.	kW	11.1 (1) / 11.3 (2)		14.5 (1) / 14.5 (2)		16.5 (1) / 15.6 (2)	
Power input	Heating	Norm.	kW	2.16 (1) / 2.91 (2)		2.91 (1) / 3.96 (2)		3.45 (1) / 4.21 (2)
CDP				5.15 (1) / 3.88 (2)		4.99 (1) / 3.65 (2)		4.78 (1) / 3.71 (2)
Space heating	Average climate water outlet 55°C	General	SCOP	3.29		3.34		3.41
			ηs (Seasonal space heating efficiency)	129		130		133
			Seasonal space heating eff. class	A++				
	Average climate water outlet 55°C	General	SCOP	4.38		4.45		4.56
ηs (Seasonal space heating efficiency)			172		175		179	
		Seasonal space heating eff. class	A++			A+++ (3)		
Domestic hot water heating	General	Declared load profile	L	XL	L	XL	L	XL
	Average climate	ηwh (water heating efficiency)	104	112	104	112	104	112
			Water heating energy efficiency class	A				
Indoor Unit		EAVH	16518D6V(G)/D9W(G)	16523D6V(G)/D9W(G)	16518D6V(G)/D9W(G)	16523D6V(G)/D9W(G)	16518D6V(G)/D9W(G)	16523D6V(G)/D9W(G)
Casing	Colour	White + Black						
	Material	Resin / Sheet metal						
Dimensions	Unit	HeightxWidthxDepth	mm	1,650x595x625	1,850x595x625	1,650x595x625	1,850x595x625	1,650x595x625
Weight	Unit		kg	109	118	109	118	109
Tank	Water volume		l	180	230	180	230	180
	Maximum water temperature		°C	70				
	Maximum water pressure		bar	10				
	Corrosion protection		Pickling					
Operation range	Heating	Ambient	Min.-Max.	°C				
		Water side	Min.-Max.	°C				
	Domestic hot water	Ambient	Min.-Max.	°CDB				
		Water side	Max.	°C				
Sound power level	Norm.		dBA					
Sound pressure level	Norm.		dBA					
Outdoor Unit		EPGA	11DV	14DV	16DV			
Dimensions	Unit	HeightxWidthxDepth	mm			1440x1160x380		
Weight	Unit		kg			143		
Compressor	Quantity		1					
	Type		Hermetically sealed scroll compressor					
Operation range	Cooling	Min.-Max.	°CDB					
	Domestic hot water	Min.-Max.	°CDB					
Refrigerant	Type		R-32					
	GWP		675.0					
	Charge	kg	3.50					
	Charge	TCO2eq	2.36					
	Control		Expansion valve					
Sound power level	Heating	Norm.	dBA			64		
	Cooling	Norm.	dBA			68		
Sound pressure level	Heating	Norm.	dBA			48		
	Cooling	Norm.	dBA			55		
Power supply	Name/Phase/Frequency/Voltage		Hz/V					
Current	Recommended fuses		A					